INTERACTIONS BETWEEN TOPOGRAPHY AND THE ATMOSPHERE: THE ROLE OF ASIAN TOPOGRAPHIES ON THE INDO-ASIAN MONSOON

A Dissertation

Submitted to the Faculty

of

Purdue University

by

Rene Paul M. Acosta

In Partial Fulfillment of the

Requirements for the Degree

of

Doctor of Philosophy

December 2018

Purdue University

West Lafayette, Indiana

THE PURDUE UNIVERSITY GRADUATE SCHOOL
STATEMENT OF DISSERTATION APPROVAL

Dr. Matthew Huber, Chair

Department of Earth Atmosphere, and Planetary Sciences

Dr. Ernest M. Agee

Department of Earth Atmosphere, and Planetary Sciences

Dr. Dan R. Chavas

Department of Earth Atmosphere, and Planetary Sciences

Dr. Cary D. Troy

Lyles School of Civil Engineering

Approved by:

Dr. Darryl Granger

Head of the Graduate Program

To Lourdes Martinez Acosta, for opening my eyes to the world and to Reynaldo Olan Acosta for teaching me how to fight for that world.

ACKNOWLEDGMENTS

R. Paul Acosta thanks his committee members and mentors:

My adviser Professor Huber for his guidance and astounding ability to motivate and cultivate a scientific mind; Professor Agee for always reminding us that one's personal life is as important as one's research; Professor Chavas for the boundless scientific and atmospheric dynamics discussion; and Professor Troy for his commitment and for relaying the idea that by imitating confidence and an optimistic mindset a person can realize those qualities in their own life; To Professor Paul Kirshen for seeing "the big picture" and reminding me that the societal implications of my work should be emphasized in one's work; Professor Alex Gluhovsky, who highlighted the statistical side of science; Professor Yutain Wu and Dr. Richard Neale for their scientific input on monsoon modeling and dynamics; and Professor Paul Koch, Professor Lisa Sloan, Professor Peter Weiss for their undergraduate mentoring.

R. Paul Acosta thanks supporting agencies:

The EAPS department and Research Computing Center at Purdue University; EPSCoR University of New Hampshire; NSF Grant (EAR-1049921); CISL Data Support Section (NSFEAR114504) at the National Center for Atmospheric Research (NCAR) for providing various scientific data; NCAR for developing Community Earth System Model (CESM), and NCAR Command Language (NCL); NCO developers; World Climate Research Program's (WCRP) Working Group on Coupled Modeling (WGCM), and the Global Organization for Earth System Science Portals (GO-ESSP) for CMIP5 output.

R. Paul Acosta thanks his colleagues, friends and family:

Members of Climate Dynamics Prediction Laboratory (Dr. Ruben van Hooidonk, Dr. Aaron Goldner, Dr. Nick Herold, Dr. Srinath Krishnan, Dr. Muge Komurcu, Dr. Jonathan Buzan, Ashley Dicks, Emma Mccabe) for helpful discussion and comments through out my Ph.D; House of 524 (Peter Robertson, Ian Pope, and Gypsy the pup) for helping get through my arduous first year at Purdue; friends from New England (Brandon Montemuro, Alley Leach, Sophie Wilderotter, Salme Cook, John McClain Justin Pelletier, Zach Lange and his pup the real McCoy, Lindsay Vierra and her pup Adie) for the hikes, beach time and for quoting "research getting in the way of life"; friends in the Midwest (Mark Haugen, Linsey Payne, Anne Dare, Tim Bowling, Rollie Rocket, Kimberly Hoogewind, Rachel Gipe, Wai Allen, Joe McConeghy) for showing the best of the Midwest hospitality, friends in California (Godfrey Tillet, Pete Siqueiros, Daniel Rodrigez, Anthony Flores, Gilbert Ramos, Julie Steers, Alex Gomez, Katie Bailey, Isaac Norman, Nina Zelcer, Gabe Matson) for keeping me down to Earth and reminding me what life is outside of acadamia); To the climbing community at Purdue for taking me away from the grind; My family (Reynaldo, Lourdes, Sheena and Ralph Acosta) for motivating me to continue forward even when things got dire; To Jordyn Miller and Lola for the endless hugs, ice cream, climbing and for brightening my mornings.

R. Paul Acosta thanks several coffee shops:

Cafe Royale, Grey House, Fuel, Star City, Adelle's, White Heron, Lil's, Flight, Book'n Bar Starbucks, Lavazza and Panera for the countless hours I spent working in them, for the Americanos and coffee I consumed, and for the random and casual conversations.

TABLE OF CONTENTS

Page

Page

LIST OF TABLES

LIST OF FIGURES

Figure Page

ABSTRACT

Acosta, R. Paul M. Ph.D., Purdue University, December 2018. Interactions Between Topography and the Atmosphere: The Role of Asian Topographies on the Indo-Asian Monsoon. Major Professor: Dr. Matthew Huber.

Topography influences climate dynamics by redirecting how the atmosphere transports moisture, and energy. By doing so, topography alters precipitation patterns, circulation of wind, riverine fluxes, and ocean upwelling distributions. This dissertation investigates the linkages between major topographic features and atmospheric dynamics within an Earth System perspective. The studies presented build upon the foundations of theoretical atmospheric thermodynamics and dynamical principles and primarily delves into the interactions between the Indo-Asian Monsoon and the surrounding topographies. First, I explore gaps in the current body of literature, mainly using observational datasets and reanalysis products. I then add in more sophisticated tools, such as general circulation models (GCMs) to investigate how terrain orogen impact the regional climatic regime with an emphasis on the monsoonal environment. To do so I explore drawbacks in using currently available GCMs and demonstrate the necessity of utilizing appropriate model horizontal-grid resolution when studying atmosphere-terrain interactions. I then delve into reexamining previously explored monsoon theories, and develop new concepts and theories for the Indo-Asian Monsoon. Lastly, I apply such model tools to further understand the orogen of the Tibetan Plateau. To do so, I examine the paleoenthalpy methods and determine its viability in measuring the paleoelevation of the Tibetan Plateau. Ultimately, we apply this method to aid the paleoclimate community in deciphering the evolution of Tibet during the Cenozoic era. Constraining the evolution of the re-

gional topography is crucial for understanding the hydrological cycle and the climatic evolution of Eurasia.

Chapter 1 discusses the importance and implications of this work and introduces known concepts and current leading knowledge about the Indo-Asian Monsoon and mountain dynamics. Chapter 2 and 3 focus on various observational and reanalysis products which help us determine which current GCM can best represent the Indo-Asian monsoon. Chapter 4 uses that model to delve into monsoon-topography interactions. Chapter 5 utilizes the GCM results to assess the drawbacks of using the paleoenthalpy method. Chapter 6 briefly discusses future directions.

1. A BRIEF INTRODUCTION TO MONSOON-TOPOGRAPHY INTERACTIONS

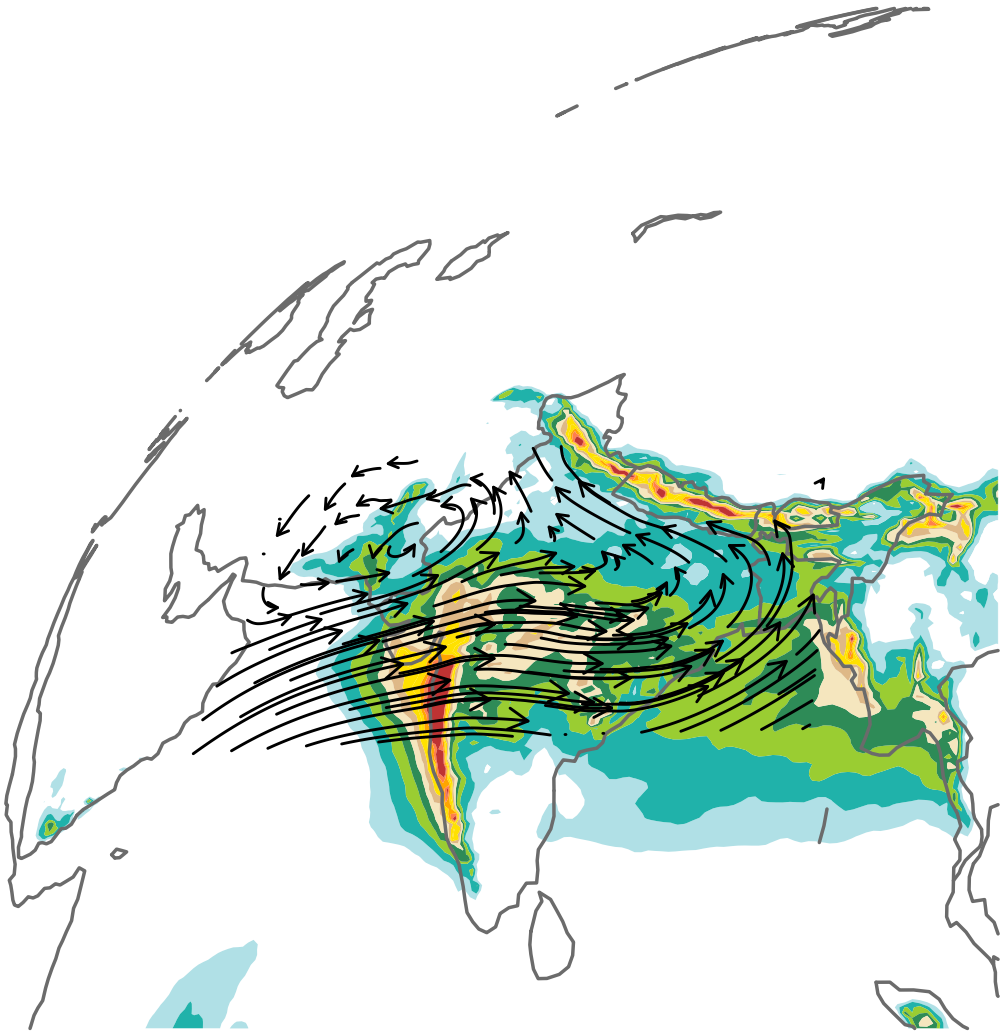

Fig. 1.1. A glimpse to the Indo-Asian Monsoon as simulated by the NCAR global climate model.

Abstract

One of the main hypothesis behind the Cenozoic global cooling trend is the orogeny of mountains [1]. Seminal works [2,3], have identified the uplift of the Tibetan Plateau as the primary suspect for inducing such global climate change, where such uplift spawned the formation of the Asian Monsoon systems and lead to regional moistening and, increased precipitation and erosion rates [4, 5]. In a longer time-scale, as the burial rate of carbon increased, such positive feedback was hypothesized to promote global cooling, whereby enhancement of the hydrological cycle ultimately allows further carbon sequestration. One of the key time periods I explore in this dissertation is during the Miocene, where global cooling and Indo-Asain Monsoon enhancement synchronously occurred [6].

More recent studies have identified the impact of topography is primarily restricted to a regional-scale [7]. In general, a topography can impose changes to atmospheric wave-dynamics, thermally driven circulations, and the hydrological cycle. Even at the most local level topography reallocates precipitation, riverine influx and can induce regional desertification.

However, such feedbacks and mechanisms are difficult to evaluate due to the concept of equifinality. Nevertheless, the advancement of physics-based climate model allowed evaluation of steady state systems with simple incremental perturbations. For this reason, I utilize such black box but ultimately hope to simplify and improve our understanding about the interactions between the Indo-Asain monsoon and the regional topographies.

The main goal of this chapter is to introduce the field and provide background for the subsequent chapters. In this chapter, I will present general knowledge of how topography influences the surrounding atmosphere and dive into previous studies on how the Tibetan Plateau influences the Indo-Asian Summer Monsoon. Then I briefly dive into the primary model we use for our studies, the National Center for atmospheric research, Community Climate System Model. Lastly, I present the hypotheses that are tested in the following chapters.

1.1 How topography influence the atmosphere

When distilled to its simplest form, as mean winds flow toward topographic relief, depending on the objects vertical extent, the fluid is either forced to flow over or around the feature. Much like river water flowing over a boulder, fluid that flows over a bump may generate internal waves with the frequency that is determined by the velocity of the fluid, the scale of the terrain and the static stability of the medium. By neglecting the process of friction, we can use scalar-analysis to understand how flow over topography interacts with the atmosphere. The primary way to do so is to utilize the non-dimensional Froude number (Fr).

$$Fr = \frac{U}{\theta}\frac{d\theta}{dz} \tag{1.1}$$

where U represents a generalized horizontal flow, θ is the potential temperature and z is the height of the mountain. The Fr number also determines if the flow over topography will allow wave propagation (i.e. gravity waves that are small enough that Coriolis can be ignored) is possible. For instance, when the $Fr << 1$ then, it is most likely the case that U is insufficient to overcome both static stability of the atmosphere or the height of the mountain, thus wave propagation is unlikely. Whereas when the $Fr >> 1$ or $U > g'H$), then flow is sufficient to flow over the terrain, where the strength of the flow determines if gravity waves propagation is possible. However, the amplitude of this type of wave over topography are often small, with frequency and waves speed to be relatively faster than buoyancy oscillation (N), these waves then decay as they propagate vertically. Examples of such waves are often associated with small topographic features where typical atmospheric velocities can easily overcome the underlying obstacle.

The most interesting situation is when $Fr = 1$, where wave amplitude and frequency are large and is more influenced by N. In this case, the buoyancy frequency, N or more famously known as the Brunt- V*àisàlà* frequency is denoted as:

$$N = \frac{g}{\theta} = \frac{U}{NH} \tag{1.2}$$

and determines the stability of the atmosphere through the downward gravitational acceleration and vertical distribution of potential temperature. Additionally, these flows typically associated with large topography. Atmospheric stability plays an important role in how waves with Fr near 1 vertically propagates. For example, strong troposphere stratification will bound the mountain wave aloft and amplify the waves between the two boundaries, these are also known as trapped lee waves. An extreme example of this is when strong stratification is developed on the lee side of the mountain and where flow over topography are funneled causing downslope winds to exceed normal wind speeds. The funneling is hindered by the critical layer where the flow $U \approx 0$.

The distribution of moisture and in particular latent heating impacts the vertical velocity of the surrounding atmosphere, which in turn affect the atmospheric buoyancy. The addition of excess energy from latent heat can allow the incoming flow of air to overcome the height of the terrain. Thus, it is important to take into account the moisture terms when calculating the Brunt-Visl Frequency. In particular, the treatment of equivalent potential temperature (θ_e) must be accounted for. This will become important in the subsequent chapters as we discuss how the onshore monsoonal flow interacts with the Himalayan Mountains. To calculate the moist Froude number ($F_m = \frac{U}{N_m h}$) we used an averaged wind speed of 5 $m\ s^{-1}$ and average mountain height of 5 km. We then calculated the modified saturated Brunt-Visl Frequency (N_m^2) use in [8, 9] as shown below.

$$N_m^2 = \frac{1}{1+q_w}[\Gamma_m(c_p + c_l q_w)\frac{1}{\theta_e}\frac{\partial \theta_e}{\partial z} + (\Gamma_m c_l \frac{ln\theta_e}{T} - g)\frac{\partial q_w}{\partial z}] \tag{1.3}$$

Where Γ_m represents the moist adiabatic lapse-rate taken from model height (z), T is the ambient air temperature and θ_e is the equivalent potential temperature. The total mixing (q_w) is the sum of liquid water ratio and the saturation mixing ratio. The following variables are gravity (g), heat capacity of dry air (c_p), and heat capacity of liquid water (c_l). For our calculation, we found the liquid water ratio to be negligible. As an example regions where $N_m^2 < 0$ represent a layer of potential instability.

As waves form on the back side of the mountain, how far they migrate is determined by the scale of energy developed. Wave dissipation is primarily done through the decay of energy as waves propagate into the atmosphere and near the surface where drag or friction is dominant. Complex vertical profile of terrains can also disrupt wave propagation due to its tendency to block the wave frequency. While the opposite can be said where abrupt changes in topographic height can accelerate wind flow at the mountain trough. These examples are due to an abrupt conversion of potential energy to kinetic energy as winds are pinged between the atmospheric boundary layer and the topography below. Most studies on flow over topography are done through 2-D Gaussian Hill- like topography, however, the complexity of in the horizontal plane is critical for understanding how atmospheric circulation is affected by flow over topography. For instance, surface winds can abruptly encounter the mountain and are unable to initially flow over (Fr $<<$ 1), which will redirect flow in the horizontal plane. This horizontal flow can either dissipate through drag or be reinvigorated and later be able to overcome the terrain.

Realistically, when the waves are substantially large, the Earths rotation, also known as the Coriolis parameter (f), imposes substantial influence on waves or eddies. For the purpose of the topic at hand, it is essential to recall that f increases as one move toward the poles; this is called the Beta effect (β). The combination of f and conservation of absolute vorticity η strongly influence the flow path and strength of eddies over topography:

$$\eta = f + \zeta \tag{1.4}$$

where ζ is the relative vorticity as viewed in the perspective of a rotating planet. A prime example of this is an aloft westerly wind encountering the Western Himalayas or Karakoram region. The layer of air, flowing about an isobaric surface, is compressed vertically and expands horizontally to converse mass. Through conservation, ζ must increase, which then alters f. The only way to increase f is to displace the aloft westerly wind poleward. Undulations represented by troughs and ridges in

the atmosphere can determine large-scale circulation and influence weather patterns across the globe [10].

As a side note, planetary-scale waves can also form without the presences of topography. For instance, over the mid-latitudes, the surface temperature gradient between land and ocean can create surface flow from high and low-pressure systems. This mechanism, also known as pressure gradient force, is balanced by the f. A balanced flow is also known as geostrophic flow and is represented by anticyclonic circulation in the Northern Hemisphere. Flows moving from trough (low) to a ridge (high) are subgeostrophic while the opposite are supergeostrophic [11]. Topographically as well as thermally induced planetary waves are also referred to as stationary Rossby Waves. They are important to mid-latitude storm tracks and are essential to how the planet transport energy.

In conjunctions to waves, eddies are the primary way the planet transports properties, whether it is heat, moisture or both, from the equator toward the poles. Eddies will be more important as we discuss them in the subsequent chapters. There are three components that contribute to the zonal and time mean transport. Here I arbitrarily pick temperature as the main variable transported.

$$[v\bar{T}] = [\bar{v}][\bar{T}] + [v'\bar{T}'] + [\bar{v^*}\bar{T}^*] \tag{1.5}$$

Where v is the meridional wind component, thus u represents zonal wind speed (both variables are discussed later). The first component on the right-hand side of the equation is the mean meridional circulation. These are the large circulation such as Hadley, Ferrell and polar cells and delineates where convergence and subsidence occurs. The secondary component is the transient eddy term, which are synoptic-scale eddies that temporally persist within 7-10 days and primarily dominate the mid-latitudes. The third component is the stationary eddy term, which are eddies that are fixed in location due to their physical constraint (topography, land-sea contrast). These eddies are large in scales which are in order of thousands of kilometers. Although stationary eddies are largely created by topographic features, regionally persistent temperature

contrast can also produce such eddies. Nevertheless, the existence of stationary eddies during a given season influences the mean meridional and zonal circulation.

For the purpose of understanding the monsoon circulation, we analyze moisture flux across the Indo-Asia during peak summer monsoon season. As noted by Walker et al., [2015] moisture flux as index incorporates and constraints both precipitation intensity and strength of monsoonal circulation, which they found more robust than using other winds shear indices. Here we relate the moisture budget to the mean vertically integrated moist flux (right-hand side) to the net change in precipitation (left-hand side), similarly to Curio et al., [2015], Walker et al., [2015]

$$IMF = \int_{P_{1000mb}}^{P_{600mb}} \rho(vq)\Delta z \tag{1.6}$$

Where the right-hand side represents the (v) mean horizontal wind speed (u and v), and the specific humidity (q) at various pressure level. For this study, we focus on the total near-surface moisture flux and integrated between 1000-600 mb.

We have discussed key atmospheric concepts, which will be implemented and further discussed in the following chapters. The next section, we will dive into a specific case which touches upon some of the dynamics we have talked about above. More importantly, it will give a general background to the primary focus of my dissertation.

1.2 Background on the Indo-Asian Summer monsoon dynamics

The Indo-Asian monsoon (IAM) is one of the most studied hydrological phenomena. Rightfully so, due to its immense influence on billions of lives. Simple delay of monsoon onset causes havoc on the Asian agriculture and changes in its magnitude create devastating floods or droughts. In colloquial terms, monsoon regions are defined as areas where the majority of its rainfall occurs during one season. In the case of India, most of the rainfall occurs during June, July, and August with seasonal growth and decay occurring during May and September.

One of the oldest definition of the monsoon is its association with strong seasonal wind reversals that is governed by strong land-sea thermal contrast between the Indian Ocean and Southern Asian landmass [12, 13]. Since the early 1960s, the Tibetan Plateau was believed to impose both mechanical and thermal forcing onto the nearby atmosphere, which influences the overall meridional circulation [14]. However, contrary to previous belief, recent controversial study [15] have shown that the Tibetan Plateau imposes little to no impact on the IAM. This section builds upon such controversy and aims to provide context to the studies presented in the subsequent chapters. This section will review influential works on the subject, both modern and paleoclimate, and summarize the current state of the field.

The IAM has been shown to be a branch of the equatorial Hadley cell during the Nothern Hemispheric summer [16–19], or a seasonal poleward migration of the intertropical convergence zone (ITCZ) onto the Eurasian continent. The IAM is a major part of the Global Monsoon (GM) system [20]. Although the migration of the ITCZ toward the subtropics is directed by the position of maximum solar insolation, the complex landscape combined with large sources of moisture, implicate the characteristic of the ITCZ over Southern Asia. As previously mentioned before, the IAM has been linked to growth and expansion of the Tibetan Plateau complex during the Cenozoic era (65 ma), where both thermal [13, 21, 22] and mechanical forcings [15, 23, 24] are hypothesize to regulate the characteristics of the IAM.

Prior to the topographical mechanisms, Halley [1686] first noted that the on seasonal change in the zonal wind over the Indian Ocean marks the onset of the Asian monsoon. He then hypothesizes that heating between the land and ocean creates a temperature difference that sets a giant land-sea breeze circulation. Thus, such a hypothesis has been used as a key component of the initialization and maintenance of the IAM. This hypothesis is predicated upon temperature gradient playing a substantial roll on how energy is redistributed over the subtropics [25], especially over the IAM

region. The total thermodynamic energy balance for the atmosphere is expressed below using time mean and deviation from the time mean in pressure coordinates:

$$\partial_t \bar{T} = \frac{\bar{Q}}{c_p} - (\frac{p}{p_0})^k - \bar{\omega}\partial_p\bar{\theta} - \bar{v}\cdot\nabla_p\bar{T} - \frac{p}{p_0})^k\partial_p(\bar{\omega'\theta'}) - \nabla_p\cdot(\bar{v'T'}) \tag{1.7}$$

where Q is diabatic heating, p is pressure, p_0 is a standard constant pressure, $k = \frac{R}{c_p}$, R is the gas constant of dry air at constant pressure and θ is potential temperature. Vertical and horizontal velocities are expressed as w and v. Near the equator, the horizontal advection term weakly contributes to the thermodynamic equation due to weak temperature gradients [26], but becomes more important toward the extratropics. The previous study [25], assumes that the mean temperature over time ($\partial_t\bar{T}$) is negligible on seasonal timescales. Additionally, it was found that transient terms were more important toward the mid-latitudes and do not play a substantial role toward the tropics. Thus, the vertical advection of θ, Q and mean horizontal gradient of T dominate the tropics.

Atmospheric heating over the Tibetan Plateau has been the longest standing theory for invoking land-sea thermal contrast that is thought to initiate the IAM. Studies using calculated soundings concluded that the equilibrium temperature of the ambient air above the Plateau was shown to be higher than the air at the same pressure level over a surface at sea level [27]. Additionally, reanalysis products which are a physical model based simulations nudge with observed state variables, illustrated an anomalously increased sensible heating at the southern range of Tibetan Plateau [28]. The components in total diabatic heating in the atmosphere can be distilled into the sum of radiation tendencies, represented by short and long-wave radiation, latent heat release as moisture change in phases, and near surface heating and sensible heat.

$$Q_{total} = Q_{rad} + Q_{sfc} + Q_{LH} + Q_{SH} \tag{1.8}$$

Detailed calculations of diabatic heating in various modern reanalysis products are presented by Ling and Zhang [29] and Wright and Fueglistaler [30].

Modeling simulations [22, 31] where topographic relief of Tibetan Plateau was altered, demonstrated that diabatic heating increased as Tibetan Plateaus elevation

increased. Modeling studies suggest that deep heating over Tibetan Plateau strongly influences the IAM circulation, while others advocate that such heating is the cause of monsoonal onset. The diabatic heating theory is thought to invoke increased vertical velocities, which corresponds to the outflow of air in the upper atmosphere. The upper-troposphere divergence (∼500 mb) is representative of a seasonally imposed high-pressure system over Tibetan Plateau [13]. Additionally, by conservation of sverdrup vorticity balance, a high-pressure system near the surface enhances the poleward flow of low-level winds (∼850) [25,32]. Enough heating of the upper-atmosphere has the potential to change the regional temperature gradient [14] and produce an asymmetric meridional circulation. A study by Tamura et al. [33] recognized a regional temperature anomaly as a function of diabatic heating that warms the lower troposphere and adiabatic warming in the upper troposphere.

Seminal work by Gill [34], used idealized models to illustrate how an imposed diabatic heating influenced tropical circulation. His work provided solutions for asymmetric forcing such that heating located in the Northern subtropics creates an anticyclonic circulation with an opposing cyclonic circulation south of the equator. It is important to note that the formation of the IAM-like monsoon can be reproduced without topography [16,17]. In fact, aquaplanet simulations demonstrated the similar rapid onset of IAM over the subtropics without any landmass [18, 35]. However, a caveat to this work is that a shallow (1 meter) ocean is required to reproduce a rapid onset that is similar to the modern day.

It is clear that for the IAM to thrive, moisture flux from adjacent bodies of water must feed the system. Thus, Gill highlights that topography can mechanically redirect moisture flow into the system. He provided solutions were a large topographic barrier like the Eastern African Escarpment (EAE) was added to the model, which acted as a western boundary (barrier where no flow is allowed to cross) and induced a low-level convergence across the equator. This flow is known as the Findlater Jet, or Somalian Jet that feeds into the Southwesterly monsoon jet [21, 36]. Moreover, several studies [25, 37] used reanalysis product to confirm that the large portion of

the easterly flowm when blocked by a highly elevated topography like the EAE, must turn poleward. The study by Gill, as well as Rodwell and Hoskins illustrated that topographic forcings play some role for generating the IAM circulation.

I briefly highlight other important mechanical forcings. Previous studies suggest Tibetan Plateau forces oncoming winter westerly winds to be deflected and become more concentrated over Southern China [28]. Such convergence of westerly wind have been coined as downwind convergence [24] and have been highlighted as a mechanical forcing important for initiating the IAM. Additionally, an AGCM study by Boos and Kuang [2010] characterize the elongated feature of Himalayan Mountain as a mechanical forcing that prevents dry and cold extratropical air from mixing with warm and moist air found over Indo-Asia. Further analysis using extensive modeling topographic sensitivity studies suggested that Tibetan Plateau is only half the answer, where the mountains over the Hindu Kush regions also play a major role in trapping warm, moist air over the region [38]. Entrapment of high entropy air has become a key component of many studies, Park et al. illustrated that topography has some role in the formation of the IAM. To further elaborate on the importance of high entropy air for the IAM, it is necessary to digress into the theory about convective precipitation and large-scale meridional circulation.

The importance of high moist entropy air found within convective regions, vertical or slantwise convection, was first proposed by Arakawa and Schubert, [39] as a potential energy source that is provided by the large-scale forcings. The study by Arakawa and Schubert postulated that convective available potential energy (CAPE) in a deep convective system is not a property accumulated but instead is released by the system (they called this the quasi-equilibrium hypothesis or QE). The QE framework assumes that convection is a mechanism that is activated to maintain a moist adiabatic temperature profile, and revert an unstable atmosphere to a neutral state [40]. The QE theory suggests high entropy air in the subcloud layer or subcloud moist entropy (s_b) are equal to that of the saturation moist entropy of the free tro-

posphere (s^*). Another form QE approximates s_b equivalent to subcloud θ_e, which again relates the subcloud θ_e to the free tropospheric θ_e.

For the context of monsoon circulation, QE theory states that convection is a response to the heating and cannot be the cause. In support, Xu and Emanuel [41] observational data to show that in a convectively neutral region where there is large ascent, the vertical temperature profile air parcels is that of a moist adiabatic lapse rate (constant with elevation). This finding, in combination with angular momentum constraints (i.e. zonal wind field is in thermal wind balance with the density field [Emanuel, 1988; 1994] illustrated that in steady state there is a relationship between moist entropy gradient and the imposed meridional circulation [Emanuel et al., 1994; 1995].

It is important to note that convectively neutral regions with the constraints mentioned above, was later reproduced by Korty and Schneider, [2007] using saturation equivalent potential temperature (θ_e^*) and the zonal and monthly angular momentum surfaces. This concept will be important as we discuss moist enthalpy in other paleoclimate systems. Korty and Schneider then demonstrated that by substituting into Ertels potential vorticity, they can use the saturation potential vorticity to show that convectively neutral region are not only found in the tropics but in the extratropics as well.

Emanuel et al., [1994] further highlighted that within the QE framework convection does not act as a heat source driving the large-scale system, but instead exist in equilibrium with the circulation. To apply QE to monsoonal circulation Priv and Plumb, [2007] illustrated that the critical θ_e in a thermally direct circulation [26] is closely related to the maximum subcloud moist static energy h:

$$h = Tc_p + ql_v + gz \tag{1.9}$$

$$\partial h_b = Ts_b \tag{1.10}$$

where l_v the latent heat of vaporization, q is specific humidity, gz is the geopotential height and subscript b denotes subcloud. We note that moist static energy is a key

concept that will be further utilized in chapter 5. This allows approximation of the zonal wind shear and illustrates the relation between zonal wind fields and subcloud moist entropy:

$$\frac{\partial u}{\partial p} \simeq \frac{1}{f}(\frac{\partial T}{\partial p})_{s^*}\frac{1}{T_b}\frac{\partial h_b}{\partial y} \tag{1.11}$$

here u is the zonal winds. Prive and Plumb used an aquaplanet simulations to demonstrate that the poleward boudary of the monsoonal circulation is located at the region of zero vertical wind shear, northward of the maximum ascent and maximum h_b. Boos and Emanuel, [2009] later on showed in reanalysis products that the maximum mean June s^* is located over the Northern Bay of Bengal and moves northwest toward northern India during July. Reevaluation of such studies by Nie et al., [2010] illustrated the IAM circulation consists of a single deep, moist circulation, with maximum precipitation equatorward of the maximum subcloud θ_e. These studies then led to the assumption that perhaps heating over topography is not a required mechanism for the IAM. This brings us back to the controversial study by Boos and Kuang [2010] where they reproduced the modern IAM without Tibetan Plateau in GCMs.

The field up to this points is divided between two opposing points of view. As mentioned above, the first view describes the monsoon circulation over Asia as a planetary scale land-sea breeze produced by thermal gradients between land and ocean surfaces [42, 43] driven by strong surface sensible heating and latent heating over the slopes of Tibetan Plateau [13, 28]. While the antithesis of this, suggest that the onset of the monsoon occurs much quicker than the continental thermal loading and stands on quasi-equilibrium theory. [16, 44, 45].

1.3 Modeling the interactions between the Indo-Asian monsoon and Tibetan Plateau

Atmospheric general circulation models (AGCMs) have long-standing difficulty properly simulating the IAM [46, 47] and monsoon processes in general, which is not surprising given their persistent tendency to misrepresent the annual migration of the

Intertropical Convergence Zone (ITCZ) toward Southern Asia [20, 48]. Nevertheless, AGCMs have been used for decades as our best tool to improve our understanding of the interaction between Asian monsoon dynamics and its connection to topography.

Because of their open-source, and community nature, the family of models developed by National Center for Atmospheric Research (NCAR) has been prominently featured in both idealized [15, 22] and paleoclimate [4, 31, 49] studies of interaction between topography and monsoons. The NCAR AGCM physics has also been ported to form the basis of other AGCMs, such as in GENESIS and FOAM, two widely used models in paleoclimate dynamics. As a consequence of the near-ubiquitous representation of the NCAR AGCMs physics in idealized and paleoclimate, systematic biases in this representation may have an outsized influence on conceptions of monsoon dynamics and engender a false confidence in the robustness of simulation results. As described below, we find that a specific feature of the IAM in the NCAR AGCMs, and others are systematically biased and consequently that one of the many of competing theories of the monsoon may have a weaker basis than commonly interpreted.

The CAM version 4 (CAM4) is the atmospheric component of National Center for Atmospheric Research (NCAR) Community Climate System Model version 4 (CCSM4). This model framework is extensively described in Bitz et al., [2012] [50], validated in Gent et al. [2010] [51], and it forms the main basis of NCARs CMIP5 contributions. For this study, we simulated 15 years with prescribed sea surface temperatures (SST) and sea ice distributions averaged over 1982-2001. We present climatological averages over the last 10 years, emphasizing on extended monsoon season May, June, July, August, and September. Regional modeling at a 1/4 resolution has been shown to reproduce important characteristics of the IAM that are not captured in low-resolution models [Ashfaq et al., 2009] [52]. Here we present the highest resolution available for CAM (1/4) and compare them against commonly used versions. Our simulations were carried out with a finite volume dynamical core on Our simulations were carried out with a finite volume dynamical core on 0.23x 0.31, 0.47 x 0.63, 0.9x 1.25, and 1.9x 2.5 grid spacing. We refer to those throughout as 1/4°,

$1/2^\circ$, 1° and 2°. To determine the difference between highly resolved dynamics and highly resolved topography, we conduct a 1/4 simulation with a 2 topography boundary condition (S1). The CAM4 utilizes 26 vertical levels and parameterizes both deep and shallow convection [53, 54].

1.4 Hypotheses

Climate models have helped us further understand monsoon dynamics, especially how it interacts with regional terrain. As our tools become more sophisticated, we find new and exciting ways to further such scientific progress. Such endeavor includes reexamining previous process and hypothesis, which can lead to a more accurate depiction of the true nature of the monsoon. Recent studies [52, 55–58] have shown that low horizontal resolution climate models cannot capture key components of the IAM. Resolution is a major component of the work presented in this dissertation. This body of work test three main hypotheses:

1. It seems evident that topographically driven low-level Jets are important for other monsoon regions. For example, the South and North American monsoon depict topographically driven low-level jets bringing majority of the moisture into their respective region. Thus we question whether the IAM also has a topographically driven low-level jet and can reanalysis and climate models help us identify such phenomenon?
2. Since high-resolution modelling enables us to elucidate key mechanisms for the IAM, are these previous monsoon theories reproducible, are they truly important feedbacks for the monsoon and can our new models present us different views on the IAM dynamics?
3. The Tibetan-Himalayan complex have been alluded to as topography that imposed global planetary scale changes in atmospheric circulation, thus it is important to understand its ancient orogen. Can we use GCMs to better assess

the viability of reconstructing of the Tibetan orogeny using the paleoenthalpy method?

Although the questions presented above are esoteric for a specialized scientific community, however, I find it important to note that the findings of my work is driven by innate desire to merge my atmospheric and geology background. Therefore, the presented atmospheric results ultimately reflect a geological context, which is focused in the discussion sections of the individual chapters.

1.5 Concluding remarks

As current theories nullify the impact of the Tibetan Plateau on the IAM, elucidating the cause of climatic changes in Asia through the Cenozoic era remain elusive. Nevertheless, the formation of the IAM and its interaction with topography is still inconclusive. Luckily it identifies a need to further delve into the topic. Thus we will further explore these topics in chapters 2-4. My primary goal throughout this dissertation is to provide evidence that topography does plays a major role for the IAM. By doing so, we can definitively highlight the importance of orogeny when discussing the climatic evolution of the Asian continent during the Cenozoic.

This chapter briefly delved into the general understanding of topography-atmosphere dynamics and physics and touched upon how winds such as the monsoon onshore flow interact with an elevated terrain. We also considered the historical and current background on the Indo-Asian monsoon and demonstrated the current controversy behind the subject. Lastly, we presented the primary method that will be applied in the study and meaningfully discussed why we chose CAM as our primary model to use. The 2nd and 3rd chapter will build upon the modeling subsection of this chapter and further dive into how models simulate the Indo-Asian Monsoonhighlighting the pitfalls of current models. The 4th chapter hopes to alleviate the controversy between the topography and the Indo-Asian monsoon. Chapter 5 touches upon why we need to better improve our understanding of paleoaltimetry of the region. There I will

discuss the issues of using paleoenthalpy as a tool for understanding past elevations of terrains.

2. THE NEGLECTED INDO-GANGETIC PLAIN LOW-LEVEL JET

(a version of this chapter is published and available in GRL:
Acosta, R. P., and M. Huber (2017), The neglected Indo-Gangetic Plains low-level jet and its importance for moisture transport and precipitation during the peak summer monsoon, Geophys. Res. Lett.)

Abstract

Accurately simulating the Indo-Asian monsoon (IAM) using atmospheric general circulation models (AGCMs) is challenging but crucial. This study uses reanalysis products ERAI, JRA55, and HAR to highlight an easterly, low-level barrier jet along the Indo-Gangetic Plain (referred from here as IG LLJ), which we identify as the primary moisture transport mechanism for the northeastern branch of the IAM. We show that the NCAR family of AGCMs (CAM) does not capture this circulation until 1/2 degree or greater spatial horizontal resolution is used. The IG LLJ develops due to a persistent low-pressure system centered over the Ganges basin and is enhanced by the Himalayas. Using diabatic heating rates and the moist Froude number as diagnostics, we find that in CAM, this branch of the IAM displays two different dynamical regimes as a function of resolution. At low-resolution, the atmosphere near the Himalayas is statically unstable, diabatic heating is strong, and the moisture flow is southwesterly from the Arabian Sea and moves over the terrain (unblocked). At high-resolution, the moist static stability near the HM is stable, diabatic heating is weak, and the flow primarily enters easterly from the Bay of Bengal and moves parallel to the terrain (blocked). During the summer season, the low-resolution CAM is locked into the unblocked mode, which has serious implications for interpreting topography-monsoon interactions. For a broader context, we demonstrate that more

than half of the CMIP5 models do not capture the IG LLJ, which further highlights model-data mismatch across the IAM region.

2.1 Introduction

The Ganges and Brahmaputra river systems are predominantly sourced from the heavy summer rains falling on the Himalayan Mountains (HM) [59], which reflect the northeastern branch of the summer Indo-Asian Monsoon (IAM). Consequently, shifts in the IAM magnitude, timing and extent cause societal, agricultural and economic uncertainty for India and the surrounding countries [60]. Controversy exists on whether or not the IAM has tipping points [Boos and Storelvmo, 2016; Levermann et al., 2016]. Nevertheless, correctly modeling the IAM in climate models is key to a more reliable future projection [61] over the region, as well as understanding the IAM spatiotemporal evolution on longer time-scales [Molnar et al., 2010]. As a whole, the IAM is a regional expression of a global scale phenomenon [62]. Certain large-scale monsoon features can be understood in terms of seasonal shifts in the Intertropical Convergence Zone [20], associated peak subcloud layer equivalent potential temperature [16, 17, 45], and corresponding off-equatorial heating [18, 34].

However, it is also well understood that at the regional level, surface-atmosphere interactions, including topography, are important for the local IAM characteristics [47, 58, 63, 64]. Thus, the correct expression of the IAM is limited by the ability of atmospheric general circulation models (AGCMs) to capture regional-scale circulation [52, 55, 65]. This has proven to be challenging, but the availability of higher resolution modeling has substantially improved the representation of the IAM in climate model simulations [55, 66–68]. Significant challenges remain, especially simulating Himalayan Water Tower [Xu et al., 2014] or extreme orographic precipitation across the HM where model-data disagreement increases toward higher elevation [61].

The subject of our study is the onshore flow of moisture into the Indo-Gangetic Plain (IGP), Ganges Basin (GB) and the HM (Fig 1 plot a). Since the monsoon field

has placed little emphasis on elucidating the phenomenology and dynamics of the northeastern IAM branch [57], we demonstrate the existence of an easterly low-level jet (LLJ) over the IGP (referred to as the IG LLJ) during peak monsoon season. The reanalysis products, model experiments and diagnostics used for the study are described in section 2. Section 3 characterizes the easterly monsoon flow using various reanalysis products, provides the mechanism for the IG LLJ primarily using the National Center for Atmospheric Research (NCAR) AGCM, and briefly considers the AGCMs found in the Coupled Model Intercomparison Project phase 5 (CMIP5) archive. Section 4 discusses the broader implications of our work and gives concluding remarks.

2.2 Methods

The analysis presented in this study focuses on peak monsoon months July and August or otherwise noted. We use three reanalysis products for this study: (1) the European Centre of Medium-Range Forecast Interim reanalysis (ERAI) at 0.70 (1°) resolution [69], the Japanese Reanalysis year 55 (JRA55) at 0.50 (1/2°) [70] and High Asia Reanalysis (HAR) at 0.28 (1/4°) [71]. The reanalysis products are based on ten seasonal averaged years. For ERAI, JRA55, and HAR we used years 2001-2010.

The primary model used in our study is the NCAR AGCM, Community Atmospheric Model version 4 (CAM4) [46, 50, 51, 72]. We also provide results from CAM5 (S1) [73]. We focus on CAM because it has been heavily used in theoretical [74, 75], idealized [76, 77], and paleoclimate studies [31, 49]. Additionally, the NCAR CAM physics schemes have been ported to several other climate models such as GENESIS [78] and FOAM [79]. For detail on the NCAR CAM models, see supplementary section 1. Simulations are carried out on various model resolutions from low 1.9x 2.5 (2 to high 0.23x 0.31 (1/4 (S1). These simulations are equivalent to 200 km and 25 km grid spacing over the equator. As indicated by Shields et al., [2016], at above 1/2 resolution, GCMs are able to represent features such as tropical lows and

cyclones, which are important for intraseasonal tropical depressions forming over the Bay of Bengal (BOB). Several studies suggest that the added accurate topography is a large driver for the improvements seen in higher resolution simulations [68]; thus, we performed a Hybrid simulation where we regridded the topographic boundary condition from the 2 model and used it in the 1/4° model. Our goal is to distinguish if better-resolved topography or horizontal dynamics are more important for simulating the IAM. Detailed information about the observations and models utilized in this analysis are listed in published version.

As a first order validation for the reanalysis products and the CAM models used in our assessment, we compare our results to a 1/2° rain gauge dataset (averaged over 1998-2007), Asian Precipitation Highly-Resolved Observational Data Integration Towards Evaluation of Water Resources (APHRODITE) and a 1/4° resolution satellite based observation (averaged over 2001-2010) Tropical Rain Measuring Mission (TRMM) 3B42/3B43 [80,81]. Similarly to the Intergovermental Panel on Climate Change 5th assessment report [82], we quantitatively evaluate simulated orographic rainfall over the HM and GB (Fig. 2.1 plot (b) denoted by the purple box) using the Pearson Correlation Coefficient (PCC). Our correlations are based on the mean of APHRODITE and TRMM.

To investigate the dynamics behind the IG LLJ, we use near surface equivalent potential temperature (θ_e) as a diagnostic for evaluating monsoon mechanisms in a moist static energy framework [16, 45], and near surface geopotential height to determine the location of the monsoon low [83]. We also use the total diabatic heating [30] and the moist Froude number (as diagnostic tools for flow over topography [8] . To calculate the , we used constant meridional flow (v = 5 m/s), mountain height (h = 5km) and the saturated Brunt-Visl Frequency [8, 9, 84] (see Supplementary). For flows over the HM, we highlight two distinct dynamical regimes. As shown by Reeves and Lin [2007], when a negative layer above topography is observed, latent heat is strong, and the is negative. As a result, the statically unstable layer allows moisture to flow over the terrain (i.e. unblocked). In contrast, a strongly positive represents

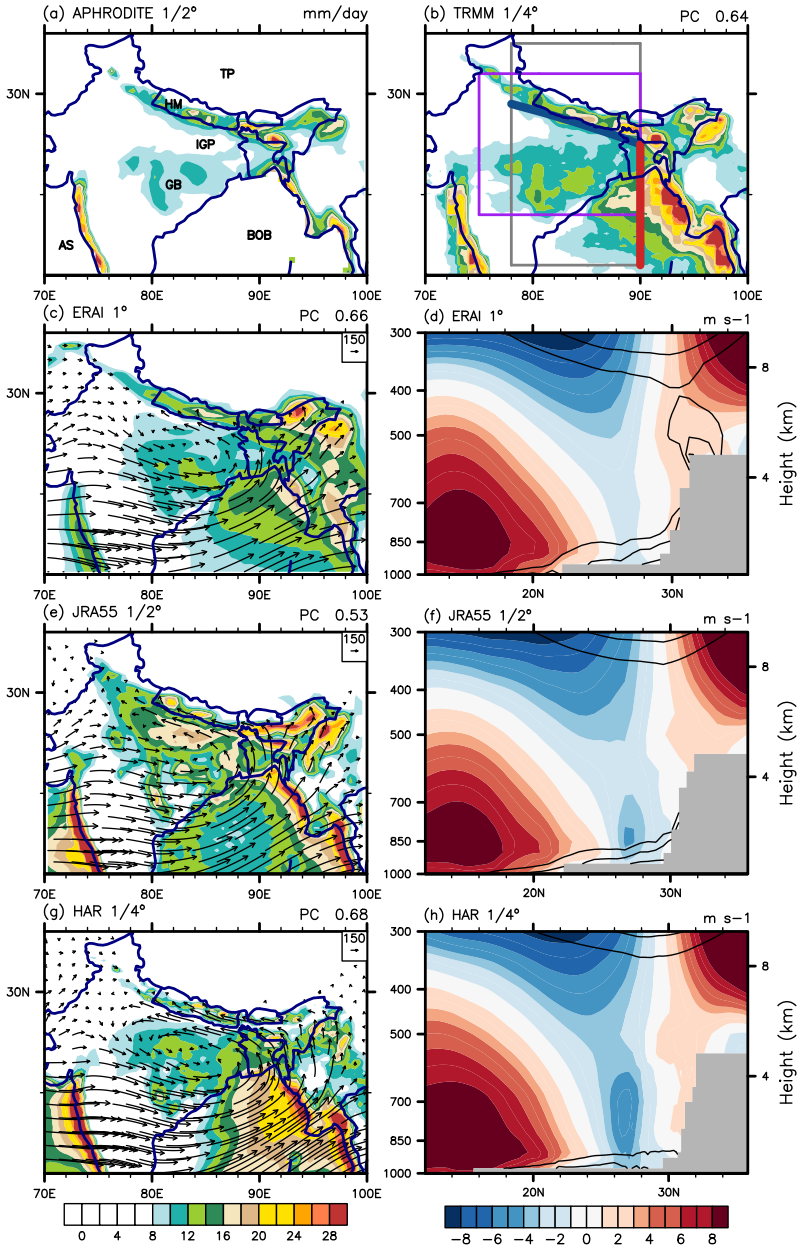

Fig. 2.1. Total precipitation (mm/day) averaged from July and August (a) APHRODITE, (b) TRMM, (c) ERAI, (e) JRA55, (g) HAR. Vertically integrated moisture flux vectors from 1000 to 600 mb. The PCC between precipitation observations and models presented above are calculated over the purple box in plot (b). plots (d, f, and h) are the respective vertical profiles of zonal winds (m/s) zonally averaged over the region indicated by the gray box in plot (b) for the products. The blue colors south of 30N represent the IG LLJ, while gray outlines demarcate area with topography. Black contours, represents maximum surface (ranging from 350-356 K). Labels on the plot (a) is as follows Himalayan Mountains (HM) and Tibetan Plateau (TP), Indo-Gangetic Plain (IGP), Ganges Basin (GB), Himachal Pradesh (HP), Arunachal Pradesh (AP), Western Ghats (WG), Bay of Bengal (BOB), Arabian Sea (AS). The red and blue thick lines in plot

a stable layer which then caps the near surface flow from rising over the terrain (i.e. blocked) [85, 86]. A typical outcome of a blocked flow is a terrain-parallel barrier jet [87].

To simplify comparison of various reanalysis products, CAM simulations (S1) and AGCMs from the CMIP5 archive (S2), we created an index that highlights the southerly-then-easterly flows relevant in this study (Fig. 2.1a red and blue transects) (referred to as the Bengal-Gangetic moisture flux (BGMF) index). The BGMF index uses the average strength of meridional integrated moisture flux across a latitudinal transect 14N to 25N (red-line on Fig. 2.1 plot (a)) and the average strength of zonal integrated moisture flux across longitudinal transect 76°E to 85°E (blue-line on Fig. 2.1 plot (a)). We placed all three-reanalysis products at the top to illustrate how the observational products are performing. We normalized the calculated BGMF index value by dividing the resulting $BGMF_{model}$ value by the average $BGMF_{reanalysis}$ value as shown in Supplementary.

2.3 Results

2.3.1 Observations

Our emphasis for this section is to characterize the nature of the moisture flux over the IGP through various reanalysis products and to demonstrate that this flow is a part of the mean monsoon circulation. The comparisons between the reanalysis products and observational datasets demonstrate that the total precipitation across various regions has some qualitatively similar features. In terms of precipitation rate magnitude, compared to observation, ERAI and HAR capture the precipitation distribution across the GB better than the JRA55. Out of the three reanalysis products, the JRA55 has the lowest precipitation PCC. Nevertheless, the PCC values for all three reanalysis products are in a narrow positive range of 0.5-0.7 (Fig. 2.1 plot b,c,e, and g top-right corner). This consistency in precipitation patterns across the prod-

ucts and observed precipitation rates gives us confidence that the regional circulation is robust.

Vertically integrated moisture flux from the reanalysis products shows strong southerly onshore moisture flow from BOB into the HM. This flux of moisture then veers easterly into the IGP. Both JRA55 and HAR has a stronger east-west flow along the IGP than ERAI (Fig. 2.1e-g). The flow magnitude is potentially due to the required horizontal resolution. Regardless of flow strength, all three reanalysis products simulate a strong cyclonic feature over the GB, which represents recirculation of moisture. To show that the cyclonic flow over the Ganges Basin and IG LLJ does not reflect the mean of many transient events and a mean flow persists, we decompose the total moisture flux over the region for the JRA55 during July and August (S2.8) and show the temporal monthly distribution of zonal winds over the IGP transect (blue line in Fig. 2.1 plot (a)) from May-September (S2.9). We briefly evaluate the possibility that the easterly flow is induced by changes in diurnal heating over topographic slopes [88] , and show four-times daily output of the zonally averaged winds for JRA55 (S2.9).

We show the zonally averaged zonal winds across the region (Fig. 2.2 plots d, f, and h, averaged over the gray box in the plot b). All three reanalysis products illustrate strong easterly flow. However, the well-defined core near 25°N, which is simulated by both the JRA55 and the HAR, is not captured by ERAI. Our results suggest the vigorousness of the IG LLJ is potentially resolution dependent. We test if increasing horizontal-resolution impacts the formation of the IG LLJ in the NCAR CAM models.

2.3.2 CAM

The low-resolution version of CAM4 produces excessive precipitation over the Himalayan foothills and lacks precipitation over the GB and IGP, which is reflected by the low PCC value. The easterly flow and the cyclonic circulation are not resolved

by low-resolution versions of CAM4 (Fig. 2.2a). The simulated precipitation rates across IAM in the 1/4° CAM4 and the Hybrid model are overall improved. Quantitatively, the 1/4° CAM4 model lies within the same PCC range as the reanalysis products (Fig. 2.2c). Although circulation is well represented in the Hybrid simulation, the spatial distribution of precipitation demonstrates resolving topography influences precipitation patterns (Fig. 2.2e).

The low-resolution version CAM4 models show that the dominant moisture transport across the IGP originates from the Arabian Sea (Fig. 2.2a) and ignores the east-west moisture transport. In contrast, 1/4° CAM4 displays a similar flow pattern to the reanalysis products and it can simulate the easterly flow of moisture flux along the IGP (Fig. 2.2 c). The 1/2° CAM4 model begins to capture the easterly flow and is fully formed at a 1/4° (S2.6), suggesting that the easterly IG moisture flux is resolution dependent in CAM. This dependence is evident in our hybrid simulation, where the easterly flow persists without the well-resolved topographic boundary condition (Fig. 2.2e). We note that the standard CAM4 1/4° and the Hybrid simulations extend the easterly flow well into the India-Pakistan Border, which is not consistent with the reanalysis products.

From the vertical profiles (Fig. 2.2 plot b, d, and f), the low-resolution CAM4 simulates the southwesterly monsoon winds extending toward the center portion of the HM. In contrast, we see that the 1/4° CAM4 model simulates an easterly wind with a fully formed core. The Hybrid simulation represents some aspects of both the high and low-resolution CAM models. Although it is well documented that high-resolution topography [68] improves the IAM circulation, our Hybrid simulation demonstrates that improvements in dynamics due to increased horizontal resolution are important for modeling the northeastern IAM branch.

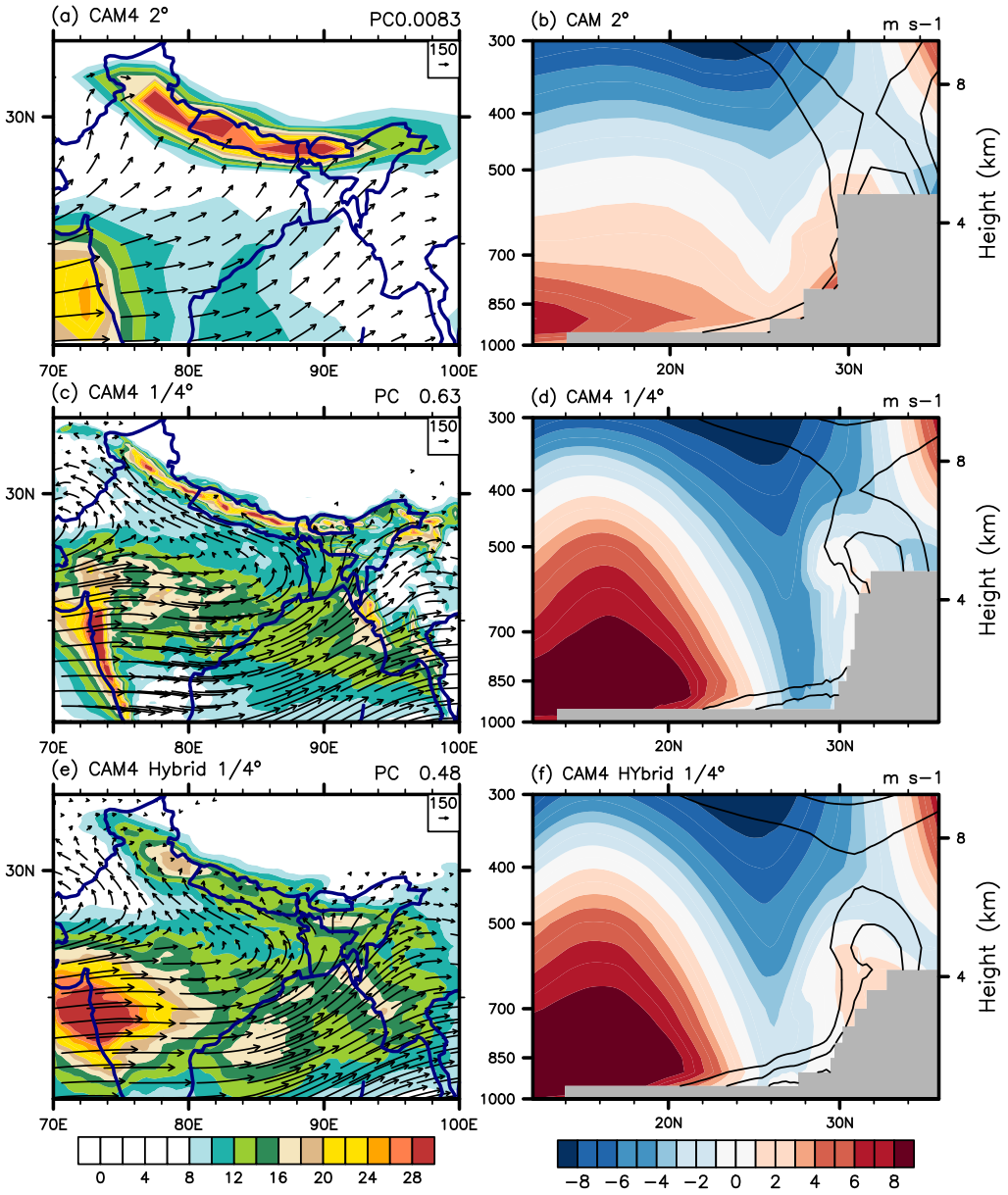

Fig. 2.2. Similar to figure 1 with (a and b) CAM4 2°, (c and d) CAM4 1/4°, and (e and d) Hybrid simulation

2.3.3 Mechanics behind the IG LLJ

The monsoon low is governed by a seasonally persistent thermal heating across the northern Indian subcontinent which is accompanied by a near-surface, stationary cyclonic circulation [83]. For this section, we show how the various CAM4 models simulate the persistent low-pressure system and maximum 850 mb surfaces. Because the HAR model simulates a similar circulation to that produced in the global reanalysis products, we consider it representative and the comparison robust (Fig. 2.3 left-hand panel). Across the CAM4 results, a strong 850 mb surface is over the entire northern Indian subcontinent, with its maxima centered on the Indian-Pakistan border. However, in HAR, the maximum is centered over the Ganges Basin and does not extend toward the Indian-Pakistan Border. Simulated surface geopotential heights across the CAM4 simulations are improved as you move toward higher resolutions, where the cyclonic circulation is more centered over the Ganges Basin (Fig. 2.3 black contours, left-hand panel plots). We find that simulating the seasonally persistent monsoon low is crucial for forming the IG LLJ. To evaluate if the cyclonic flow over the Ganges Basin and easterly LLJ are not primarily driven by transient events, we decompose the total moisture flux over the region (S2.8).

Here we investigate how the CAM models simulate flow over or around the topography. In figure 2.3, the negative are arbitrary values that represent regions dominated by moist instability, and in contrast, positive values are statically stable layers (Fig. 2.3 right-hand panel plots). Across our CAM4 simulations, we show that the layer of neutral buoyancy is located at 700 mb (Fig. 2.3 right panel, white layer) and moves up near the HM. Focusing on the front of the HM, the 2° CAM4 model readily extends the unstable layer over the HM (Fig. 2.3 plot (b), blue layer). Alternatively, the 1/4° CAM4 model completely cuts off the near surface unstable layer from reaching the atmosphere aloft (Fig. 2.3 plot (d)). Interestingly, the Hybrid model simulation has both aspects of the low and high-resolution model. It readily moves the unstable

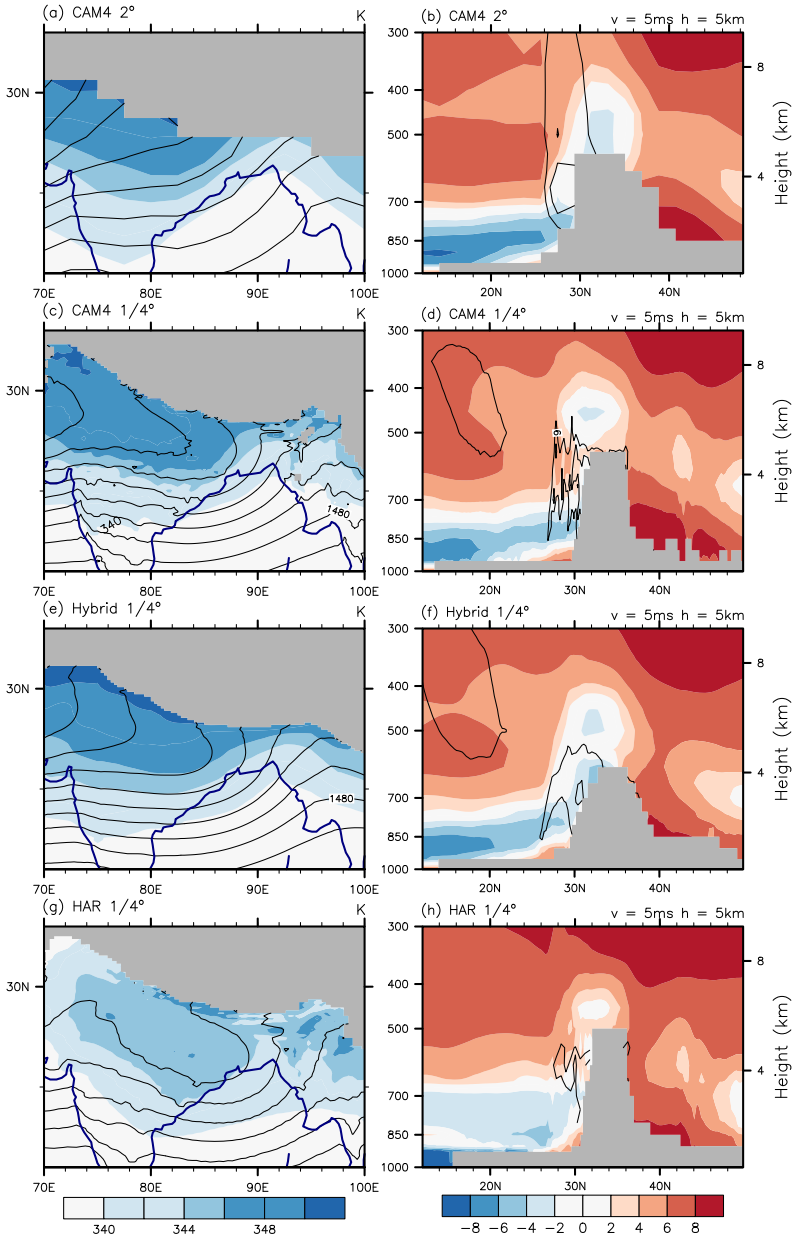

Fig. 2.3. Left-hand panel shows Equivalent potential temperature surfaces, and black contour with geopotential height (1400-1500 m) at 850 mb. Right hand panel shows vertical profile of , overlain with diabatic heating (6-12 K/day) in black contour. Plot is in order (a and b) CAM4 2°, (c and d) CAM4 1/4°, (e and f) Hybrid, and (g and h) HAR 1/4°. Variables are derived from June, July, and August climatology.

layer over the mountain but produces a neutral layer above the mountain top. We identify that a well-defined terrain is crucial to producing a blocked flow.

We suspect that strong orographic diabatic heating is playing a role in our CAM simulations (Fig. 3 black contours, right-hand panel plots). We show that an overly strong diabatic heating extending above 300 mbis simulated in our model. (Fig. 3 b). In contrast, both the 1/4° CAM4 and Hybrid model simulated diabatic heating closer toward the overlying surface and does not extend above 300 mb (Fig. 2.3 d and f). Since heating tendencies are unavailable for the HAR product, we utilize available diabatic heating rates from JRA55 (contour overlay in Fig. 2.3 plot (h)). Orographic diabatic heating rates in JRA55 are simulated near the Himalayan slopes and do not extend as high up as the CAM4 2 model.

2.3.4 CMIP5 Models

The goal of this section is to demonstrate how AGCMs from the CMIP5 archive simulate the northern IAM sector. We present results from our BGMF index and precipitation PCC (Fig. 4). For reference, see figure 2.1 plot (b) for the transects and area where PCC was applied. For detailed information on BGMF index see section 2 and Supplementary section 3. Briefly, we use the reanalysis products found in Fig. 2.1 to demonstrate how the AGCMs should simulate the precipitation and flow along the IGP. For example, all three products show a positive (red) meridional moisture flux from BOB into HM, then a negative (blue) zonal moisture flux along the IGP. Thus, we should expect strong positive values for the left-hand side and strong negative values for the right-hand side of the plot from the AGCMs.

Figure 2.4 shows that many AGCMs poorly capture the strong southerly moisture flux across BOB and do not simulate the easterly flow across the IGP. Alternatively, based on our index, some models even produce a strong westerly flow across IGP (Fig. 2.4). The precipitation PCC values widely vary across the AGCMs presented here, and requires further analysis. Nonetheless, we conclude that properly simulating the northeastern IAM branch requires capturing both the easterly IGP moisture flux and

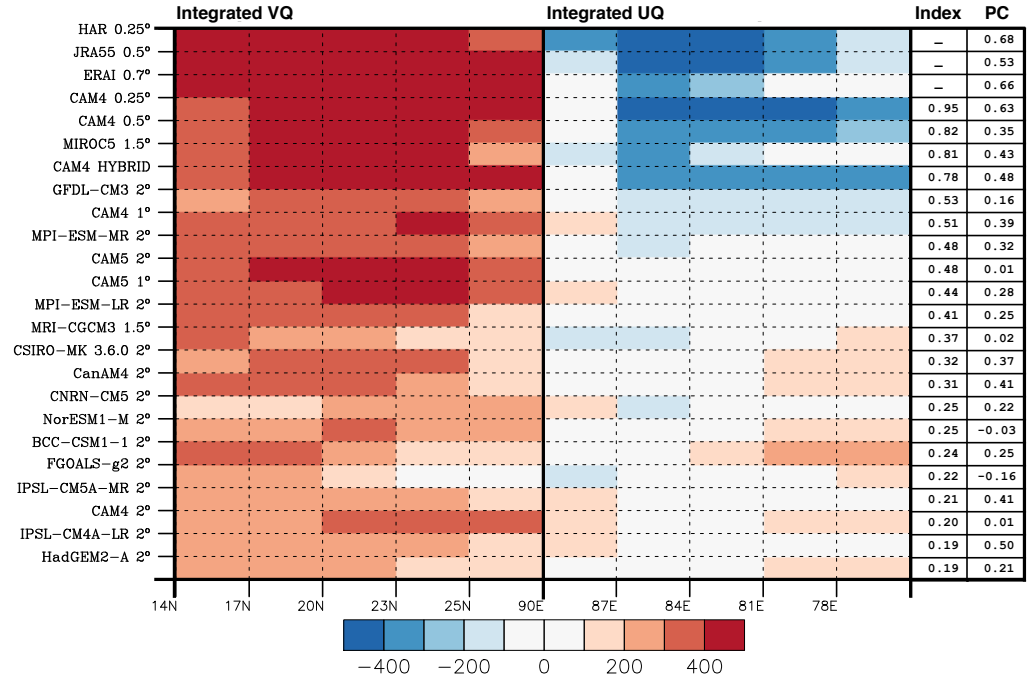

Fig. 2.4. Bengal-Gangetic moisture flux index. The order of various reanalysis products, CAM model resolutions, and CMIP 5 models was determined by using a flux index described in supplementary. The left-hand side represents the average meridional integrated moisture flux over red polyline in Fig. 1a. The right-hand side represents average July-August zonal integrated moisture flux over blue polyline in Fig. 1a. The values from the normalized BGMF index are shown on the 3rd column. The PCC values over topography (purple box in figure 2.1 plot (a)) between various results and observations are shown on 4th column.

a strongly positive precipitation PCC. From our brief analysis, most AGCMs in the CMIP5 archive poorly simulate the northeastern IAM branch.

2.4 Discussion and Conclusion

It is evident that vigorous moisture transport over the IGP exists in global and regional high resolution reanalysis simulations during peak monsoon season [57], which suggests that there is a crucial flow that is understudied in the region. The influx of moisture from the BOB into the IGP has long been recognized as a part of easterly propagating tropical depressions associated with advancement and retreat of monsoon trough [58, 89–93]. However, here we demonstrate that much of the time this should be thought of as a topographic barrier jet.

We highlight that the IG LLJ is distinct from the southwesterly monsoon jet. We also identify that the major supplier of moisture across the IGP and Himalayan foothills is by the mean flow, which persists throughout the monsoon season and is strongest during July and August. The reanalysis products and the high-resolution CAM4 simulations show that increasing the horizontal resolution tends to better reproduce the easterly flow and precipitation pattern across the northeastern sector of the IAM. In contrast, based on our BGMF index, most of the climate models from the CMIP5 archive, which tend to have a coarser resolution, do not capture the easterly flow across the IGP, and the cyclonic flow over the Ganges Basin. Misrepresentation of this circulation is problematic for interpreting future projections. Addressing how precipitation in the Himalayas will behave in the future, including its possible tipping points [75,94,95], is beyond the scope of this paper. Nevertheless, it may require fully resolving the LLJ identified here, because this is the primary flow that transports water vapor into the region. We conjecture that because of the role of moist static stability and blocking in the region, moisture flux over the central HM most likely exhibits a bimodal behavior [58]. Therefore, this branch of the IAM may exhibit

tipping behavior [95]. Considering this process is only captured at high-resolution versions of CAM, it will not have revealed itself in prior analysis [75].

Better representation of topography was alluded to as the solution for the observed improvements in simulating the IAM [55, 68, 96]. We demonstrated with our Hybrid simulation that increasing horizontal resolution is important as increasing topography resolution when modeling the northeastern IAM branch. This is further highlighted when simulating the monsoon low over the Ganges basin. Additionally, analysis by Mishra [61] on various regional climate models agrees with this conclusion. Although the height and geometry of the topography impact the flow over the terrain, we speculate that the production of excessive orographic diabatic heating in CAM is modulated by the adjustments in convective and large-scale parameterizations [97]. Additionally, the mediating role of moist static stability over the Himalayas may also explain some of the inter-model difference in monsoon behavior, since different physics schemes may change the degree of blocking and flow over topography. We are aware that coupled atmosphere-ocean modeling was suggested to improve simulated representation of the IAM; however, from our previous work [31], and from a more recent study using 1/2° CAM4 model [68], we believe that increasing the atmosphere horizontal resolution is more important for the IAM than adding the coupled system.

From our CAM simulations, we find that poorly resolving topography enables the constant flow of statically unstable moist layer over the HM, while not resolving the monsoon low and excessive production of orographic diabatic heating disables the formation of the IG LLJ. This unblocked mode simulated by the CAM4 and 5 models has serious implications for studies that suggest the IAM is triggered, driven or maintained by orographic heating [22,31,98,99]. If so, then perhaps theories regarding orographic surface heating should be revisited using higher resolution models [67,100] and the diagnostics applied here.

2.5 Acknowledgments

The authors would like to thank the anonymous reviewers, Dr. Rodrigo Caballero, Dr. Richard Rotunno, Dr. Richard Neale, and the members of the Climate Dynamics Prediction Laboratory whose insightful comments and discussions greatly improved the manuscript. This research was supported by the University of New Hampshire NSF EPSCoR grant, (NSFEPS1101245), NSF Grant (EAR-1049921) and Purdue University. We appreciate the CISL Data Support Section at the NCAR (NSFEAR114504), for providing data for ERAI and JRA55, and TUB Chair of Climatology for the HAR simulation. For their roles in producing, coordinating, and making available the CMIP5 model output, we acknowledge the climate modeling groups listed in this paper, the World Climate Research Program's Working Group on Coupled Modeling, and the Global Organization for Earth System Science Portals. The data used in this manuscript are listed in the supplementary table, and references. We are grateful for the CISL NCAR Command Language and Data Support group for aiding with interpolating the various data sets provided in this literature. We acknowledge the Information Technology at Purdue University for providing computational support.

2.6 Supplementary: BGMF Index

We analyze moisture flux across the Indo-Asia during peak summer monsoon season. Additionally, as noted by Walker et al., [101] moisture flux as index incorporates and constrains both precipitation intensity and strength of monsoonal circulation, which they found more robust than using other winds shear indices. Here we relate the moisture budget to the mean vertically integrated moist flux (right-hand side) to net change in precipitation (left-hand side), similarly to Curio et al., [57], Walker et al., [101]. See Chapter 1 for moisture flux calculation.

The Bengal-Gangetic moisture flux index was determined by taking the difference between the mean integrated meridional flux across a transect over the Bay of Bengal

(BOB) and mean integrated zonal moisture flux across the IGP (represented by the red and blue line in Fig 2.1a.) as shown below.

$$BGMFindex = \int (Vq_{bob}) - \int (Uq_{IGP}) \tag{2.1}$$

Poleward transport from the Indian ocean into the Asian continent is well understood and should result in a positive meridional transport. Additionally, the dominant flow across the region is the propagation of westerly winds from the cross-equatorial Somalia Jet, however, since the zonal moisture flux across the IGP is negative, the difference should move toward a positive magnitude. To apply our index to the climate models presented in our analysis, we normalize the BGIMF values of GCMs by dividing by mean BGMF of the reanalysis products as shown below.

$$BGMFIndexNormalize = \frac{BGMF_{model}}{BGMF_{reanalysis}} \tag{2.2}$$

Models that are not properly simulating such east-west transport will lead to a lower index value.

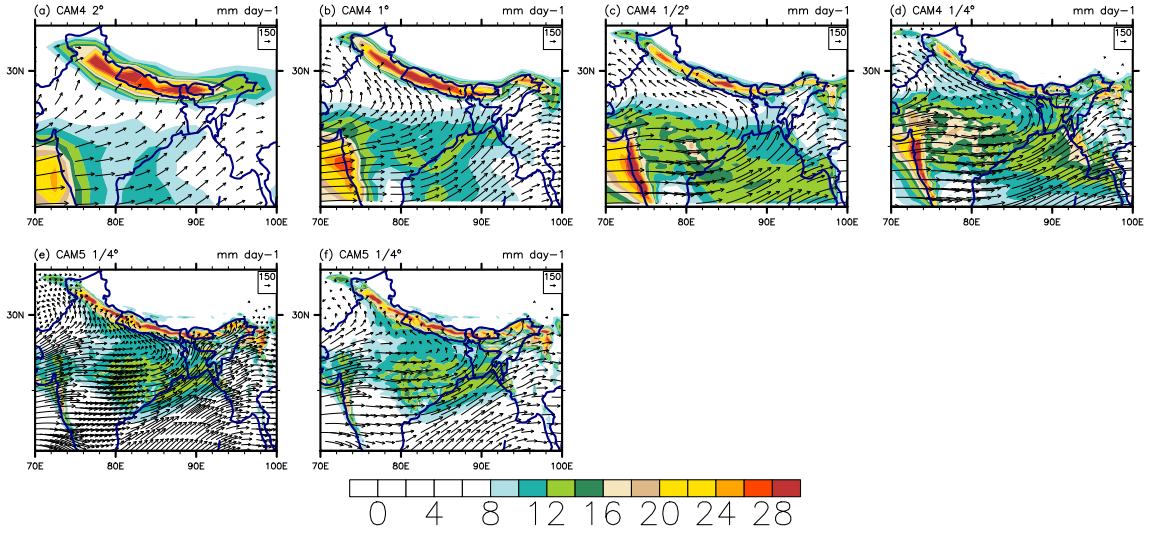

Fig. 2.5. Total precipitation (mm/day) averaged from July and August for the various resolutions of CAM 4 and 5 models. Integrated moisture flux vectors from 1000 to 600 mb

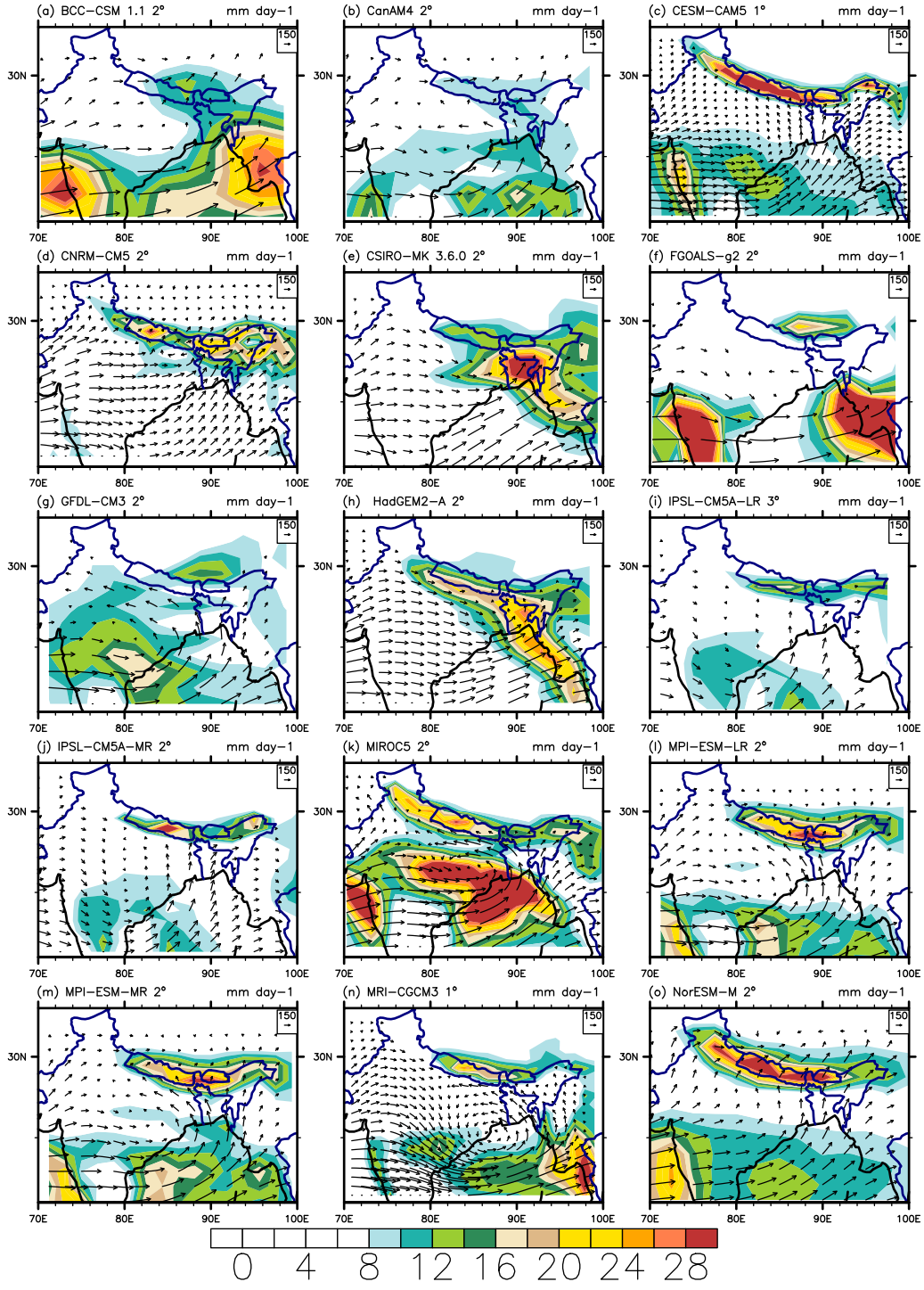

Fig. 2.6. Same as Fig. 2.5 except for the various resolutions of CMIP5 models.

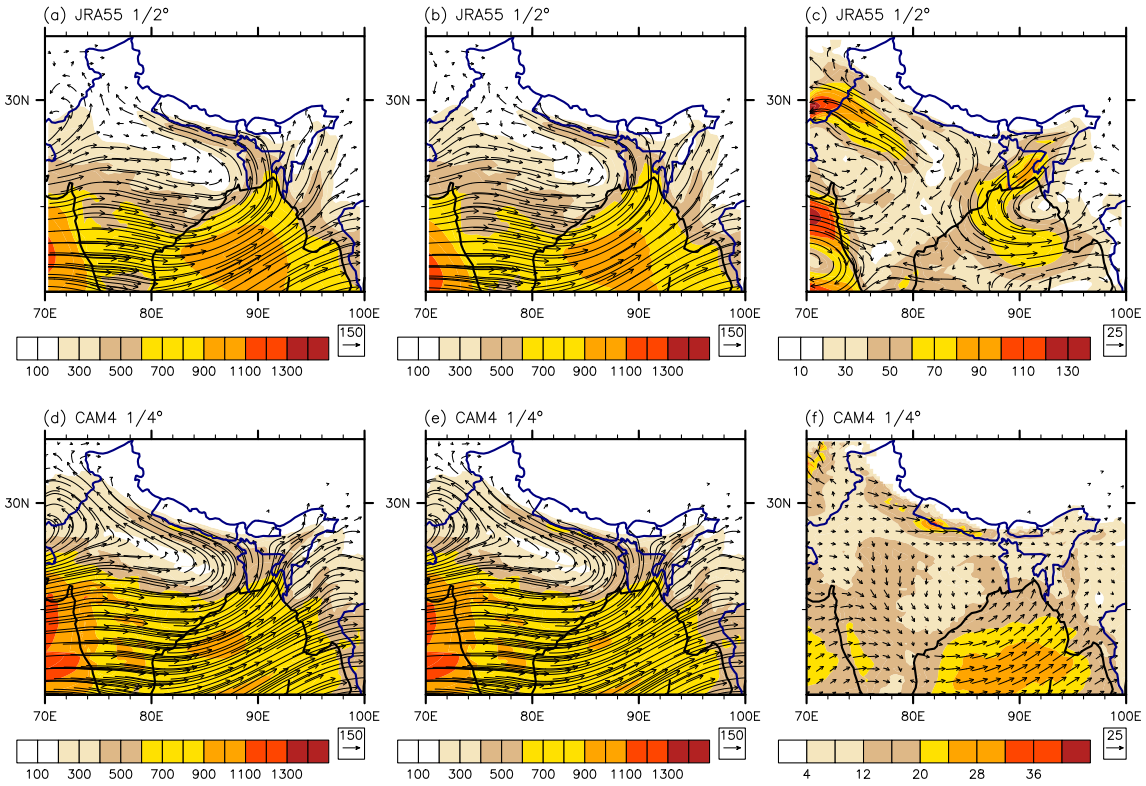

Fig. 2.7. Peak monsoon season vertically integrated moisture flux (kg m-1 -s1) from 1000-600mb. Color shade denotes strength and length of arrow is proportional to flux magnitude. Plot (a and d) shows the total $\bar{UQ}$, plot (b and e) are the mean flux $\bar{U}\bar{Q}$and plot (c and f) is the residual representing the calculated transient vertically integrated moisture flux $\bar{U'Q'}$.

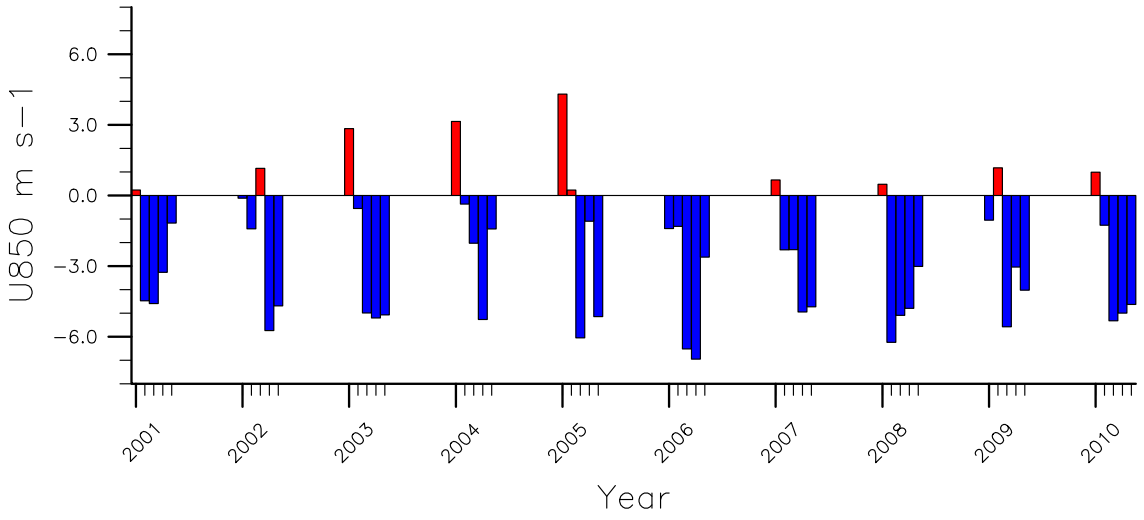

Fig. 2.8. MJJAS temporal distribution during 2001-2010 of Mean U850 calculated over the blue line in figure 1 plot(a). Red represent westerly, while blue shows easterly winds.

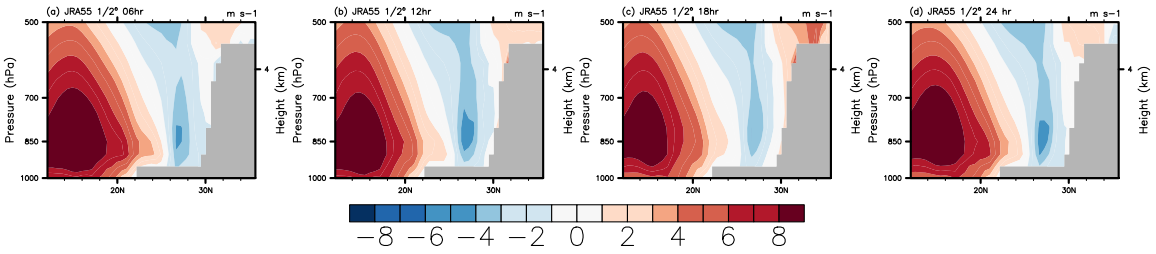

Fig. 2.9. Vertical profile of regional zonal winds as in Fig. 2.1 Plots presented represents JA averaged four times daily output for JRA55

3. OROGRAPHIC FORCING: A DIABATIC HEATING PERSPECTIVE

(Major aspects of this chapter is published and available in GRL:
Acosta, R. P., and M. Huber (2017), The neglected Indo-Gangetic Plains low-level jet and its importance for moisture transport and precipitation during the peak summer monsoon, Geophys. Res. Lett.)

3.1 Background

Atmospheric general circulation models (AGCMs) have long standing difficulty properly simulating the Indo-Asian Monsoon (IAM) [46, 47] and monsoon processes in general, which is not surprising given their persistent tendency to misrepresent the annual migration of the Intertropical Convergence Zone (ITCZ) toward Southern Asia [48]. Nevertheless, AGCMs have been used for decades as the best tool to improve our understanding about the interaction between Asian monsoon dynamics and its connection to topography. Seminal work linked the formation of the modern summer IAM to the uplift of the Himalayan Mountains and Tibetan Plateau (HMTP) [2, 23] and much subsequent work has revealed various topographic mechanisms and processes that are important to the IAM [14, 22, 31, 77, 102–105].

The models developed by National Center for Atmospheric Research (NCAR) has been prominently featured in both idealized [15, 38, 76] and paleoclimate [4, 31, 49] studies of interaction between topography and monsoons. The NCAR AGCM physics has also been ported to form the basis of other AGCMs, such as in GENESIS, FOAM, and FGOALS, which are some of the most widely used models in paleoclimate dynamics. As a consequence of the near ubiquitous representation of the NCAR AGCMs physics in idealized and paleoclimate, systematic biases in this representation

may have an outsized influence on conceptions of monsoon dynamics and engender a false confidence in the robustness of simulation results. As described below, we find that a specific feature of the IAM in the NCAR AGCMs, and others is systematically biased and consequently that one of the many of competing theories of the monsoon may have a weaker basis than commonly interpreted.

As summarized in Wu et al. [2007], Nie et al., [2010], Molnar et al., [2010] and Zhisheng et al., [2015] [7, 28, 45, 105, 106] various mechanisms for this monsoon have been proposed: some of which emphasize the role of heating and the formation of a land-sea breeze initialized by surface heating over the front range of the HMTP [13, 14, 27, 28, 76] , while others focus on the maximum boundary layer moist static energy found over Northern India [37, 107], which sets-up the poleward extent of meridional overturning circulation or Hadley-cell like feature [16, 45]. It is generally the case that once a summer IAM-like circulation has initiated, most studies emphasize the role of deep diabatic heating [31, 77, 108] and its association with vertical velocities [21, 36], upper-level divergence [62], and low-level convergence [42]. While basic physical reasoning demands that deep diabatic heating over the HMTP can maintain the IAM, it remains controversial whether it actually drives the monsoon circulation. The strong precipitation-driven deep (extending above 500 hPa) diabatic heating centered over topography-sometimes called, the candle- has become a key target for understanding the response of climate models to changing HMTP topography. Understanding the location, depth and strength of this feature is important, since it can be linked directly to the various theoretical underpinnings of monsoon dynamics. Despite the fact that this feature has been heavily interpreted in simulations [76, 109], no studies ascertained whether it is a real feature of the atmosphere in the IAM region.

Nonetheless, this strong thermal forcing is predicated upon a constant supply of moisture from the nearby body of waters, whereby, strong moisture flux from the equator to the poles is key to understanding the maximum poleward extension of the IAM [110]. As previously shown by Curio et al., [2016], various reanalysis products

suggests that majority of moisture flux across the Himalayan mountains is drawn from the Bay of Bengal. While it is the case for the high-resolution version of CAM, CAM at 2 and 1 has moisture flux originating from the Arabian Sea. While observations shows deep convection is prevalent across the Western Himalayas it maybe the case that CAM at low-resolution produces excess deep convection over the region.

3.2 Observations and Reanalysis

In this study, we use physical observations from various sources such as Global Precipitation Climatology Project (GPCP) at 2° resolution [111], Asian Precipitation-Highly Resolved Observational Data Integration Towards Evaluation of Water Resources (APHRODITE) at 0.5° resolution [81] and Tropical Rainfall Measuring Mission version 7 (Product 3B43) at 0.25° resolution [112] (Fig. 3.1 a-c). Additionally, we incorporate reanalysis products, which are simulated observations optimized by various observed quantities such as winds, temperature and mixing ratio. The reanalysis product used in this study include Modern Era Retrospective-analysis for Research and Applications (MERRA) at 1 resolution [113], the European Centre of Medium-Range Forecast Interim reanalysis (ERA-I) at 0.70° resolution [Dee et al., 2011] [69], and Japanese 55-year Reanalysis (JRA55) at resolution [70] (Fig. 3.1 d-f). For moisture transport, we used the method from Curio et al., [2015] and compare our results to observation products ERAI and JRA55. For diabatic heating we use MERRA and JRA55 and divide the Indo-Asia monsoon region into two, an eastern portion zonally averaged over 88E-98E (BB) (highlighted as a red outline in Fig. 3.1b), and a western half zonally averaged over 74E-88E (HK) (highlighted as a black outline in Fig. 3.1b). Measurements of total diabatic heating in the atmosphere are difficult to obtain [114]. Since direct observations of global diabatic heating are lacking, data assimilation products are currently the best way to validate global scale, vertical structure of diabatic heating. Detailed calculations of diabatic heating in various modern reanalysis products are presented in Ling and Zhang [2013] and Wright

and Fueglistaler [2013]. Reanalysis products also contains biases, specifically in the tropical region [29, 30, 115] hence we use multiple reanalysis products: MERRA and JRA55. Reanalysis output, precipitation data sets and models were regridded for the sake of comparison.

3.3 Further Analysis

3.3.1 General Monsoon Precipitation and Wind Distribution

We evaluate how the family of CAM models simulate peak summer (June, July, August) monsoon characteristics by comparing total precipitation rate and low-level (850 mb) winds against observations: GPCP, APHRODITE and TRMM (Fig. 3.1 a-c), and reanalysis products: MERRA, ERAI and JRA55 (Fig. 2.10 d-f). We primarily emphasize on CAM version 4 (Fig. 3.1g), but include results from CAM5 (Fig. 3.1h) and SPCAM4 and SPCAM5 (Fig. 3.1h). Additionally, we provide context to CAM sensitivity to resolution by simulating CAM4 at various resolution and a hybrid simulation, where the 1/4 topography is replaced with 2topographic boundary condition (Fig. 3.1k and 3.1l).

Similarly to Cash et al., [2015], we divide the Indo-Asian into multiple subsections: Bay of Bengal (BoB), Bhutan-Bangladesh (BB), Ganges basin (GB), Western Ghats (WG) and Himachal-Kashmir (HK) as indicated in Fig. 3.1a. Analysis of the observed total precipitation suggests resolving rainfall at a higher spatial resolution has a major impact on the magnitude of precipitation over a region but a minor influence on the spatial distribution. For instance, comparison between GPCP and TRMM illustrate that precipitation maxima exist over the BoB, BB and WG when looking at GPCP, however, precipitation maxima over regions of high topography such as the central Himalayan Mountains and Western Ghats Mountains, are only characterized as spatial resolution are increased. The importance of resolution is corroborated by ground observations from APHRODITE (Fig. 3.1b). The spatial distribution of to-

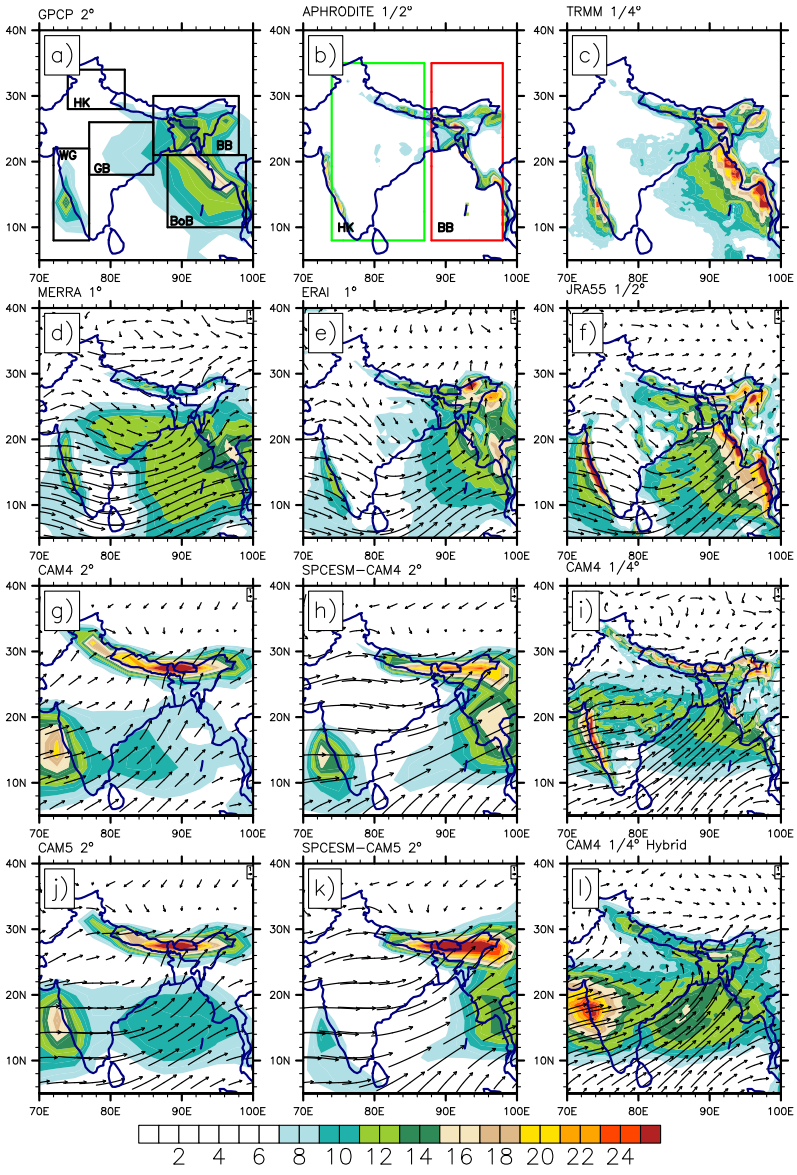

Fig. 3.1. Average summer (MJJAS) total precipitation rate (mm day-1). Panels (a)-(c) display observations: GPCP, APHRODITE, and TRMM. (d)-(f) show reanalysis products MERRA, ERAI and JRA55. Plots (g, h, j and k) illustrate CAM4 simulations 2° for CAM4, CAM5 and SPCAM. Plots (i) shows the highest model resolution, 1/4° and l° shows the hybrid simulation. Boxes on plot (a) are used to define regions of interest for rainfall analysis and plot (b) illustrates region of interest for diabatic heating.

tal precipitation rate across reanalysis products vary, however common patterns arise regardless of spatial resolution [116]. Rainfall magnitude and distribution over the Ganges Basin and large parts of Bay of Bengal spatially differ and are biased compared to observations. In contrast, regions of complex terrain are better captured by ERAI and JRA55 than MERRA when compared to TRMM and APHRODITE.

Precipitation maxima in the CAM4, 2 model is distinctly separated between two latitudinal regions, the Himalayan Ranges and Indo-gangetic plains which is primarily located toward the continental interior at 30 N and Southern coastal reagions at 15° N (Fig. 3.1g). Strongest simulated precipitation is located primarily on the foothills of the Himalayas or at northern part of BB region. Compared to observation and reanalysis product, simulated rainfall rates over the eastern parts of Bay of Bengal and Bangladesh are substantially weaker. Additionally, although precipitation rates over the HK does appear in observations during July (not shown), CAM4 consistently over estimates rainfall over this region as well as the greater western half of the Himalayan Mountains when compared to observations. These results are similar for CAM5 model and suggested that added cloud micro-physics schemes have minimal influence on the simulated monsoon precipitation (Fig. 3.1j). As the CAM model steps away from convective and large-scale parameterization (SPCAM), the model at the same resolution begins to simulate precipitation over BoB and BB (Fig. 3.1h and 3.1k). Additionally, average precipitation over HK region is minimal, which is much closer to observations. However, orographic precipitation across the BB are over simulated and has a biased magnitude compared to observations and reanalysis.

The SPCAM5 model has a similar spatial pattern as SPCAM4, but orographic precipitation over Bhutan are exacerbated, while rain rates over WG become weaker (Fig. 3.1j). Simulations with the CRM model, suggest that the convective and large-scale precipitation schemes are partly to blame for the behavior of the model [117], which will be explored in subsequent section. As we increase model resolution to 1/4°, the spatial distribution of precipitation rates across BB, and WG are more similar to high resolution observations and reanalysis products (Fig. 2.10k). However,

rain rates are over simulated in the GB, and BoB. Rainfall over HK are improved in the 1/4° when compared to the 2° model. The hybrid simulation has similar precipitation patterns as the 1/4°. However, regional rainfall peaks, especially over the mountains are better simulated when the high-resolution topography is utilized. Moreover, strong precipitation over the Arabian Sea as well as western half of Bay of Bengal are similar to the low-resolution version of CAM, which suggested that resolving the mesoscale topography [118] like the Western Ghats has a large impact on the southern section of the IAM. This highlights the importance of resolving topography, but also suggests that resolved terrain is only part of the solution.

The low-level wind fields across Indo-Asia for the reanalysis products are overall consistent with one another (Fig. 3.1d-f). Strong westerly winds flow across the Arabian Sea, interacts with topography over Western India and continues an eastward trajectory until it encounters the Bay of Bengal. This flow then shifts toward a north or northeast direction. Flows that are fully northward encounter the Himalayan Mountains and are forced to either climb over or flow around. Wind fields over the Indo-Gangetic plains and Ganges Basin are much weaker than the prevailing westerly winds. Mean wind speeds over the Ganges Basin moves southeast and reenters BoB. Over Indo-Gangetic plains surface wind speeds moves east to west, then flows into HK region. The 850 mb winds that flow over the Eastern Himalayas continue in a northward direction.

Simulated Indo-Asia 850 mb wind fields in CAM4 2° consist of westerly winds moving across the Arabian Sea into Western India, then shifts to a northward flow and heads toward the Himalayas. Wind speeds over BoB also follow a north and northeast trajectory that flows into and over the Himalayas. The 850 mb winds climbing over the Eastern Himalayas and into Tibet have a northeast trajectory, while winds located at the western and central portion of the Plateau are directed southward. Interestingly, despite the changes in micro physics scheme in CAM5 or application of CRM in SPCAM, the winds speed and direction are similar to those in CAM4 2°. The noticeable difference are wind fields over BB in the SPCAM model where they

are stronger than the control CAM4 model. Since, the topographic boundary condition is identical between CAM and SPCAM simulations, the convective scheme is more likely controlling how the winds are distributed. When we increase the models resolution to 1/4° the wind fields are closer to the reanalysis product. For instance, the east-west flow across the Indo-Gangetic plains are captured by both 1/4° and hybrid simulations (Fig. 3.1i and 3.1l). Since the distribution of winds between the 1/4and hybrid simulation are similar, this indicates that resolved topography has partial influence on monsoonal winds.

3.3.2 Diabatic Heating, Vertical Velocities and Equivalent Potential Temperature

It has been a long standing question whether convection in over the Indo-Asian monsoon region is merely a product of the large-scale dynamics [37, 45] or whether second order processes such as strong diabatic heating [22, 31, 77] through moist convective processes [36] influences and maintains horizontal meridional surfaces fluxes. The theory of convective quasi-equilibrium (CQE) implicitly uses convective rainfall as a threshold mechanism that removes convective instability and resets the atmosphere to an equilibrium state [44]. The latter view emphasizes on the response of the atmosphere when perturbed by moist heating, which is directly linked to enhanced vertical velocities. Through conservation of mass, strong vertical ascent influences both upper and lower horizontal wind distribution [119]. Inevitably, the properties of convection are closely tied to boundary layer moist static energy or maximum subcloud equivalent potential temperature. Any changes in distribution leads to subtle but important characteristic changes to the IAM and further deviations from strict CQE [67]. In this section, we provide context to the validity of this atmospheric heating in the CAM models, and its connection to distribution. As mentioned above, the 2 model simulates moisture flux across India poorly, whereby having unlimited

moisture supply. In this section, we demonstrate how this enhance moisture flux overall impact precipitation, diabatic heating and the overall monsoonal circulation.

To understand how orographic convection influences large-scale overturning circulation, we plot zonally averaged total diabatic heating, meridional circulation, and , during extended summer (May-September) monsoon season in our analysis (Fig. 3.2). We depict regions that are in CQE by approximating the upper-level saturated equal to maximum boundary layer (Fig. 3.2 black contour line). Additionally, to understand the co-occurrence of peak diabatic heating and with rainfall and vertical velocities (w) we plot simulated zonally average total precipitation rate and at 300 mb (Fig. 3.2 bottom panel, black and red lines). To provide validity to these variables we compare them to TRMM and reanalysis products MERRA (Fig. 3.3 bottom panel, grey and pink lines) and JRA55 (Fig. 3.3d, 3.3e, 3.3i, and 3.3j). We divided our zonal averages into two regions that focus on the Eastern and Western Portion of the Himalayan Mountains and Tibetan Plateau: Bangladesh and Bhutan (BB) (88-96) region which includes majority of BoB and Himachal-Kashmir (HK) (74°-82°) regions, which incorporates the Western Ghats on the south. The purpose of analyzing the the HK sector is to understand why the IAM in the CAM models extends well beyond the bounds of an average Hadley cell circulation. Since the spatial pattern of the simulated precipitation rates and wind fields over the Indo-Asia are similar between CAM4 and CAM5, SPCAM 4 and 5, and CAM4 1/4° and hybrid, we omit CAM5 versions of the model as well as the hybrid model for this analysis.

The total diabatic heating across BB sector for the CAM4 2° illustrates a dual heating region one near BoB and stronger more dominant feature across the Himalayan Range and into Tibetan Plateau (Fig. 3.1a and 2.11f), which is not surprising due to the nature of how precipitation is distributed across the region. The orographic diabatic heating has the highest values near the surface but extends up to 250 mb. The maximum distribution is located over the front range of the Himalayan mountains and Tibetan Plateau, with northward extent of the meridional over turning circulation extends to 30°-35° N. This is also the location of maximum

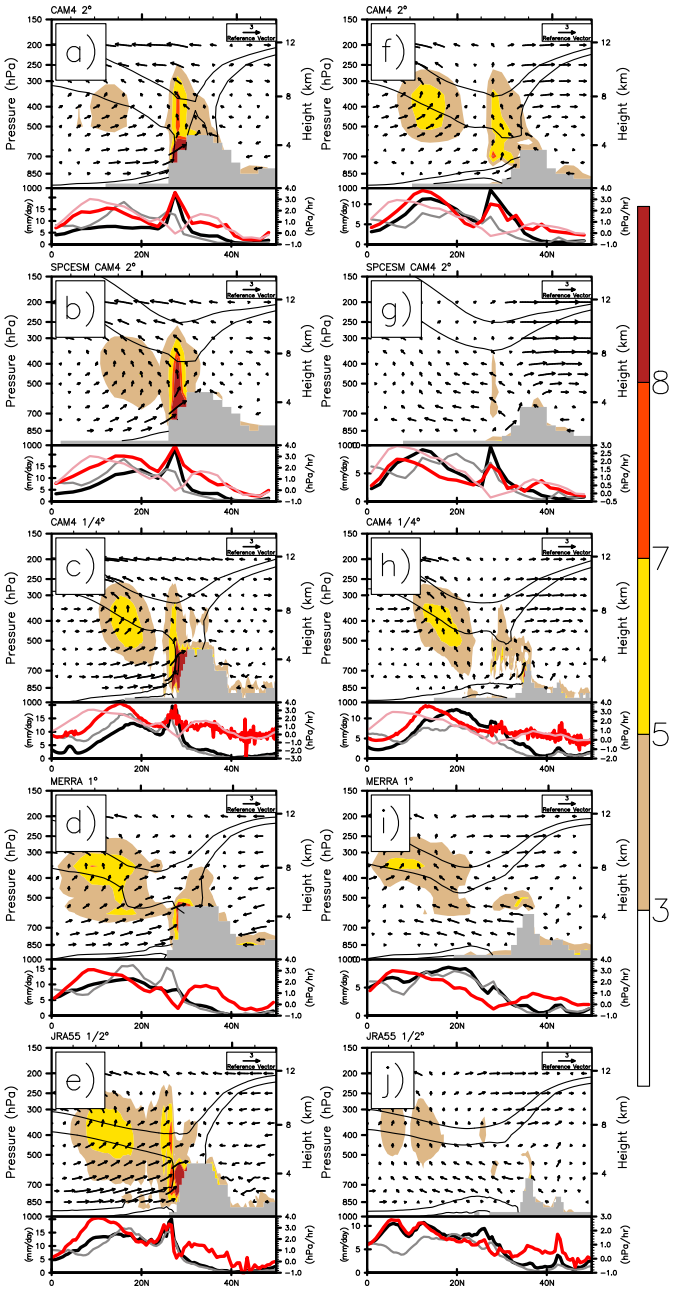

Fig. 3.2. Zonal average of total diabatic heating over Indo-Asia monsoon region during extended summer months of May, June, July, August, and September. Panels (a)-(e) are focused on BD region and are averaged over 88°E-98°E and shows latitude from 0°-50°N (Fig. 3.1b red box). (f)-(j) are focused on PR region, averaged over (74E-88E) and shows latitude from 0-50N (Fig. 3.1b green box). The grey outline represents Himalayan-Tibetan Mountains. The diabatic heating ranges from 3-8 K day-1 and vectors are omega (hPa/hr) scaled with meridional wind components (m s-1) to highlight vertical wind velocities. The lower panel displays, zonally averaged total precipitation rate (black) and vertical velocity at 300 hPa (red) over the region. Dark colors represent model output, whereas light colors are observed: GPCP and MERRA. Black contour lines overlaying diabatic heating profiles represents θ_e surfaces ranging from 342-347 K.

precipitation and the maximum vertical velocity in the CAM4 2° model. Similar analysis over the HK region demonstrates that this orographic heating is persistent across the Himalayan Front range. Additionally, strong diabatic heatng over WG section is also identified. Enhanced zonally averaged vertical velocity and precipitation are still simulated over 30°N. The location of maximum is between 25°-30°N. Analysis on the zonal averaged precipitation and vertical velocity, the 2° version of CAM has two distinct precipitation and vertical velocity maxima for both regions, where as TRMM and MERRA does not illustrate this over HK region.

Orographic diabatic heating over BB region, for the SPCAM4, has a similar vertical extent as the CAM4 model, however the magnitude is greater and BoB heating is closer toward the Himalayan Mountains (Fig. 3.2b and 3.2g). The SPCAM4 simulation has maximumat 30°N with co-located maximum vertical velocity, precipitation. Over the HK and WG region, both the heating and vertical velocity are weaker. Unlike the 2° model, the meridional overturning circulation is closer toward the equator, with 850 mb to 700 mb meridional wind speeds flowing equatorward. Analysis on how spatial resolution influences the distribution of total diabatic heating, the 1/4° CAM4 model suggest that deep orographic diabatic heating over BoB and BB is maintained regardless of horizontal grid spacing (Fig. 3.2c and 3.2h). However, the distribution and magnitude of zonally averaged precipitation and vertical velocity are qualitatively similar to both reanalysis products. For instance, even though orographic diabatic heating extends to the upper troposphere, maximum diabatic heating is concentrated near the front range of the Himalayan Front. This maximum near the front range intuitively follows where maximum orographic precipitation should occur. Additionally, orographic heating over HK region is dissipated monotonically as you move from low to high resolution, such that orographic heating is shallower than CAM 2°. It is worth to note that in our hybrid simulation, the upper-level diabatic heating is also weaker, however, a much stronger BoB heating is produced. These results hold true when using CAM5 versions of the model.

To identify the validity of these heating features, we analyze reanalysis products MERRA and JRA55 (Fig. 3.2d, 3.2e, 3.2i, and 3.2j). In the reanalysis products, two dominant heating regimes are also shown over the Bhutan-Bangladesh region, but the vertical and horizontal extent are distinctly different between the two products. For instance, the dominant upper-level heating over BoB in MERRA and orographic diabatic heating is much weaker. These are consistent with how precipitation rates are distributed across the BB region (Fig. 3.1d). Although, meridional low-level wind speeds are converging toward topography in the Bhutan-Bangladesh region, strong vertical velocities are focused toward the equator. We find vertical velocities over the Plateau in the reanalysis products are much weaker than the CAM models. We consider the strong vertical velocities at 15-20°N over the BB region as poleward extent of the overturning circulation for MERRA. However, considering results from the JRA55, between the two heating regimes the orographic diabatic heating is more dominant, whereby extending meridional overturning circulation at 25°N. The zonally averaged precipitation rates between JRA55 and TRMM are nearly identical. In JRA55, the maximum distribution is found over front range of Himalayas, while in MERRA we identify it at the foothills of Himalayas. Strong vertical velocities are aligned with maximum, however, the maximum vertical velocities are not strictly co-located. Over the Hindu Kush and Kashmir region, diabatic heating distribution is much weaker than CAM4 2° model, with maximum vertical velocities near the equator. The distribution between MERRA and JRA55 are similar and away from topography (20°N). We find it important to identify that near surface wind speeds associated with enhanced diabatic heating and vertical velocity over the Himalayan foothills for the CAM models are flowing into topography for the HK region, which is opposite of SPCAM, MERRA and JRA55.

Recent studies looking at monsoon circulation in reanalysis product ERA-40 by Nie et al., [2010], suggest that the averaged monsoonal circulation over Southern Asia (60E-100E) extends to 25°N, with precipitation maxima located southward of the maximum. Our analysis suggests that when BB and HK are zonally averaged

together, such simplified version of the monsoon is observed, however, our results suggest the ascending branch of a Hadley cell like circulation is constrained at 15-20°N, while northern parts of the Indo-Asian Monsoon circulation at 20°-30°N are dynamically influenced by regional forcings provided by local terrain [24, 120]. Differences in diabatic heating rates, meridional circulation, equivalent potential temperature, precipitation rates, and vertical velocities between BB and HK region further clarify this conclusion. However, the impact of regional topography on the general circulation are exacerbated in the low-resolution version of CAM. Since, strong vertical velocities influence the distribution of low-level horizontal circulation, it is key to understand how the general circulation is impacted by the excessively strong orographic heating in the low-resolution version of CAM.

Regional distribution of upper-level diabatic heating

To further understand how the distribution of diabatic heating influences horizontal circulation, we analyze the total diabatic heating at 300 hPa and low-level winds at approximately 850 hPa between our simulations and the reanalysis products over Asia (Fig. 3.3). In addition, we extend our analysis to sensitivity studies where parameterizaion of convective processes such as deep and shallow are turned off. Not surprising, maximum upper-level diabatic heating is associated with regions of maximum precipitation. For example, the CAM4 model exhibit substantial upper-level diabatic heating over the foothill of the Himalayas when compared to 1/4° CAM4, MERRA and JRA55. Wind speed anomaly shows wind fields over the Indo-Gangetic plains for the CAM4 2° are predominantly moving toward the Himalayan Mountains and regions of increased diabatic heating. Both heating and wind speed anomalies over BoB are greater in 1/4° CAM4, MERRA and JRA55.

Comparisons between CAM4 2° and SPCAM4 demonstrate that upper-level heating is greater over the WG and HK regions with the cloud resolving model. Similarly, surface wind speeds are primarily moving toward regions of increased diabatic heating. Strong diabatic heating over BB region simulated by SPCAM4 weakens the wind speed anomaly over the region. Suggesting winds over this region between the two

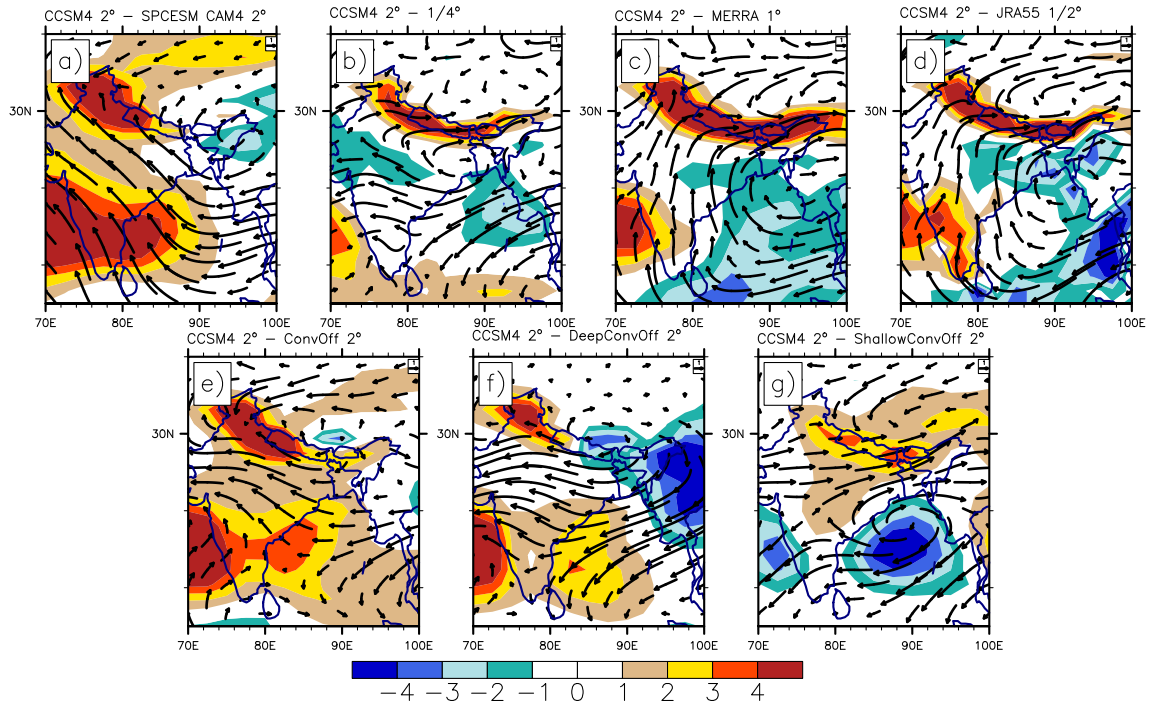

Fig. 3.3. Anomaly color contour map of diabatic heating at 400 hPa, overlaid with low-level winds at 850 hPa over Asia. The vectors are in hybrid coordinates equivalent height of 850 hPa. a, b, and c shows CAM4 simulations in 2°, 1°, and 1/4° resolution. d, and e illustrates MERRA and JRA55. Plots (e-f) shows anomaly plots of sensitivity cases where various convective schemes are turned off: deep and dhallow Convection schemes turned off, only deep convection off and only shallow Convection off.

models are nearly equal in magnitude. Interestingly, sensitivity analysis where both deep and shallow convection is turned off has similar upper-level diabatic heating and low-level wind speed patterns to SPCAM4. As we turn off deep convection the shallow convection and large-scale precipitation begin to dominate the BB and BoB region. Shutting off shallow convection while maintaining the deep convection on, simulates strong precipitation and upper-level diabatic heating across the Himalayan Mountains. The lack of heating at HK region suggests that the Zhang McFarlane scheme primarily dictates exceedingly strong precipitation occurring over the region and sets up the overturing circulation northerward in the commonly used CAM models. We find it important to note that strong precipitation and heating over WG and Arabian Sea is not simulated when the deep convection scheme is turned off. Furthermore, the cross equatorial low-level winds over the Arabian Sea are substantially weakened when deep convection is turned off. These results illustrate that diabatic heating over HK is primarily connected to the deep convective scheme, while orographic heating over BB region is produced by all three precipitation types, but are mostly dominated by large-scale and shallow convection.

The low-level circulation patterns near terrain, especially over northern India into HMTP are substantially improved as we increase CAM4 resolution to $1/4^{\circ}$. We associate the reduction of winds converging toward topography with weaker topographic heating. The exacerbated strong topographic heating stimulates low-level convergence, such that simulations with excessive heating exhibit a land-sea breeze type monsoon. Analysis on the HK region in the CAM4 2° model supports this interpretation, which illustrated that strong diabatic heating allow rising air parcels to move pass lines of potential temperature, impacts the distribution of vertical velocities in the upper atmosphere and the location of . The CAM models that simulate excessive heating over topography suggests that two dynamical regime exist in the CAM4 models. A deep moist monsoonal circulation, BB region and a mixed type, HK region [45]. However, we demonstrate that both reanalysis products do not produce this mixed type circulation over the HK region. In addition, analysis on the maximum

suggest that the the Indo-Asian monsoon region during extended summer monsoon season is in quasi-equilibrium, but are regionally modified by strong orographic heating. In summary, this heating is tied to moisture transport across the region and at lower-resolution, the monsoon circulation is a land-sea breeze type monsoon. At higher resolution the Hadley cell like circulation extends up to 15-20°N and orographic precipitation across the Himalayas is primarily due to regional mechanisms.

3.3.3 Impact of horizontal resolution

We analyzed the breakdown of total precipitation rate over Indo-Asia during extended summer months (May-September) to understand the spatial distribution of large-scale versus convective precipitation as we change spatial resolution (Fig. 3.3). Total precipitation in the model is quantified by summing the convective and large-scale (stratiform) precipitation. In CAM4, the convective precipitation parsed between deep and shallow convection. Deep convection is parameterized using the Zhang and McFarlane, [1995] scheme mainly using undiluted bulk mass transport with a convective available potential energy threshold as the closure function. Deep convective scheme was updated by adding a dilute plume approximation, and convective momentum transport by Neale et al., [2008] [73, 121]. Shallow convection uses the Hack, [1994] [53] scheme and similarly to the deep convection scheme it uses simple mass flux approach. The large-scale precipitation in CAM uses prognostic cloud microphysics, which are described in Rasch and Kristjnsson, [1998] [122]. We also provide detailed breakdown of percent amount of convective precipitation over a specified region shown in figure 1 plot a.

General analysis on precipitation anomaly plots suggests that in the standard CAM4 2 model orographic precipitation over the Himalayan front as well southern India are largely from convective processes. In contrast, increased production of large-scale precipitation is found over the Ganges Basin and Burma region in the CAM4 1/4° simulation (Fig. 3.4 a-c). Overall, as we increase model resolution the con-

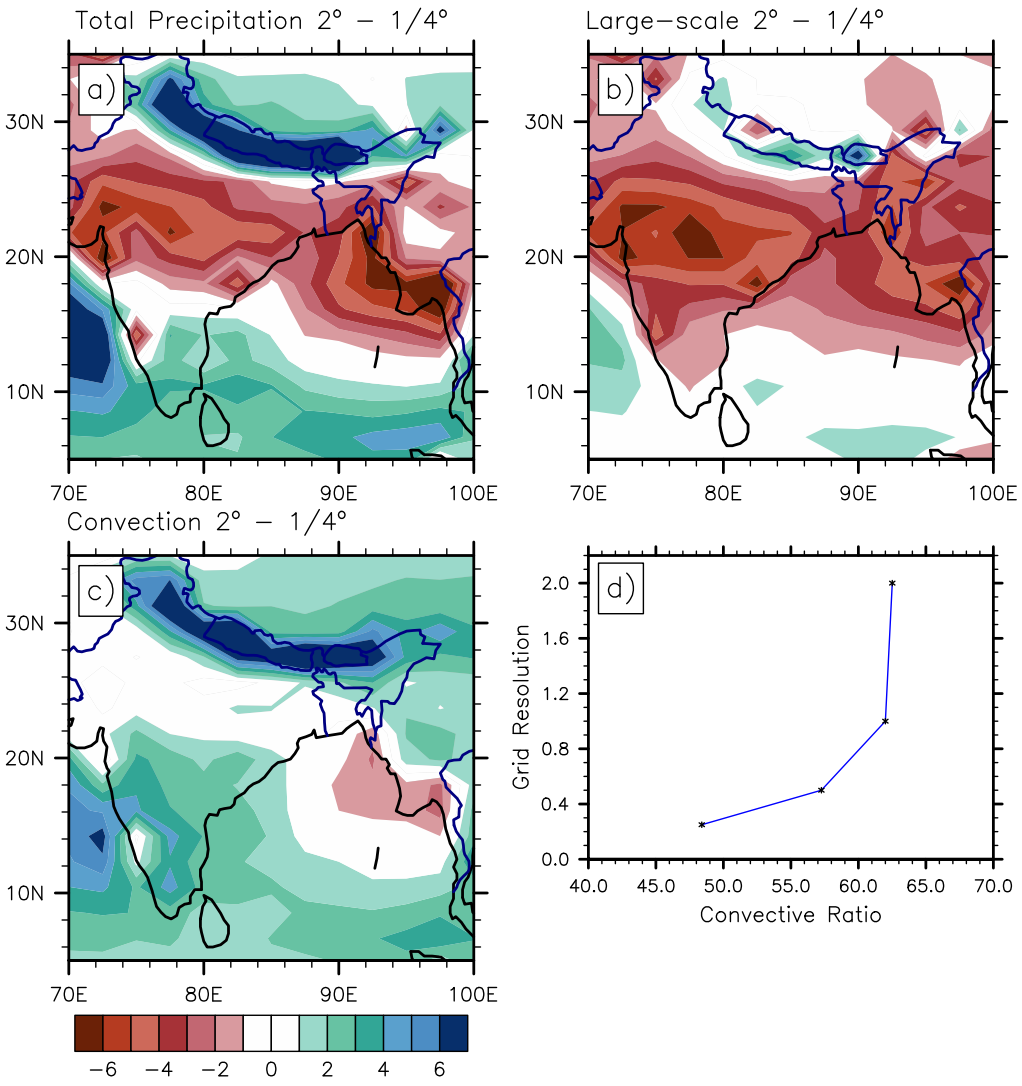

Fig. 3.4. Difference color contour map of total precipitation rate (mm day-1) (plot a), large-scale precipitation rate (b) and convective precipitation rate (c) between the CAM4 2° and 1/4° over Indo-Asia monsoon region during peak monsoon months June-August. Plot (d) scatter plot of model grid resolution versus the convective ratio (convective precipitation to total precipitation) for various CAM4 simulatons.

vective ratio drastically decreases (Fig. 3.4d). Percent breakdown of convective to total precipitation as we increase resolution shows convective processes dominating precipitation over Indo-Asia, with 62%, when using the lower resolution model, while the large-scale precipitation dominates the higher resolution model with convective rain at 48%. The amount of convective rainfall decreases monotonically as we increase CAM4 resolution. Similar results has been found [123] when looking at specific events in the Maritime continents and by Li et al., [2011] analyzing high-resolution aqua-planet simulations. Convective percentage from the reanalysis products suggest that the IAM region mostly consist of convective processes. Out of the three products we used JRA55 had the most convective rainfall at 84%, where MERRA estimates convective precipitation much lower at 57%.

Detailed break down of convective rainfall to total precipitation rates over specified regions are shown in Table 1. For the low-resolution versions of CAM4 (2° and 1°), the HK, WG, GB, and BoB predominantly consists of convective precipitation, which are in agreement with JRA55 and ERAI. In contrast, the BB region for the low-resolution CAM4 models are dominated by large-scale precipitation and are consistent with MERRA and ERAI. Results from the high-resolution models (1/2° and 1/4°) only has BoB dominated by convective precipitation, while BB, HK, GB and WG has large-scale precipitation occurring more frequently. Overall, the production of convective rain in the low-resolution CAM4 compares better with JRA55 but poorly against MERRA, while the opposite results are found for the high-resolution models. Recent study by Sen Roy et al., [2014] [124] using TRMM V7 with a 9 year climatology, illustrated that toward the peak and late monsoon season, build up of large stratiform precipitation occurs more frequently over BoB, BB and GB, while convective precipitation mostly persist at the Western India, primarily at WG and Western Himalayas. Additionally, as suggested by Sen Roy et al., [2014], these persistent stratiform rain over BB and GB observed in TRMM are from low-pressure systems [89,90] originating from BoB and migrating across Central India and moving parallel of the Himalayas bringing rain into the Indo-Gangetic plains.

Table 3.1. Ratio convective precipitation rate to total precipitation for JJA over specified regions: Bhutan-Bangladesh (BB), Hindu Kush-Kashmir (HK), Western Ghats (WG), Ganges Basin (GB), Bay of Bengal (BoB) and the general Indo-Asian Monsoon (IAM). Units are in percent (%)

Model	BB	HK	WG	GB	BoB	IAM
CAM4 2	44.85	57.19	67.19	63.88	73.59	62.51
CAM4 1	43.44	45.3	63.71	64.61	69.41	62
CAM4 1/2	37.49	38.27	55.92	54.05	64.94	57.26
CAM4 1/4	30.97	34.51	50.96	38.48	55.12	48.4
MERRA 1	42.15	43.69	51.52	52.93	59.39	57.84
JRA55 1/2	69.53	75.8	80.14	80.28	87.27	83.4
ERAI 1	47.23	50.45	68.84	66.35	75.99	68.58

As noted by Li et al., [2011], changing model resolution, the model time-step (the length of coupling interval between the physics and dynamics) both effectively impact how the model resolves precipitation. However, decoupling the two has been found difficult [97]. To sparse out if the timestep applied on 1/4° is strongly moderating the changes we observe as we move model resolution, we produced a 2 simulations where the time-step was modified from f 1800 to 900 seconds and a secondary simulation where other parameters applied on the 1/4° simulation were modified. These simulations did not change our results, which suggests that convective timescale do not strongly impact how the model is producing IAM precipitation. However, this indicates that resolving stratiform rain is one of the reasons for the improvements seen in the 1/4° CAM simulation.We note that Li et al., [2011] and OBrien et al., [2013] mentioned that the CAM4 at 1/4°, globally over produces stratiform rain and in depth analysis from OBrien et al., [2013] indicated that convective parameterization begin to lack awareness of the sub-grid scale components of convection and which allows the micro and macro physics to be more active. The similar distribution of total precipitation between the SPCAM, the Convective off simulation and GPCP demonstrates that the convective schemes are largely the root cause of the problem. Recent study by Gustafson Jr. et al., [2014] [125] demonstrated that appropriate tuning such as adjusting the convective timescale of the model can produce a better total precipitation distribution, which corroborate with our results.

3.4 Discussion

3.4.1 Model improvements

This study investigated the root cause of excessive precipitation over the Himalayan Mountains when using commonly used low-resolution versions of CAM. We identified that the lack of east-west, low-level circulation across the Indo-Gangetic plain in the 2° model allows continuous moisture transport from the adjacent bodies of water to the front range of Himalayas. This in turn, produces excessive total

precipitation and associated diabatic heating, and vertical velocities in commonly used versions of CAM, when compared to reanalysis products. The most notable bias is found over Himachal-Kashmir region, where strong diabatic heating extends the ascending monsoonal branch well into the subtropics. Although differences are known to exist between reanalysis products [29, 30]. However, since diabatic heating is strongly associated with precipitation, and both APHRODITE and TRMM are converging toward the similar results as the reanalysis products (Fig. 3.1 a-f), we conclude that biased orographic heating found in CAM does not fully represent the mean precipitation distribution in the reanalysis products presented here, especially on the western half of Himalayan Mountains (Fig. 3.2 d, e, i, and j). However, mesoscale precipitation events have been observed during extreme cases [Houze et al., 2011; Lau and Kim, 2012; Rasmussen and Houze, 2012; Palazzi et al., 2013; Viterbo et al., 2016]

We showed that even with the more advanced cloud microphysics in CAM5, increasing model resolution is more important when simulating the IAM. This is further supported by a recent study by Jian et al., [2015], where higher resolution versions of CAM5, AGCM shows large improvements in orographic precipitation over complex terrain. We find that the decrease production of deep and shallow convection in the $1/4^\circ$ over terrain is the reason for the improved precipitation distribution. These results corroborates with studies by OBrien et al., [2013], where the authors demonstrated the changes in precipitation ratio due to changes in horizontal resolution are robust throughout different dynamical cores. Ideally the ratio of convective or stratiform rain to total precipitation between model resolution should be scalable and should not drastically change as one changes model resolution. Boyle and Klein, [2010] and Li et al., [2011] have found similar results in other tropical regions, their studies suggest that CAM at $1/4^\circ$ may be over predicting stratiform rain. Results from OBrien et al., [2013] suggested that convection parameterization has a scale-incognizant problem. However, analysis on convective versus stratiform precipitation using TRMM, showed that Indo-Asia is largely dominated by stratiform precipita-

tion, with strong convective regions restricted over the Western Ghats and Burma [Sen Roy et al., 2014]. Nevertheless, Boyle and Klien [2010] suggests that better atmospheric heating profiles during simulated events, as well as the model resolving complex wind flow patterns between terrain are the reason for the changes. While, Li et al., [2011] attributed the change in convective ratio to better representation of extreme precipitation events, as well as the prognostic parameterization of the large-scale precipitation becoming more sensitive as the model increase resolution.

Regardless the scale-incognizant problem with the convective schemes, we demonstrated that such overly strong heating on the foothills of the Himalayan Mountains persist in the low-resolution versions of CAM even when various convective parameterizations are turned off. This result extends to SPCAM model with regards to BB region. Additionally, we briefly tested if changing model time-step which is important for the formation of convective rain [Li et al., 2011] could provide a solution to this problem, however, we find that the CAM 2was unaffected by such changes. We find that the excessive diabatic heating, especially over the HK region is primarily due to the overly productive convective schemes over terrain. We find that when the shallow convection is turned off but the deep convection is maintained, the east-west over Indo-Gangetic plain are partially simulated (Not shown) and orographic precipitation over the Himalayan Range is better simulated. This result further demonstrate the importance of correctly simulating the eastwest flow over Indo-Gangetic plain. Although it is beyond the scope of this paper, it may be fruitful to identify which models found in the CMIP5 archive also have a large heating discrepancy over the greater Asian monsoon region [126] and more importantly identify which models accurately represents the east-west flow found over the Indo-Gangetic plain.

Increased horizontal resolution improves CAM simulating the Indo-Asian monsoon system, especially at $1/4^{\circ}$ resolution. A recent study by Gent et al., [2010] suggested that a more realistic interaction between the surrounding topography and the atmosphere when using high-resolution versions of CAM is one of the reasons why such improvements are observed. Although our 1/4results are in keeping with Gent

et al., [2010], the Hybrid simulation suggests a more realistic topographic boundary condition is only moderately driving improvements in the resolution simulations. Increased production of stratiform rain, in addition to better-resolved circulation are responsible for the improvements. The more accurate surface-winds across the Indo-Gangetic plains as well as better spatial distribution of precipitation over BoB and BB region supports this interpretation. Nonetheless, major improvements in the model should encourage the field to use high-resolution version of CAM when studying the Asian monsoon system and its sensitivity to topography.

3.4.2 Impact on monsoon dynamics

The paleoclimate community extensively uses the NCAR family of AGCMs, CAM, to understand the mechanisms associated with the maintenance of a mature IAM. In our own work, we have also emphasized the role of deep diabatic heating over the HMTP [31] as derived from analysis of CAM3 paleoclimate simulations. Moreover, recent study [38] used CAM4 to simulate different topographic boundary conditions. These sensitivity studies used CAM to show that stronger diabatic heating, associated with the height of subtropical topography is the primary cause for the existence of the modern day IAM. These results could overweight the role of diabatic heating, or candle mechanism as opposed to other hypotheses. We find that the commonly used CAM version shown in paleotopography studies [38] possessed similar biases. We demonstrate that overly strong heating on the HK region maybe influencing such results. Its perhaps not the case over the BB region where the heating profiles as well as meridional circulation are consistent with reanalysis products. Nonetheless, weaker diabatic heating over the Himalayan front range does not strongly influence the onset of the equator to pole moisture flux. This indicates that the heating is a response to the large-scale circulation [Nie et al., 2010b; Boos and Kuang, 2013], but once initiated can influence the regional circulation and allow the atmosphere to deviate from quasi-equilibrium [71].

Earlier we illustrated that such focused heating influences the regional distribution of maximum , this is primarily observed over Bay of Bengal region. Nonetheless, both reanalysis products as well as the 1/4 simulation show that the classical Hadley cell like circulation primarily extends up to 15°-20°N, while precipitation regimes found further inland is a product of the interactions between local circulation and terrain. Recent study by Ma et al., [2014] using high-resolution (1/2°) global Weather Forecasting Model demonstrated that the height of the subtropical topography determines the amount of moisture trapped in Indo-Asia. This stratification of stable moist air provides the deviations from idealized monsoon theories [26], hence altering how precipitation is distributed over IAM region. The interaction between surfaces and maximum diabatic heating has implications for the IAM circulation. Results from the reanalysis products, as well as the high-resolution version of CAM are in general agreement with quasi-equilibrium theory. Whereas the low-resolution version of CAM, which have overly strong diabatic heating rates, will generate anomalously extended meridional circulation. Such models are not in compliance with theory suggested by Nie et al., [2010a], but instead have maximum precipitation occurring at the subcloud maxima. This can be thought of as standard CAM versions have an overly strong land-sea breeze centered type monsoon overlain on top of a system that is in quasi-equilibrium.

3.5 Conclusion

The primary focus of this study was to illustrate the robustness of the east-west flow found across the Indo-Gangetic plain, during peak monsoon months (July and August). We compared a suite of CAM4 simulations across a range of horizontal resolutions from low (2°) to high (1/4°) with reanalysis data products, and analyzed how low-resolution version of CAM lack the ability to simulate the prevailing east to west flow. Instead, in low-resolution version of CAM, dominant southern wind flow supplies moisture directly into the Himalayan range which in turn produce excessive

orographic precipitation rate. The biased rain band is associated with excessive diabatic heating and vertical velocities. As a consequence, monsoonal circulation is extended further poleward, which has implications for monsoon characteristics and of critical importance in maintaining IAM in steady state. A key outcome of this research is how a 1/4° resolution, the CAM model can accurately simulate this east-west flow which mitigate excessive production of orographic diabatic heating across the Himalayan Mountains. We conclude that using CAM at a lower resolution will produce an IAM circulation that follows that of a dominant land-sea breeze circulation, while reanalysis products as well as the high-resolution version of CAM are in compliance with quasi-equilibrium theory. Results presented in this study extends to CAM5 version of the model as well as paleoclimate simulations that alter topography. We note that increasing the resolution of topography is part of the reason for these improvements, however, we demonstrated the models ability to increase large-scale to convective precipitation which is due to the convective parameterization, are key to model improvements and more accurate representation of the IAM.

4. COMPLEX INTERACTIONS BETWEEN TOPOGRAPHIES AND THE MONSOON

(a version of this chapter is submitted and is under review)

Abstract

The Indo-Asian Monsoon (IAM) circulation is an exemplar for how tectonic processes alter regional-to-global climate systems. However, the interactions between topography and the IAM are not simple and are challenging to model. Competing monsoon theories place different emphasis on low-level enthalpy distributions, diabatic heating, and mechanical forcing, and these processes respond differently to varying tectonic configurations. The evolution of the regional topography is also complex in space and time, and understanding the IAM at a specific period involves the consideration of multiple interacting large-scale terrains within a finely resolved climate model framework. Here we investigate such contingent, non-linear interactions, using high (0.25) resolution global climate simulations. We find the Iranian Plateau, by itself, can support the major features of the modern IAM, by acting as a gatekeeper that insulates the Indo-Gangetic Plain from the low-enthalpy westerly air. Furthermore, expected general relationships between topographic forcings, winds, and rainfall do not follow previously proposed concepts. For example, the Somali Jet is largely unrelated to monsoon rainfall in Tibet and the Himalayas; the Himalayas are not required for monsoon rain over central Asia, a Tibetan Plateau suffices; left by itself, the Tibetan Plateau dries and weaken the IAM. Our study reconciles several different frameworks for understanding the IAM, suggests a need to revisit previous assumptions made in the reconstruction of paleo-monsoons, and implies that the timing of the Iranian Plateau orogeny may be crucial to the IAMs history.

4.1 Introduction

The role of topography in modulating the Indo-Asian Monsoon (IAM) circulation has long been studied [2, 13, 127, 128] and the orogenic history of the region is complex and actively debated [7, 129, 130]. Classic monsoon theory regarded large-scale terrains as external forcing on the Indo-Asian Monsoon [15, 22, 24, 99, 104, 131]. However, paleoclimate proxy data and modeling studies [31, 49, 100, 132] demonstrate that an active IAM persisted during the early Cenozoic Era, prior to the formation of the modern-day Himalayan-Tibetan complex. The height and extent of the Tibetan Plateau during the early Cenozoic is controversial [7], and there is even less agreement on the rise of surrounding terrains such as the Iranian Plateau. A large elongated topography much like the modern day Himalayan Mountains have been estimated to be present during the Eocene, where paleoclimate modelling of such feature highlighted the IAM productivity [31, 49]. Evolution of the IAM across the Cenozoic Era suggests enhancement during the Miocene [5, 133]. Such enhancement have been proposed to be linked to the full development of the Tibetan Plateau [6, 134]. However, inconsistency arises when considering the insulation theory of Boos and Kuang, [2010] has cast doubt on the importance of the Tibetan Plateau orogeny.

Less attention has been paid to other regional topographic features, such as the Iranian Plateau. Geological evidence suggests Iranian Plateau orogeny [McQuarrie et al., 2003; Mouthereau, 2011] [135,136] occurred during the same period as the Miocene IAM enhancement. Modeling evidence has highlighted the thermal properties of the Iranian Plateau for the IAM [137] and other works has hinted at the importance of its mechanical mechanism [Tang et al., 2013; Zhang et al., 2015] [38, 130]. Yet, a full demonstration of how the Iranian Plateau influences the IAM has not been done.

The core of our study is to understand how the three large-scale terrains, especially the Iranian Plateau, redistributes the monsoon circulations and rainfall distributions. Although the key role of topography in redirecting onshore monsoon flow have been well-studied, low-resolution models tend to misrepresent various important IAM pro-

cesses and features [138, 139]. Thus, it is crucial for the next generation of monsoon studies to implement high-resolution modeling. For our study (Fig. 4.1) we used the high-resolution (1/4°) Community Atmospheric Model version 4, which was found to adequately represent the regional characteristic of IAM (see modeling details in section 2). Modeling detail are found in section 2. The results of our study are presented in section 3. Section 4 will touch upon the broader context of our results and summarizes our study.

4.2 Model, Experiments and Diagnostics

CAM4 is the atmospheric component of National Center for Atmospheric Research (NCAR) Community Climate System Model version 4 (CCSM4). The model framework is described in Bitz et al., [2012] [50]. For model validation see Gent et al. [2010] [51]. For studies highlighting monsoon circulation see Shields et al., [2016] [68] and Acosta and Huber, [2017] [139]. The CCSM4 has also been evaluated within the Coupled Model Intercomparison Project [140]. We use the finite volume dynamical core version of CAM4, which have been found to provide a better representation of the hydrological system compared to the spectral dynamical core [50]. Simulations are carried out on model resolution 0.23x 0.31 or equivalent to 28 km grid spacing over the equator. The CAM4 utilizes 26 vertical atmospheric levels and parameterizes convective precipitation processes into two separate schemes deep convection [54, 121], and shallow convection [141]. Cloud microphysics, which controls the amount of large-scale precipitation are also parameterized in CAM4 [122]. The CAM4 interacts with Community Land Model version 4 (CLM4) [142] and uses prescribed monthly-observed fixed sea surface temperature and sea-ice that were compiled and averaged from 1982 to 2001. We primarily focus on climatological averages of equilibrium fixed SST simulations and emphasized on monsoon season June, July, and August.

The two reference state cases provided in this study are a modern-day simulation (referred to as MODERN) and a simulation where the Himalayan Mountains, Tibetan

Plateau and Iranian Plateau was removed (referred to as FLAT). We revisit the experimental case of BK10 with two modifications: (1) we use higher-resolution, (2) and explore the dependence of both the Himalayan mountains and Tibetan Plateau on the existence of the Iranian Plateau (referred to BK10). We then simulate an opposite end-member where only the Tibetan Plateau was present (referred to as TP). To identify the impacts of the Iranian Plateau on the IAM we then compare a case without the Iranian Plateau otherwise maintains both Himalayan Mountains and Tibetan Plateau (referred to as NO IP), and case where only the Iranian Plateau is added to a FLAT case (referred to as IP). It is important to note that since high-resolution modeling enables us to look at how smaller terrains such as the Western Ghats and Mizoram Mountains impact the regional circulation, all our cases keep these mountain ranges, which is unique to all topography-monsoon sensitivity studies. For further information on the sensitivity cases, see Figure 4.1 and 4.2 far left panels.

We present monsoon metrics such as total precipitation, integrated moisture flux and near surface geopotential height. Precipitation and moisture flux anomalies are presented figure 1k, 1o, 2c and 2g. Diagnostic analysis on the convective quasi-equilibrium environment includes horizontal lower and upper equivalent potential temperature (θ_e) following the methods of Boos and Kuang, [2010], Nie et al., [2010] and Emanuel, [1994]. To facilitate quantitative comparison between theoretical arguments of Boos and Kuang, [2010] and Nie et al., [2010] and our results, we compare vertical profiles of between our simulations and a generalized critical distribution derived in Emanuel, [1995]. To use equation 11 in Emanuel, [1995], we fit our simulated maximum found at a specified , but allow the maximum to vary in the vertical (profiles are presented in figure 4.1c, 4.1g, and 4.3).

4.3 Results

In our MODERN case (Fig. 4.1a), the strongest precipitation rates are located on or near topography such as the Himalayan Mountains or the Western Ghats and

Mizoram Mountains (Fig. 4.1b). In keeping with expectation, the dominant integrated moisture flux moves toward the Asian continent, following isobars associated with a low found across the India-Iran border and Western China (Fig. 4.1d). Both the Somali Low-Level Jet across India and the Indo-Gangetic Low-Level Jet as well as their associated orographic precipitation features is well represented [Acosta and Huber, 2017]. As expected from quasi-equilibrium theory [Emanuel, 1995b], the vertical gradient of θ_e is very weak at 30°N where subcloud has its maximum (Fig. 4.1c). Subcloud θ_e peaks in: (1) Northern India, spanning across most the Indo-Gangetic Plain; (2) Western China which is often associated with the East Asian Monsoon; and (3) Tibetan Plateau surface (Fig. 4.1d). The maximum upper-level θ_e corresponds to the maximum subcloud θ_e that is found over India. At all heights, the meridional gradient of θ_e are in general agreement with Emanuels theory for critical θ_e gradient (Fig. 4.1c, grey lines). Strong diabatic heating is found near 15-20°N and some near topography 3°0°N. In other words, this MODERN control case is an excellent match to observations and can be understood within the context of a robust theory.

We can contrast this with a highly idealized, opposite end member in which the Himalayas, Tibetan Plateau and Iranian Plateau are removed (Fig. 4.1e), which we call the FLAT case, although it retains all other topography. This FLAT simulation maintains a strong Somali Low-Level Jet with associated strong orographic precipitation over the Western Ghats and Myanmar (Fig. 4.1f), and rainfall is at near modern level in central India. The region of convective neutrality is located at 20°N, and maximum subcloud and free troposphere θ_e are found over the Bay of Bengal (Fig. 4.1g,h). The high enthalpy air in the northwest of India and the Himalayan rainfall are entirely missing. The rest of the circulation is nearly unaffected. It also maintains a meridional, onshore flow and moisture flux into Central Asia, reminiscent of the MODERN case, but without the three large topographies (Fig 4.1f). In contrast with the MODERN case, enhanced diabatic heating is only simulated at 15-20°N and is associated with precipitation of the Western Ghats. The FLAT case is an important reference point in this study: many of the basic aspects of the IAM circulation persist

in the region without any of the large-scale terrains that are commonly attributed to them. What is sensitive to the topography is rain in the location of topography itself, not the circulation.

To demonstrate that these results are congruent with the dynamical perspective in BK10 that identified the insulation effect of the Himalayas by removing the Tibetan Plateau, so for the sake of comparison, we conducted the BK10 sensitivity study at higher resolution (Fig. 4.1i). The results are similar to their study and our MODERN case, although the Indo-Gangetic Low-Level Jet is better captured at higher resolution (Fig. 4.1j), thus corroborating at higher resolution, the importance of the Himalayan insulating effect in building high subcloud θ_e over central India (Fig. 4.1l). As the impact of the Himalayan Mountains and Iranian Plateau are removed from the MODERN case, the anomalous cyclonic circulation introduced by the Tibetan Plateau mainly acts to weaken the Indo-Gangetic Low-Level Jet (Fig. 4.1k), which further suggests that the Tibetan Plateau plays a minor role in the IAM of today, as previously noted by BK10.

The results of BK10 may depend critically on the current modern configuration of the other terrainsremoving the Himalayas to the modern-day (referred to as NO HM case) could present similar results to BK10 (Fig. 4.1m). As expected the results are strikingly similar to the MODERN and BK10 cases. Strong orographic precipitation occurs over the Western Ghats, and Myanmar and is further enhanced in Central Asia (Fig. 4.1n). Although strong onshore moisture flux from the Somali Low-Level Jet occurs, the Indo-Gangetic Low-Level Jet is not present (Fig. 4.1n). The insulation mechanism persists in the NO HM case, but the high subcloud θ_e air buildups further in the interior of Asia, setting the region of convective neutrality further north (Fig. 4.1p). The incorporation of the Tibetan Plateau presents an anomalous cyclonic circulation over Eastern Indo-Asia (Fig. 4.1o). Since the insulation mechanism is activated the cyclonic circulation enhances the IAM.

Adding the Tibetan Plateau to a flat reference state (TP case) present different impacts to the IAM than removing the Tibetan Plateau from the modern world. With

the Tibetan Plateau isolated, the strong anomalous cyclonic circulation persists over Eastern Indo-Asia (Fig. 4.2b, 4.2c), similarly to the MODERN and NO HM case. However, unlike the previous cases, the cyclonic circulation enhances intrusion of dry, low-enthalpy air into the IAM system, effectively drying Northern India (Fig. 4.2b, 4.2d). The subcloud θ_e maximum over Northwest India is substantially disrupted and does not coincide with the maximum upper-level (Fig. 4.2d) and the region is no longer in convective quasi-equilibrium. Although the Himalayas are removed, onshore flow persists from the Bay of Bengal and is orographically lifted when it meets the Tibetan Plateau instead. Indeed, in the TP simulation, enhanced orographic precipitation occurs further north than the MODERN case (Fig. 4.1b, 4.2b). The main low-pressure and associated local subcloud θ_e maximum now occurs over the Tibetan Plateau (Fig. 4.2d). An enhanced near surface θ_e above Central Tibetan Plateau is collocated with the upper-level θ_e maximum found at 30°N (Fig. 4.2d). In the TP simulation, precipitation persists in Central Asia, although the influx of dry low-level westerly air has disrupted the high subcloud θ_e across India (Fig. 4.2b, 4.2d). Disregarding the distribution over Northwest India, the northern margin of the IAM precipitation shifts further North when the Himalayas are removed. A maximum over Tibetan Plateau exist in equilibrium with the monsoonal flow originating from the Bay of Bengal, demonstrating that the Himalayan insulation effect is not a necessary condition to produce the northern extent of the IAM precipitation.

To evaluate the type of non-linear responses of the commonly used approach in anomaly topography studies, we make the appropriate comparisons and focus on the cyclonic circulation surrounding the Tibetan Plateau. Comparison of the BK10 when the reference state is the MODERN case, the anomalous cyclonic circulation is centered over Northwestern India (Fig. 4.1k), however, when the reference state is the FLAT case the cyclonic circulation is centered over the eastern Tibetan Plateau (Fig. 1o and 2c). In several cases, when the Himalayas and Iranian Plateau are present, such cyclonic circulation enhances the IAM. However, left alone, the Tibetan Plateau and the induced cyclonic circulation acts to reduce enthalpy in Western India (Fig.

4.2b, 4.2c, 4.2d), but by virtue of its different position, has a complex interaction with region precipitation distributions. Seminal work [Zhisheng et al., 2001] has shown enhancement of cyclonic circulation when a Plateau like topography is added to Asia, which has been interpreted as the IAM becoming more vigorous. However, evidence provided in our analysis suggests that by solely adding the Tibetan Plateau, major portions of the IAM can be disrupted and does not overall lead to the IAM strengthening.

One aspect that emerged from the previous analysis was the key role that the Iranian Plateau has in modulating the response to the other major topographies. In a similar vein to the previous analysis, we perform two experiments. In one, we remove the Iranian Plateau (NO IP case, hereafter) from the MODERN case (Fig. 4.2e). In the other, we add an Iranian Plateau to the FLAT case (IP case, hereafter) (Fig. 4.2i). The NO IP case shows similar precipitation, moisture flux features as our MODERN case (Fig. 4.2b). Qualitative comparison with the NO HM case, demonstrate the Himalayan Mountains is crucial for the Indo-Gangetic Low-Level Jet to occur. The presence of the Iranian Plateau in the modern world enhances the Somali Jet and an anomalous anticyclonic circulation in the west (Fig. 4.2g). Indeed, without the IP, the regional subcloud θ_e maximum shifts eastward to Bangladesh, Nepal and Central Tibet (Fig. 4.2h). As can be seen by comparing the enthalpy distributions in figures 4.1l, 4.1p, 4.2h and 4.2d, the Iranian Plateau in the modern world has a bigger impact on the location of the subcloud θ_e and the associated precipitation than the Himalayas.

Turning now to the evaluating the impact of adding the Iranian Plateau to a flattened Asia, strong precipitation over the Western Ghats and Myanmar persist (4.2j). This is supported by the anomalous cyclonic circulation over Western Indo-Asia and enhancement of the Somali Low-Level Jet, which operates to enhance water vapor transport into the IAM (Fig. 4.2g, 4.2k). The IP simulation qualitatively demonstrates that with neither the Himalayan Mountain nor the Tibetan Plateau, most of the IAM circulation, and subcloud θ_e distribution is preserved (Fig. 4.22l).

Additionally, the bulk of the insulation effect of BK10 can be maintained without the Himalayas. Precipitation across the southern section Indo-Asia is comparable to our MODERN case (Fig. 4.1b, 4.2j). Key features that are not generated by the Iranian Plateau include the Indo-Gangetic Low-Level Jet and orographic precipitation over the Himalayas.

In these results, the Iranian Plateau plays as large a role as the Himalayas in determining the regional θ_e distribution and the IAM circulation, and an even larger role than the Tibetan Plateau. The lack of changes in precipitation anomaly over the Western Ghatsin the presence of an Iranian Plateau suggest that the Tibetan Plateau orogeny is unnecessary to produce strong onshore flow over the Arabian Sea as well as orographic precipitation over the Western Ghats. Analysis of the isolated impact of the Himalayan Mountains yielded similar results as our HMTP simulation.

4.4 Discussion

It is useful at this stage to review what we would expect the monsoon to look like in the absence of the Tibetan and Iranian Plateaus or the Himalayas. Regardless of ones preferred monsoon theoryinsulation and deviation of subcloud θ_e from a critical gradient, latent or sensible heating over elevation [22, 137], orographic mechanical forcing, land-sea breezethat the major, broad terrains figure prominently and the expectation is that major monsoonal features should be missing. We cover those in more depth subsequently, but first we discuss the features that remain.

Even without those terrains, a monsoon similar to modern extends to 20°N; there is a low-pressure system in the region of the Himalayas and an onshore flow from the Bay of Bengal that extends to 30°N as in the modern. It appears that the Himalayas and Tibetan Plateau in the modern restrict the poleward transport of water vapor in the region, rather than enhancing it. Precipitation in the Western Ghats and a strong Somali Jet also remain close to modern. This allows us to invalidate the hypothesis that the major terrains, via the various theories, are the leading order

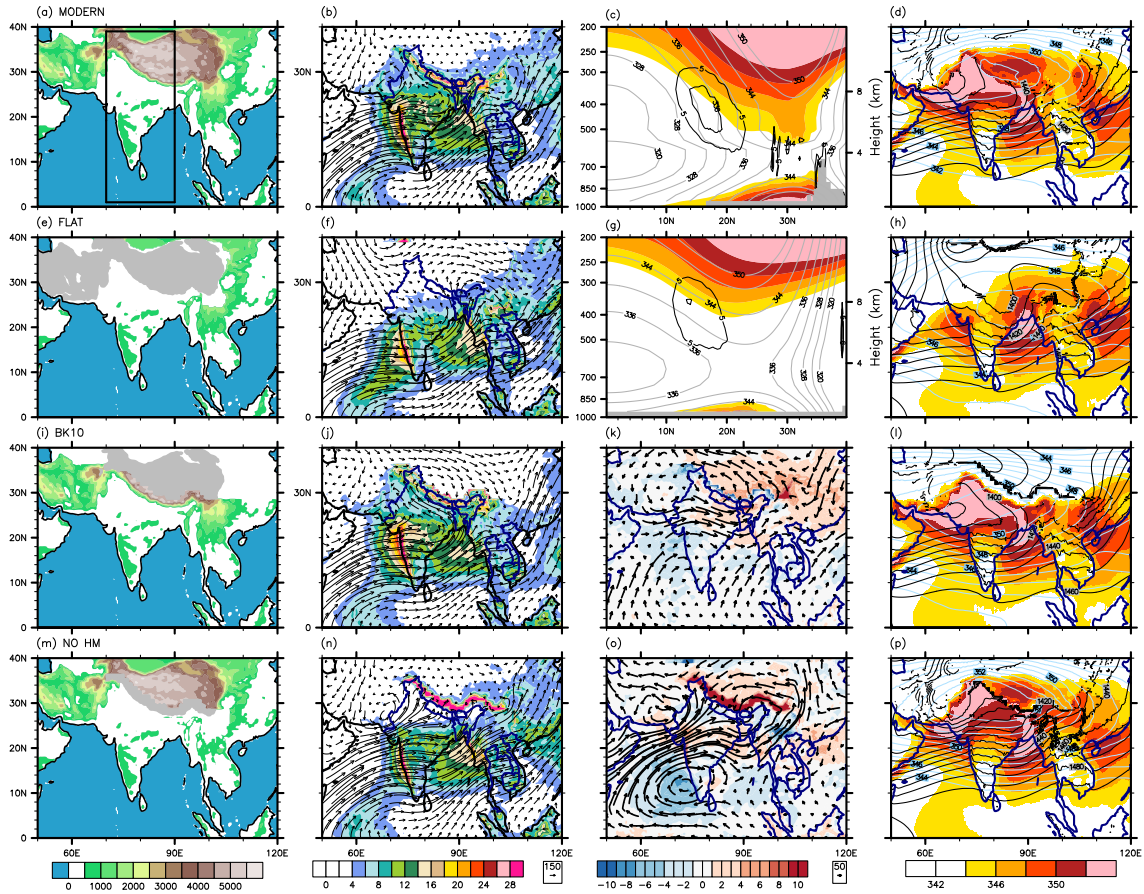

Fig. 4.1. Topographic boundary conditions for the Modern-Day, Removed, BK10, and NO HM case (plots a, e, i and m). The grey shaded area in plots a, e, i and m are topography removed. Total precipitation rate [mm day-1] overlain by integrated meridional and zonal flux (1000-600 mb) [kg m/s] (plots b, f, j and n). Two end-member analysis (with and without topographies) on the vertical profile of θ_e (K) overlain with calculated critical (same range of color bar) distribution from Emanuel 1995 in gray contours and total diabatic heating (3-9 K day-1) in black contours (plots c and h). The zonal averaged area spans over the black box on plot a. Near surface θ_e 900 mb overlain with 200 mb θ_e in light blue contour and 850 mb GPH [m] in black contours (d, h, l and p). θ_e plots share common label bar. Anomaly of integrated moisture flux and total precipitation between our Control and test cases (plots k and o). Plot k represents the impact of the Tibetan Plateau referenced with the Modern-Day simulation (Modern-Day minus BK10). Plot o represents the impact of the Tibetan Plateau with respect to a flattened Asia (Tibetan Plateau simulation subtracted with the Removed simulation).

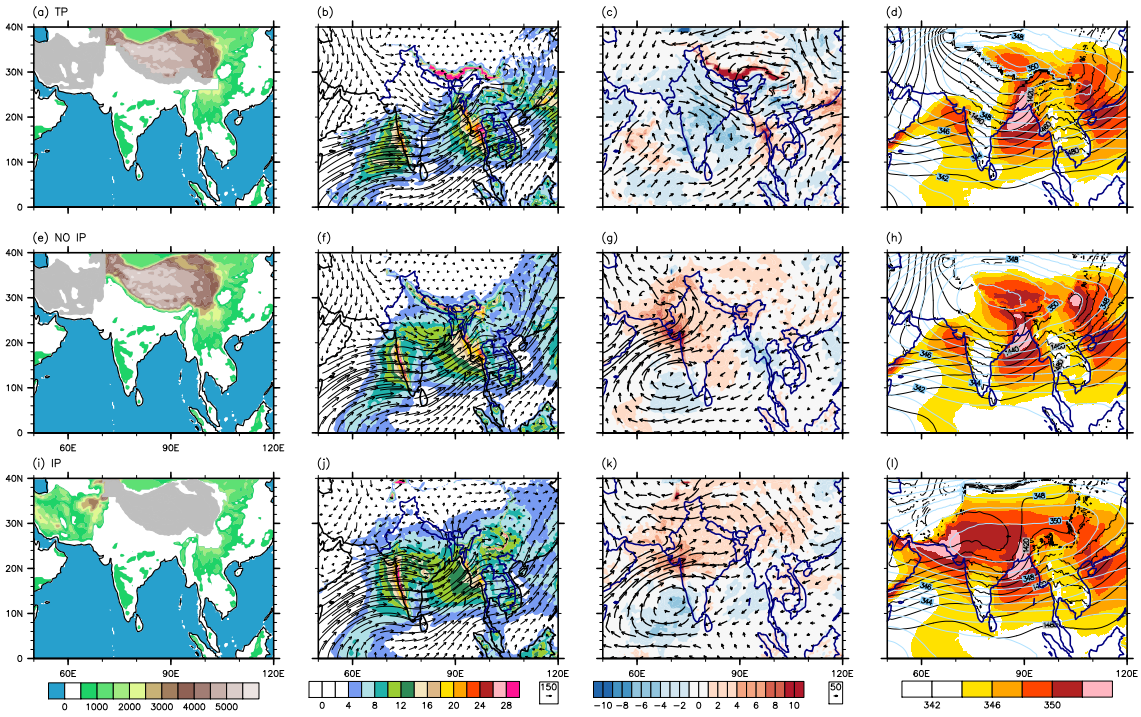

Fig. 4.2. Plots has the same caption as figure 1 except simulations are for the TP, NO IP case and the Iranian Plateau case. Anomaly plot c shows the impact of the Iranian Plateau referenced with Modern-Day (Modern-Day subtracted with the HMTP). Anomaly plot f shows impact of the Iranian Plateau with respect to Removed case (Iranian Plateau simulation subtracted with the Removed simulation).

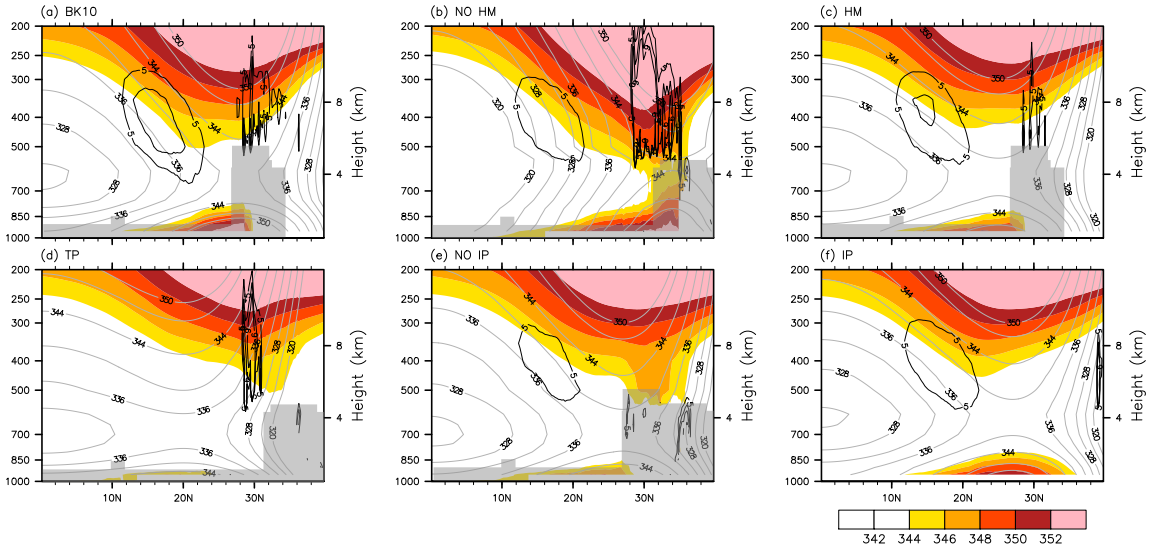

Fig. 4.3. Vertical profile of θ_e overlain with calculated critical (same range of color bar) distribution from Emanuel 1995 in gray contours and total diabatic heating (3-9 K Day-1) in black contours.

drivers of the southern half of the IAM and the poleward flow in Bay of Bengal. These southern IAM circulation and precipitation features are persistent, and the existence of this part of the IAM is not in the details of Indo-Asian topography, but in factors governing the larger scale sea surface temperature (SST) gradients in the region [Lindzen and Nigam, 1987; Bordoni and Schneider, 2008] [18, 143]. The circulation is set up by these SST gradients and the precipitation is a passive response to the resulting flow over topography. While diabatic heating may occur, it is not driving the flow. This result is consistent the convective quasi-equilibrium theoretical framework and previous studies [139, 144] that demonstrate simulating the IAM at higher modeling resolution better captures the modern monsoon without deep diabatic heating.

Five main features are indeed missing in the FLAT case: a maximum across northern Indian, precipitation in the Himalayas, moderate mid-level diabatic heating along the front of the Himalayas, and a strong low-level easterly jet. From this experiment by itself, little can be gleaned about which theory for these features at the northern margin of the IAM is more correct. The piecewise comparison carried out in this study do enable this discrimination between theories to be carried out. A flattened Asia does not allow the buildup of high-enthalpy air past 20°N. Our study corroborates BK10 such that without the Asian topographies, insulation of the high-enthalpy air found in northern India from westerly cold, dry flow does not occur. However, which topography provide most of the insulation and does insulation provide a predictive theory for the disposition of the IAM? BK10 interpreted the Himalayas as the primary topography that activates the insulation effect [16, 45], but did not perform a case without Himalayas or by changing other topography. In the absence of the Himalayas (NO HM case) there is still a local maximum over in the northwestern Indian region, what is lost is the broader maximum through the Indo-Gangetic Plain. Convective quasi-equilibrium in the region can be maintained without the Himalayan Mountains as the Iranian Plateau alone can provide much of the insulation. This shows that the Himalayas are not the only terrain causing insulation; they are neither

a necessary or sufficient condition for a maximum at this northern margin of the IAM to occur. Rain still falls over topographic highs, and deep diabatic heating at higher latitudes is much stronger. The Himalayas are not necessary for a monsoon at all.

On the contrary, if the Tibetan Plateau existed without the Himalayas, precipitation would occur further north and be enhanced. Additionally, the surface energy budget which maintains high air can create a local maximum over Tibetan Plateau even without the Himalayas. This is because strong meridional transport of water vapor from the Bay of Bengal occurs even without topography. Thus, in the TP or NO HM case, when such moist enthalpy air reaches the Tibetan Plateau, rainfall occurs, regardless of the Himalayan insulation effect. Although the insulation effect has a minor role on the precipitation over the central part of Southern Tibetan Plateau, it does have an impact on the rainfall that occurs over the western portion. When the Iranian Plateau exist with Tibet Plateau (NO HM case), strong onshore flow from the Arabian Sea with an associated buildup of over Northwest India exist, which is then results into enhanced orographic precipitation over the Karakoram. The importance of topography is not to drive the circulation, but to mechanically steer it and to orographically lift it causing precipitation. In the NO IP case, a Northwest India local maximum is non-existent, but the Indo-Gangetic Low Level Jet and precipitation over topography is vigorous.

This analysis is limited in multiple ways. The coupling between the atmosphere-ocean is crucial in terms of paleoclimate analysis [145, 146], while changes in greenhouse gasses [68], aerosol emissions [147], orbital parameters and gateways [100] also impact the regional climate and can ultimately modify the monsoon. Although the modeling parameters mentioned above are not investigated here, our simple single parameter sensitivity tests allow us to isolate the impact of topography on the system. This study only looked at the seasonal response to topographic forcings and did not touch upon seasonal initiation of the IAM. Although the integrated impact of transient events is included in our simulations, the explicit role of topography concerning

triggers for rapid onset and transient eddies dynamics [148], is beyond the scope of this study.

4.5 Conclusion

This study focused on how the surrounding Asian terrain modulate the high enthalpy air delivered by the Indo-Asian Monsoon system. We presented high-resolution global climate simulations where we highlighted the individual mechanisms of the Himalayan Mountains, the Tibetan Plateau, and the Iranian Plateau. Our results demonstrate the following:

1. Meridional inshore flow of high enthalpy monsoon air occurs without any of the large terrains, but rain does not occur.
2. The Tibetan Plateau by itself provides a source of mechanical lifting that can cause this flow to precipitate, even though it also allows strong downstream convergence that enables low enthalpy westerly air to enter the Indo-Gangetic Plain. When acting in conjunction with the Iranian Plateau the IAM precipitation extends further north and yields more vigorous precipitation than in the modern state.
3. The Himalayan Mountains mechanically lifts the onshore high enthalpy air and is the primary topography that invigorates the Indo-Gangetic low-level jet.
4. The Iranian Plateau produces a maximum θ_e in Northwestern India. The Iranian Plateau can block much of the cold, dry westerly air from disrupting the monsoon environment along the Indo-Gangetic Plain. Additionally, its presence strengthens the Somali low-level jet and can further moistens Northwestern India. However, the insulation mechanism is not sufficient to produce strong precipitation over Central Asia, such that the northern IAM precipitation regime is better explained with an orographic framework.

Interpretations of proxy records regarding the IAM have been closely tied to the uplift or existence of the Himalayan-Tibetan complex [7, 149]. For example, marine

sedimentary records from the Indian Ocean, which primarily reflect shifts in the strength of the Somali Low-Level Jet, have been used to interpret changes in the uplift rate of the Tibetan Plateau [5, 6]. However, strengthening the Somali Jet and precipitation found over the Western Ghats can be explained by the uplift of the Iranian Plateau rather than the Himalayan-Tibetan complex. This is supported by recent flora proxy records, identifying monsoon intensity along Bhutan remained relatively constant during the monsoon enhancement period [150]. Our results confirm that the Tibetan Plateau influenced the IAM during the early Cenozoic, but had little role in the Miocene IAM enhancement [5, 133] and that the Himalayas and Iranian Plateau may have been equally important. Our results are consistent with the interpretation that the IAM was present during the Eocene, or even prior to the uplift of the Tibetan Plateau [31, 49, 100, 132]. Studies that suggest that the uplift of the Tibetan Plateau during the Miocene was the consequence of the poleward shift in the ITCZ are probably incorrect [151]. Our findings show the northern branch of IAM is tied to the terrain in Central Asia and implies that the poleward precipitation regime could not have existed without the aid of local topography.

As shown, topography by itself only plays a role in the northern branch of the IAM and does not play the leading role in maintaining the greater IAM as previously suggested [4]. The current results show that while many features of the modern IAM can be correlated and are often related through simple diagnostic relationships, the frameworks are not prognostic. The IAM in large points boils down simply to large scale flows transporting water vapor set up by regional SST gradients which either lifted airmass over topography generating rain, or the same locked-in flows do not rain of there is not local topography; processes on land are of secondary importance. This highlights the importance of answering the question of what sets up or changes the sea surface temperature gradient across the region, in the past or future.

Our results have important implications for interpretation of pale-monsoon records. We fully expect through the Miocene, where much of the evidence for an enhanced monsoon is available, that there was major re-organization in the ocean circulation

and vertical temperature gradient within the ocean column [152]. This raises the interesting possibility that the major changes in the IAM during the Miocene, especially near 20°N, are not in fact due to topography but instead largely governed by changes in the ocean circulation and thermocline properties. This is counter to the interpretation that monsoon caused a re-organization of the ocean-atmosphere system. This conclusion is not surprising since cooling in upwelling zones occurred throughout the world during the Miocene and subsequently in the Pliocene, not just in the monsoon regions. Thus, we should be looking for one common causes, not a special cause having to do with paleogeography in the monsoon region [129]. Although local SST records [6] demonstrate a sharp cooling at a crucial interval in the Mid Miocene (10-14 ma) this is consistent with the hypothesis that the secular trend in global cooling led to an abrupt local temperature transition as the sharp temperature gradients of the thermocline shoaled enough to seasonally outcrop. This sudden enhancement of SST gradients would have would clearly have impacted low level atmospheric circulation and the IAM and would show strong correlation with IAM proxy records, but it may be unnecessary to suggest a sudden change in the IAM drove the SST changes.

As we pointed out, regional topography does play a role in the spatial distribution of precipitation, thus, interpretations of sediment records, especially those found in the Bay of Bengal or the Arabian Sea should be recognized as a regional signal. Since oxygen isotopes are also constrained by the regional moisture source and attempts in modeling such methods should be conscientious of model limitations. For example, in our previous analysis, using low-resolution models may have erroneously assumed that the moisture originates from the Southwesterly monsoon, while in fact, it originates from the Bay of Bengal. Thus, application of high-resolution models should be considered when performing isotope modeling over Southern Asia.

4.6 Acknowledgement

We are grateful for funding from National Science Foundation Grant (OCE-1602905, EAR-1049921) and Purdue University for funding our study. We acknowledge the Information Technology and Research Computing at Purdue University for providing computational support. The authors would like to thank members of Climate Dynamics Prediction Laboratory for helpful discussion and comments during the preparation of the manuscripts.

4.7 Supplementary: Complete Sensitivity Study

4.7.1 Background

The role of topography on the South Asian Monsoon (SAM) circulation is actively debated [22,67,76,104,144]. The foremost topographic theory compares the amount of solar insolation that occurs over the Tibetan Plateau versus the surrounding low-lying regions. The substantially larger solar insolation the TP receives was considered as the primary off-equatorial forcing that thought to allow any thermally-direct circulation, like monsoons, to occur [153, 154]. However, simplified theories [26, 34, 155–157] that suggest that a substantially sufficient off-equatorial thermal loading ultimately invokes a steady-state asymmetric overturning circulation, and the identification of the global monsoon system [20, 62] where the characteristics of monsoon systems can be grossly simplified to be the regional imprint of the Intertropical Convergence Zone, imply that topographic controls on a monsoon circulation can be regarded as an unnecessary mechanism. This is further highlighted by more recent results from idialized aquaplanet simulations, where the non-linear abrupt transition from seasonally dry to a wet regime was obtained even without the presence of land [16–18, 35]. Nonetheless, theory suggests that any thermally driven circulation is constrained by conservation of absolute angular momentum, which inevitably limits the poleward extent of the monsoon overturning circulation. However, the SAM migrating poleward further than

any other monsoon system suggests that other mechanisms allow it to deviate from the typical Hadley cell-like circulation [45]. Thus, understanding the transition from a theoretical Hadley cell circulation to a more complex monsoon system like SAM is an utmost interest to the field.

The various forcings related to topography are divided between thermodynamic and mechanical theories. More specifically, the debate is whether sensible heating along the slopes of the TP forces near-surface wind convergence allowing orographic latent heating to maintain the monsoon overturning circulation [22,120]; maintenance of high subcloud θ_e moist entropy through the Himalayan Mountains mechanically blocking the low entropy extratropical air from entering southern Asia] [15] encouraging the monsoon overturning circulation to occur well into the Asian continent; or the elongated feature of the TP or HM, which allow mechanically produce downstream convergence of westerly winds on the eastern side through conservation of potential vorticity [24]. Nevertheless, current theories support a Himalayan-like topography plays a crucial role in initiation and maintenance of the SAM. However, paleoclimate studies [31, 49, 100, 132] demonstrate that the characteristics of the SAM during the early Cenozoic have largely been unaltered, alluding to an active modern-like SAM during Tibetan orogeny prior to the formation of the Himalayan Mountains. Although the height and extent of the Himalayan-Tibetan complex during the early Cenozoic is unknown, determining how active the SAM prior to uplift incentivizes the need to reevaluate the various topographic mechanism.

A common crucial feature for the proposed mechanisms is the availability of high entropy moist air. In general, the flow of moisture into monsoonal regions is invoked by a subtropical heat-low over land that induces a low-level convergence from ocean toward the respected continent [36]. However, the SAM is a more complex monsoon system because the mechanisms that feed moisture into the system highly interacts with the surrounding terrains. Thus, it is an utmost importance to deduce how topography impact such mechanisms. More recently, the SAM was characterized as a region with two distinct Low-Level Jets (LLJ) that distribute moisture. First is the

well-known Southwesterly LLJ, which originates from the western Indian Ocean and enters India from the Arabian Sea [21]. The second branch is an Easterly LLJ, which is sourced from the Bay of Bengal and the Ganges Basin, and delivers moisture across the Indo-Gangetic Plains and Himalayan Mountains [139]. Together, these two LLJs provide the necessary environment for the modern-day SAM to thrive. Regardless of either wind feature, the suppression of the surface heating over northern India results into a weakening of onshore flow [144]most likely due to the weakening of the persistent summer monsoon low (hereafter referred to as monsoon-low) [83]. It remains unclear how the regional environment, especially regarding topographic forcings, influence the LLJs.

The core of this supplementary section is to more broadly present how the Asian topographies modulate the SAM monsoon-low and the Southwesterly and Easterly LLJs. As previously shown [139] many models found in the CMIP5 archive cannot properly simulate the Easterly LLJ, and thus display high variability in regional precipitation regimes. Therefore, for our sensitivity cases (Fig. 4.3) we used the high-resolution 1/4° Community Atmospheric Model version 4, which was found to adequately represent the regional characteristic of SAM. In addition to the modern day topographic boundary condition (CNTRL), we provide seven sensitivity cases where various terrain(s) over Asia is removed (Figure 4.3). We analyze key monsoon metrics which include (1) the formation on monsoon-low, as it relates to (2) Equivalent potential temperature (θ_e), (3) surface geopotential height (4) regional meridional moisture flux and (5) distribution of total precipitation. To analyze tropical convective regions, we use the basic quantities of quasi-equilibrium theory and plot near-surface θ_e at 850 mb as a proxy for subcloud moist static energy and its upper-level covariation the saturated free troposphere (400-200 mb), which is commonly referred to as θ_e^*. We also show the location of the monsoon-low using near-surface geopotential height at 850 mb. (Fig. 4.4 and 4.5 left-hand panel). Additionally, to understand the regional circulation we plot the total precipitation as well as the integrated moisture flux (Fig. 4.4 and 4.5 right-hand panel). Lastly, we present a

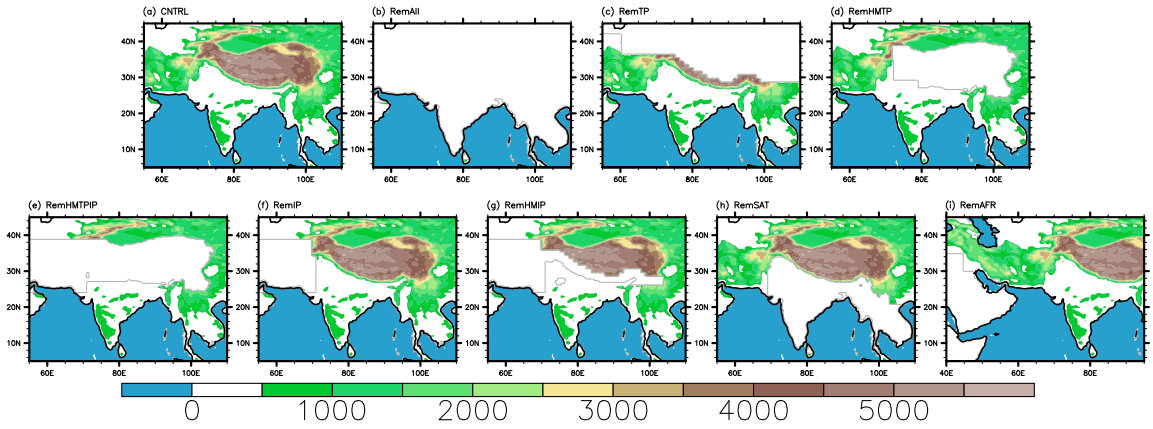

Fig. 4.4. Cases for the topographic sensitivity studies (elevation in meters).

vast array of surface energy quantities to further delve into the regional influence of topography.

4.7.2 Further Analysis

From the classic monsoon theory, large-scale terrains such as the HM, TP, and IP have been regarded as an important land-surface features that impose external forcing on the South Asian Monsoon. Such interpretations are postulated upon comparisons between a modern-day simulation (CNTRL) (Figure 2a, 2b) and the simulation where all the topography is removed (RemAll) (Figure 4.4c, 4.4d). In general, there are two locations where peaks: (1) Northern India, spanning across most the Indo-Gangetic plain; and (2) north of Myanmar which is often associated with the East Asian Monsoon. However, the maximum when all topography is present corresponds to the maximum surface is found over India, and does not coincide with the maximum surface found north of Myanmar. Additionally, low geopotential height coincides with the maximum surface in both CNTRL and RemAll simulations, again primarily residing along northern India. The general monsoon features are accentuated when all three large terrains are present. Strongest precipitation rates are collocated with

orographic fronts such as the HM or the Western Ghats and Mizoram Mountains. Overall, our results demonstrate that the onshore flow during peak monsoon season is contingent on the development of the monsoon-low across Southern Asia, which occurs without the aid of topography.

Prior work [15] as well as our own, shows that the modern day monsoon can be induced without the TP (Fig. 4.5a and 4.5b). Here we show that without the HM nor TP (RemHMTP) (Figure 2e, 2f) major characteristics of the southern branch of the SAM are relatively unchanged. For example, the onshore moisture flow from the Arabian Sea and Bay of Bengal into central Asia is unaltered. This is accompanied by the maintenance of the high , and low geopotential height found in northern Indiawe refer to as the monsoon-low. Additionally, precipitation along the Western Ghats and Mizoram Mountains are unaffected by the removal of HM and TP. Such results are important because the HM is linked to maintaining the high air found in Northwestern India or inducing the southwesterly LLJ and here we show the HM plays a minor role in influencing the general monsoon circulation. Additionally, the build-up of moisture and high in Northwestern India was thought to be the critical thermal property that sets the monsoon overturning circulation.

We find that the Iranian Plateau is also a major component of the insulation mechanism. Without the IP, low-entropy air from the mid-latitudes enters Northern India, and disrupts the buildup of high air (Figure 4.4g, 4.4h). This is even further highlighted In the RemIP simulation where we find that the high air shifts eastward and moving the monsoon-low along with it. However, even when the strong found in Northwest India is disrupted, a modern-day monsoon precipitation regime persists may persist. We perform simulations where the HM and IP were removed and similar results such as easterly shifts in the monsoon-low and largely unaffected precipitation regime were simulated (Fig. 3). We find resulting regional dynamics from the RemH-MIP results similar those previously highlighted as strong downstream convergence of air over the Southeastern Plateau. Such mechanical mechanism was emphasized as

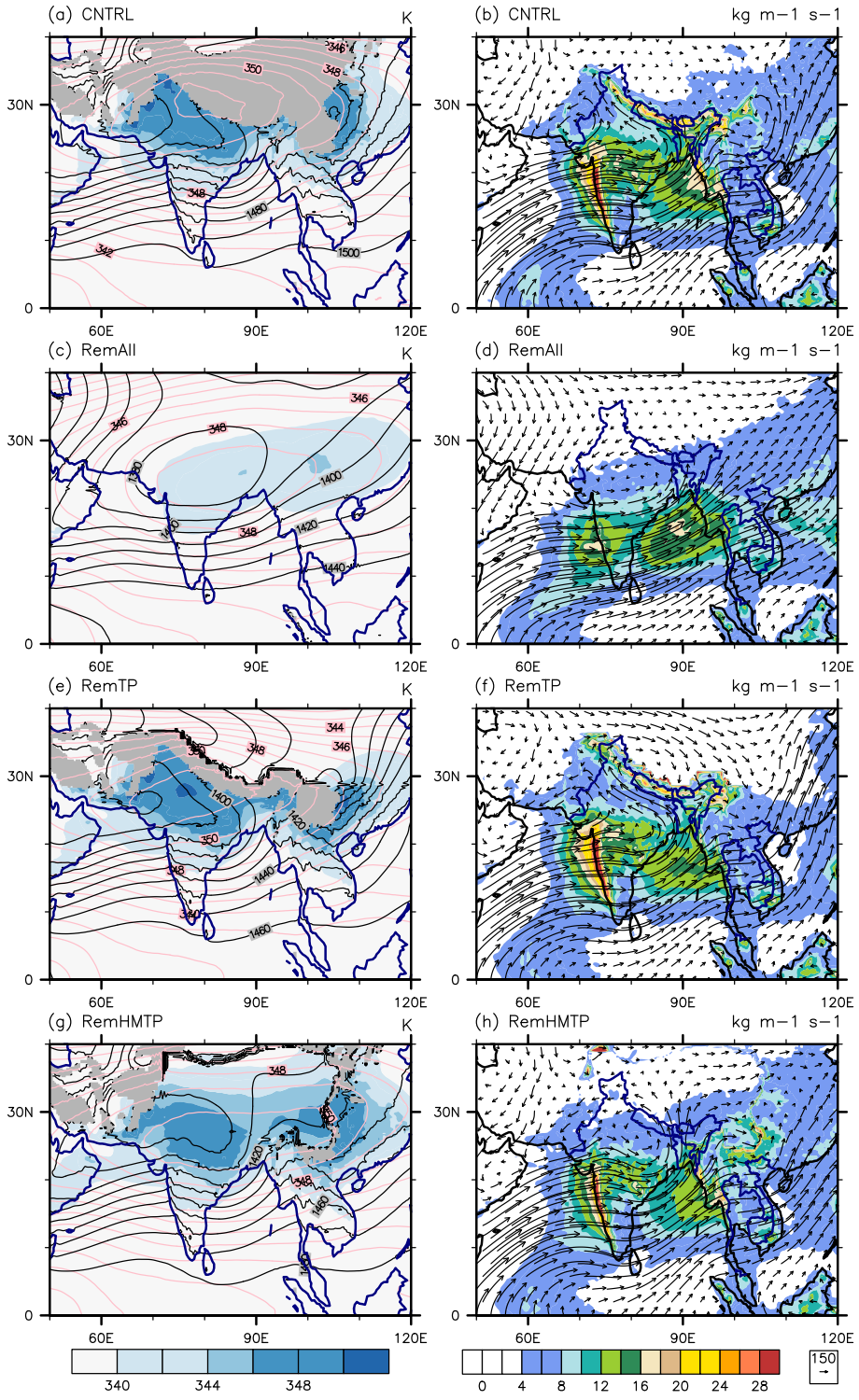

Fig. 4.5. Various monsoon attributes for cases: (a, b) CNTRL, (c, d) RemAll, (e, f) RemHMTP, (g, h) RemIP. The left-hand panel shows surface at 850 mb, and is overlain with surface geopotential height at 850 mb (black contour) and integrated from 400-200 mb (pink contour). The right-hand panel displays total precipitation rate in mm day-1 and is overlain with integrated moisture flux from 1000-600 mb (black vectors). The boxes in figure 2b were used to calculate figure 3. The red boxes represent the regions where the difference in Geopotential height are calculated, and the gray box is where the average precipitation, zonal winds at 850mb and zonal moisture flux from 1000-600mb were taken.

an important forcing during premonsoon season [24], but is muted in the cases when the IP is present.

Nevertheless, precipitation along the HM does not occur due to the lack of orographic lifting and steering of the onshore flow, which alludes to the SAM having a strong regional orographic dependence. This is demonstrated by relating the moisture flux and precipitation brought by the Southwesterly LLJ to the magnitude of the monsoon-low and the meridional pressure gradient it imposes. We quantitatively show that the presence of HM, TP and IP linearly influence the monsoon-low which then alters the pressure gradient between the Indian Ocean and Northern India (Fig. 4.6). We first note that precipitation and moisture flux along the Western India are present regardless of topography since the Southwesterly LLJ is present in all simulations. This is due to the dry thermal forcings from increased summer solar insolation and sensible heating found across Central Asia. From our analysis, we find the meridional gradient is changed in the cases where the IP is removed. Suggesting out of the three-main topography (HM, TP and IP), removing the IP reduces the overall wind and precipitation fields across Western Ghats. This is most likely due to the increased in downstream convergence over the Southeastern Tibet, and an eastward shift in .

The key monsoon characteristics identified above are subject to the changes in the monsoon-low found in Northern India and eastern China. Here we provide an in-depth surface energy budget between our CNTRL and RemAll simulations to diagnose the formation of the monsoon monsoon-low (Fig. 4.7). Not surprising, the monsoon-low consist of high temperature and moisture found in central Asia, such that there is a compensating effect when topography is removed (Fig. 4.7a). By eliminating the terrain, we find higher temperatures over northern India, but with a much lower specific humidity (Fig. 4.7b, 4c). The lower regional humidity weakens latent and diabatic heating across Southern Asia. However, we find that the climate system is then balanced by increasing the total net shortwave radiation and sensible heating at

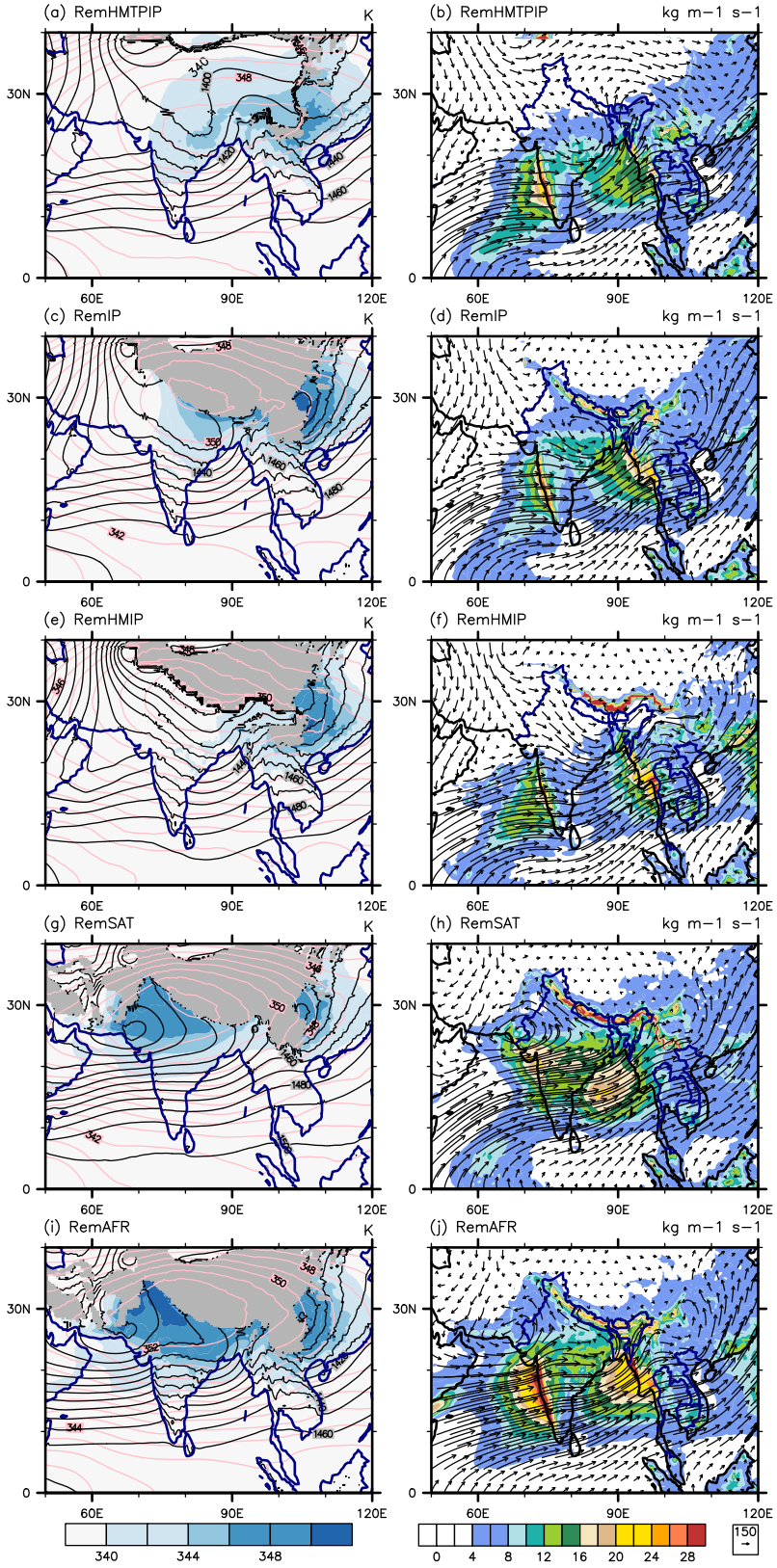

Fig. 4.6. As is in figure 4.4, but for cases (a,b) RemHMTPIP, (c,d) RemIP, (e,f) RemHMIP, and (g,h) RemSAT.

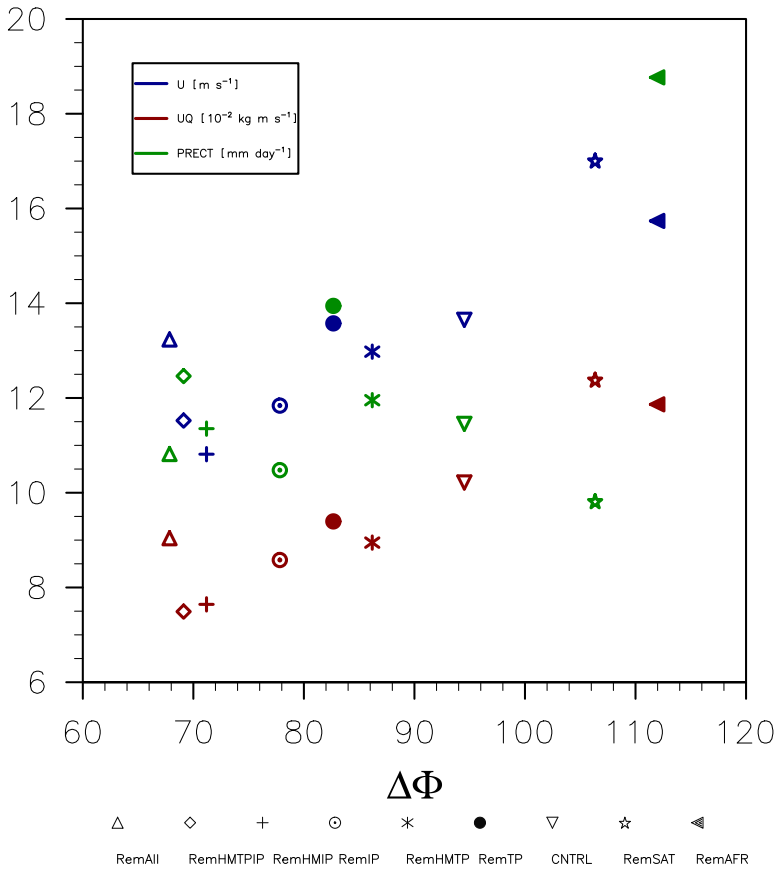

Fig. 4.7. The Markers represent average magnitude of 850 mb zonal wind (blue), Intergraded (1000-600 mb) zonal moisture flux (red), and total precipitation rate (green) across the Western Ghats. The x-axis shows the change in geopotential height (850 mb) between the set locations in figure 1b. The location where the averages were taken is found in figure 2b.

the surface (Fig. 4.7 d-g). These compensations in the surface energy budget is then accountable for maintaining the formation of the monsoon-low.

Analysis on the vertical structure of the zonal wind shows the Southwestern LLJ is persistent and weakly impacted, while alternatively the Easterly LLJ is heavily influenced by presence of topography. We note that removing the topography over Africa imposes the largest positive change on the Southwesterly LLJ (Fig.4.8d), which is supported by previous results [103]. The Easterly LLJ was originally described as a barrier jet that is driven by the topography and maintained by the monsoon-low. We use our results to test such hypothesis. We find that the cyclonic circulation centered near northern India is geostrophic in nature. This is especially the case for the RemAll and RemHMTP simulations (Fig. 4.8b). However, this flow is strongly modified when the HM is present (Fig. 4.8c). We simulate a more vigorous jet along the Indo-Gangetic Plain as the onshore Bay of Bengal flow is then funneled by the Himalayan Mountains. Removing the IP weakens the Easterly LLJ, and removing both HM and IP while maintaining the TP changes its sign. The reversal of flow is most likely a product of the mechanical downwind convergence by the TP [24]. Since the easterly LLJ is present in our RemAll simulation, we can robustly say that topographic blocking only augments the vigorousness of the IG LLJ.

4.7.3 Further Discusion

Prior work [15] as well as our own, shows that the modern day monsoon can be induced without the TP. Such results have also been previously interpreted as (1) thermal heating on the slopes of HM inducing a land-sea breeze or (2) a mechanical insulator that blocks cold extratropical air. However, we demonstrated that first order mechanism which sets up the continuous flow of moisture into the Central Asia is the monsoon-low that is set up by strong net solar insolation found in Northern India and Central China during the summer season. This monsoon-low is geostrophic in nature but is augmented by the surrounding terrain. Simplistically topography acts as

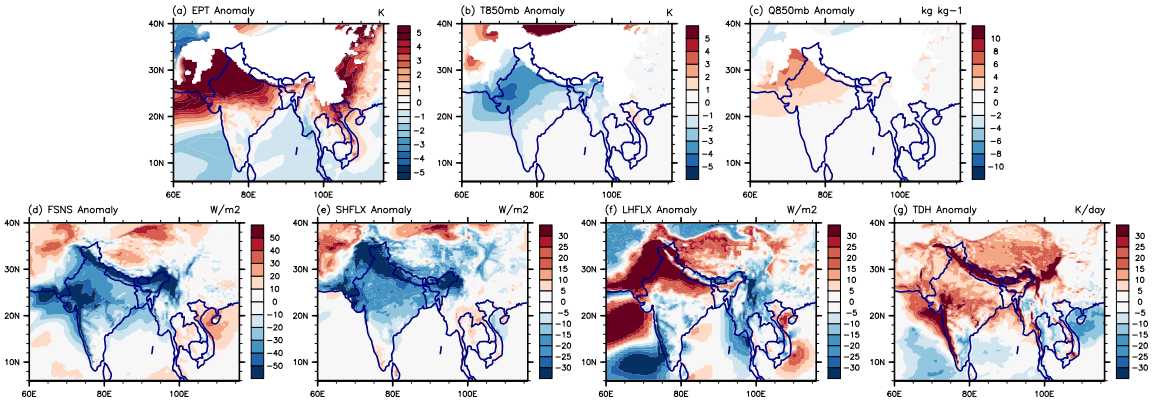

Fig. 4.8. Surface energy budget anomaly between our CNTRL and RemAll cases: (a) equivalent potential temperature at 850mb, (b) temperature at 850mb, (c) specific humidity at 850mb, surface net shortwave radiation, surface sensible heating, surface latent heating and integrated total diabatic heating 1000-100mb.

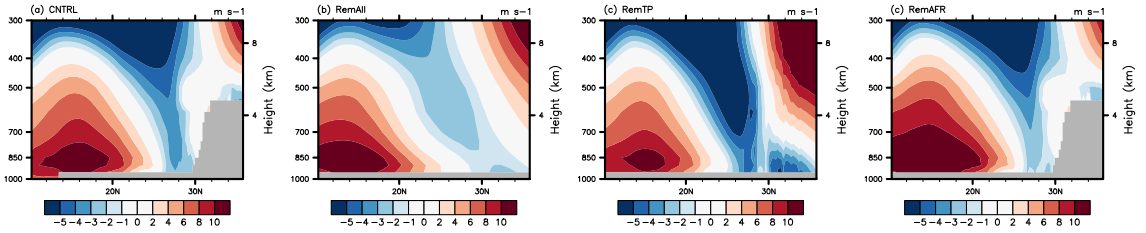

Fig. 4.9. Vertical profile of JJAS zonal winds averaged over 70E and E for the four key cases: (a) CNTRL, (b) RemAll, and (c) RemTP. Red contours represent Southwesterly Low-Level Jet and blue contours are Easterly Low-Level Jet.

barrier that funnel, lift and enhance the onshore moisture flux. In this view, the mean onshore flow of moisture can then be divided into two distinct systems: a southern branch that is derived from the Southwesterly LLJoccurring regardless of topographic presence and a northern branch that is derived from the Easterly LLJpredominantly reliant on orography to redistribute and uplifting the supply of moisture from the Bay of Bengal.

Nevertheless, topography is still a key component of the SAM, which allows the thermal overturning circulation to move further into the continent. For instance, we find the SAM diagnostically follows radiative convective equilibrium theory [45] especially in the RemAll case, however, topography moves its moist convective region further than other tropical monsoon systems. We note that the distribution of can be grossly predicated with theory that does not include topography as a parameter. Additionally, we find the SAM having a unique system where the boundaries of the Himalayan Mountains and Iranian Plateau not necessarily insulate, but allow the onshore flow to build up over the region [67]. We find that intrusion of dry low-entropy air from the northwest region is only valid when the Tibetan Plateau downstream convergence mechanism is present, and a form of subtropical orographic precipitation persists when the HM and IP is removed. Such results contradict the importance of the high air found in northwest India, as well as the criticality of the insulation effect [15, 131].

Although the Easterly flow is invoked by the monsoon-low and can exists without topography, a vigorous jet is not simulated without the HM. From our analysis, we conclude that the strength of the Easterly LLJ relies on both the vigorous of the monsoon-low and orographic blocking by the Himalayan Mountains. We note that the cyclonic circulation modulates cross Northern India is does experience reversals in synoptic scales [158, 159]. Interestingly, the zonal component of the Southwesterly LLJ is not strongly tied to the topography and such flow becomes stronger when the mountains over Africa are flattened [103]. Such results contradicts the importance of the cross-equatorial flow such that the African Horn is key for inducing the Somalia

Jet [37]. Additionally, the importance of the Western Ghats Mizoram mountains in Southern Asia have been shadowed by the Tibetan complex, however, results from high-resolution models highlights how they can alter the Southwesterly LLJ. Lastly, this study only looked at the seasonal response of the Southwesterly and the Easterly LLJ to topographic forcings and did not touch upon onsets. Thus, triggers for rapid onsets is beyond the scope of this study.

Interpretations of proxy records regarding the SAM is closely tied to the uplift or existence of the TP [7,149]. Often, interpretations from a paleorecord are extrapolated to try and explain the broader climatic regime or the elevation of TP. For example, marine sedimentary records from the Indian Ocean, which primarily reflect shifts in the strength of the Southwesterly Somali Jet, have been used to interpret changes in the uplift rate of the TP and the evolution of Asian climate [6, 106]. However, our simulations show that the southern branch of the SAM is largely unaffected by changes in TP nor HM, therefore, such interpretations about the height of TP based on the Southwesterly Jet may require revaluation. As we pointed out, regional topography does play a role in the spatial distribution of precipitation, thus, interpretations of sediment records, especially those found in the Bay of Bengal or Arabian Sea should be recognized as a regional signal. For instance, the flux of sediment into the mouth of Northern Bay of Bengal and Arabian Sea can be presumably linked to the height of the TP, while the sediment further from the origin should be considered as an integral of fluxes from Tibet and other mountain ranges like the Western Ghats and Mizoram Mountains.

Our results demonstrate that the SAM can exists without the presence of topography in Central Asia and supports the conclusion that the SAM was present during the past when the Tibetan Plateau configuration was more variable [31, 49, 100, 132]. This conclusion disputes studies that suggest that the uplift of the HMTP during the Miocene was the consequence of the poleward shift in the ITCZ [Allen and Armstrong, 2012]. Our findings show the northern branch of SAM is tied to the terrain in Central Asia and implies that the poleward precipitation regime could not have existed with-

out the aid of local topography. Thus, it is more likely that uplift must have occurred first. In addition, since oxygen isotopes are also constrained by the regional moisture source and attempts in modeling such methods should be conscientious of model limitations. For example, from our analysis using low-resolution models may have erroneously assumed that the moisture originates from the Southwesterly monsoon, while in fact, it originates from easterly flow from the Bay of Bengal.

5. DRAWBACKS OF USING THE THERMODYNAMICS PALEOALTIMETRY

Abstract

The focus of this work is to highlight the strengths and weaknesses of the thermodynamic paleoaltimetry method or paleoenthalpy method. The paleoentalphy method is predicated upon the annual mean atmospheric temperature profile along an air mass trajectory being close to a moist adiabat. Rigorous tests of this method are lacking, however. As a self-consistent assessment of this method, we simulate a suite sensitivity tests on is the Himalayan-Tibetan complex. The model presented in this study is the family of climate models developed by the National Center for Atmospheric Research: Community Climate System Model version 3 and 4, and the Community Earth System Model. The three questions we highlight are (1) how does simulating the climate system in a higher model resolution impact the paleoenthaly estimates, (2) is there an elevation limit to the method, and (3) how does altering the climate system to a warmer world impact estimates.

Our results demonstrate that changing the model resolution has a small impact, which is crucial for the future application of this method. However, planetary-scale changes to the Tibetan Plateau elevation suggest that the paleoenthalpy method is unreliable with low and high mountain ranges. Lastly, moist static enthalpy estimates increase as we increased global temperature, which results in a decrease in calculated maximum elevation. In general, calculated paleoenthalpy has a 1 km uncertainty [Forest, 2007] and such uncertainty increases as we increase global mean temperatures.

5.1 Introduction

The height and morphology of an elevated terrain, coupled with the regional atmospheric circulation dramatically alter local climate systems. Mountains dictate regional wet or dry regimes and ultimately impact their surrounding ecosystems. For example, the windward side of a mountain range can create a healthy cloud forest like those found in Central America [160]. Alternatively, the lea-ward side can induce a Rain-Shadow effect [100] that produces discrete dessert regions on the back side of mountain ranges much like the Basin and Range located on the Western side of North America or even widespread continental desertification such as Central Asia. Understanding the uplift history of topography is fundamental to unraveling the regional climatic evolution.

One iconic example of such mountain dynamics is the interactions between the Tibetan Plateau (TP) and the surrounding atmosphere. The orogeny of TP was hypothesized to influenced both the global climate and is tightly connected to the paleoclimatic evolution of the Asian continent throughout the Cenozoic [7, 134]. The surface uplift history of the TP is currently still under debate [161]. Perhaps, the only well-recognized event is that the Indian and Asian continent collided during the early Eocene (55 Mya) [162], which in turn caused crustal shortening and further surface uplift over Eurasia [161, 163].

The subsequent orogen history is still an active research. For instance, studies have hypothesized three main scenarios for the rise of the Tibetan Plateau during the Cenozoic. Many convey that prior to the collision, Central Asia possessed an Andean like mountain belt, with relief that is nearly equal at height as the modern day Tibet (4000 m) [164]. While others estimate even higher elevations [165] and rule out theories that suggest continuous growth after the Indo-Asian collision [166]. Contradictory to these studies, others suggest that the surface uplift began in the early Eocene and did not reach modern like elevation until the Miocene [167–169]. Lastly, others believe Tibet was approximately half of the modern elevation during the early

Miocene and surface uplift halted after the Miocene, which requires rapid uplift and follows that of a step-wise uplift model [170, 171]. In short, the paleoelevation history of TP is circumstantial and makes it the ideal location to test our paleoenthalpy studies. The discrepancies in estimated paleoelevtion between fossil leaf, and stable isotope proxy emphasis the need to further understand the tectonic history of the region.

Various approaches to studying paleoelevations of Tibet include paleotemperature reconstructions [161], stable isotopes [163, 167, 172], clumped isotopes [173] , and leaf physiognomy with moist enthalpy [132, 165, 168]. For the purpose of our study we focus mainly on the paleoenthalpy method. The paleoenthalpy method relies on ranges of temperature and humidity that a modern leaf taxa can tolerate [174]. This method also requires an empirical relationship between altitude, temperature, and humidity derived from modern calibrations, which has been the primary criticism when applied to different paleoclimate regimes.

Estimating ancient topographic relief using paleoenthalpy assumes that foliar characteristics of leaf fossil correlate to that of a modern leaf morphology of plant assemblages [175]. Leaving aside vital effects of species as they succumb to different environments, methods that use leaf physiognomy can back calculate paleoenthalpy by using modern leaf physiology and making an assumption about their environmental habitats. Paleoenthalpy is derived from conservative thermodynamics process, moist static energy:

$$H = C_p T + L_v q + gz \tag{5.1}$$

The measure of an air parcels moist enthalpy primarily relies on temperature and amount of water vapor in an air parcel. These values are the sum of none conservative fluxes and conserved potential energy processes corresponding to ascent or descent of the air parcel. Moist static energy is useful for inferring paleoelevation due to its tendency to be nearly conserved as air parcels move up altitude. Additionally, is

strongly constrained by convection, such that the subcloud and surface moist enthalpy (h) should be closely equal.

$$h = C_p + L_v q \tag{5.2}$$

Ultimately, we can back track the height of a terrain by calculating the difference between the moist enthalpy proxy found an the sea level and another found over the elevated topography [176].

$$Z = \frac{h_{sealevel} - h_{topography}}{g} \tag{5.3}$$

As described in Forest [2007] the paleoenthalpy method assumes that moist enthalpy of an air parcel is nearly conserved along trajectories such that it follows that of a moist adiabatic profile. Such assumption holds true in regions that are actively in convectively neutral state. Thus, application of this method in tropical environments has given estimated heights of various iconic terrains [168, 177].

By coupling both proxy records and GCM output, Spicer et al., [2003] were able to apply this method to the Tibetan Plateau. In their analysis they used Miocene age fossil leaves assemblages collected from Namling Basin. However, since coeval fossil leave assemblages were not found near sea level, they then used a Miocene simulation for the sea level moist enthalpy. This combined method gave an estimated Tibet height closer to the modern day (4,689 m) 15 Myr ago.

Nevertheless, there are many assumptions regarding terrestrial lapse rate when calculating the paleoenthalpy of a mountain range. For instance, from Forest [1995,2007] we can discern that low-elevation terrains present complications when using the moist enthalpy method. Additionally, Meyer [2007] showed that the difference in mean annual temperature between coastal and continental areas differ from 2-10 C/km. Such difference accounts for uncertainties in calculated elevation estimates. Meyer, [2007] further allotted such differences to (1) influence for maritime cooling effects, (2) difference in lowest elevation used, (3) orographic barrier effect and (4) furthest extent to moist regions, which are demarcated by the subtropical high-pressure zones. One solution proposed by Meyer, [2007] is the use of general circulation models (GCMs)

to calculate accurate mean sea level temperatures. By doing so, the effects of continentality, orographic dynamics and changes in past climate regimes can be mitigated.

This work builds upon Meyer [2007] work and aims to understand the limitations of the paleoenthalpy method. Our analysis is done using GCM output from the National Center for Atmospheric Research Community Earth System Model, further described in section 5.2. Section 5.3 test various parameters of the paleoenthaly method. Section 5.4 discusses the broader implications of our work, discern its usefulness for estimating orogen and gives concluding remarks.

5.2 Model Description

This study utilize the National Center for Atmospheric Research (NCAR) Community Climate System Model version (CCSM) with the Community Atmospheric Model version 4 as the primary atmospheric component. This model framework is extensively described Bitz et al., [2012], validated in Gent et al. [2010], and it forms the main basis of NCARs CMIP5 contributions. The CAM employs a finite volume dynamical core that provides a better representation of the hydrological system when compared to the spectral model. Specifically the CAM utilizes 26 vertical levels and parameterizes both deep and shallow convection using Zhang-McFarlane scheme [Hack, 1994; Zhang and McFarlane, 1995; Bitz et al., 2012]. The CAM interacts with Community Land Model version 4 (CLM4). For the sake of our experiments we will use both a slab Ocean and a prescribed sea surface temperatures (SST) and sea ice distributions. The slab ocean mode also referred to as swamp models, is equipped with a thermal mixed layer depth that allows heat flux across the ocean profiles. The temperature profiles are constructed from 30-year climatology of a control fully coupled model in slab ocean mode and a flux coupler that transfer conservative fluxes between models. The fix SST simulation uses monthly-observed SST and sea ice that were averaged over 1982-2001. The simulations used applied in our study is shown in table 1.

Table 5.1. Simulations used for the study. CNTRL for modern day land and surface properties, M-number represents double of CO2 used.

Case	Ocean Model	CO2 (ppm)	Resolution	Description
CNTRL	Slab	355	2	Modern day
TP-0	Slab	355	2	Remove Tibet
TP-1/2	Slab	355	2	Half Tibet
Low-Res	Fixed	355	2	Modern day
High-Res	Fixed	355	1/4	Modern day
Hybrid	Fixed	355	1/4	Low-res topography
M-3	Slab	2240	2	3xdoubling
M-4	Slab	4480	2	4xdoubling
M-5	Slab	8960	2	5xdoubling

We are aware that model is limited in multiple ways. For instance, analysis on Coupled Model Intercomparison Project 5 suggests that individual models can produce either a dry or wet climate over the monsoon region. We primarily used the family of NCAR models, which have yielded proficient results simulating the climate over the Indo-Asia, especially when using the high-resolution version. The coupling between the atmosphere-ocean is crucial in terms of paleoclimate analysis [Goldner et al., 2014]. We mitigated this error by utilizing a slab ocean model for some of our results. Lastly, changes in greenhouse gasses [Shields et al., 2016], aerosol emissions [Bollasina et al., 2011], orbital parameters and gateways [Roe et al., 2016] have effects on the regional the surface energy budget, which are not considered in our study.

5.3 Results

The spatial distribution of the h in both the low and high-resolution version of CAM largely similar (Fig. 5.1). However, the h distribution in the low-resolution model monotonically decreases as you move from lower to higher elevation. In comparison, the h distribution in the high resolution model is more heterogeneous. Comparison between the two simulations shows higher h values found in northern Tibet in the low-resolution simulation, while negative anomalous values over southern Tibet in the high-resolution model. Low values found in Southern Tibet are indicative of the model better representation of the peaks found in the Himalayan Mountains.

Values across our transect, we show an inverse relationship between the height of the terrain and the magnitude of h (Fig. 5.2). Such an inverse relationship is referenced across the subsequent plots, shown below. We note that in our low-resolution model the highest point in Tibet is located at the center and not in the Southern Himalayan range. This further illustrates the crude representation of topography in the low-resolution model. The high-resolution model shows abrupt h values at 25°N. As demonstrated by Acosta and Huber, [2017] the moisture source across this region is different between model resolution, where the low-resolution model has the mois-

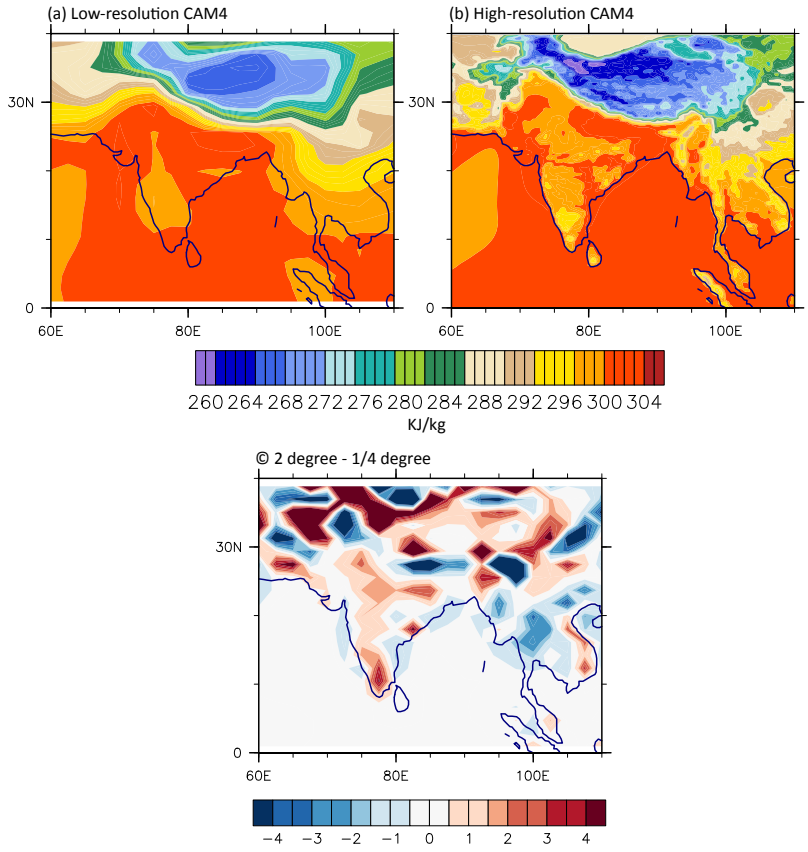

Fig. 5.1. Moist enthalpy distribution between high (a) and low (b) model resolution and the anomaly (c).

ture sourced from the Arabian Sea and the high resolution sourced from the Bay of Bengal. To distinguish if the discrepancy between the high and low model resolution is due to the topographic boundary condition or changes in circulation we plot the result from our Hybrid simulation (Fig. 5.2 purple line). The moist h distribution of the Hybrid simulation follows that of the low-resolution model, indicating that the increasing model resolution does not dramatically change the temperature and moisture distribution. There are lower h values from 20-25°N.

We use a suite of low-resolution simulations to test if h estimates are truly conserved when we change topographic boundary conditions. In this analysis, we vary the height of Tibet from a flattened Asia to double Tibetan Plateau. The transect of h between our sensitivity models shows that increasing the height of Tibetan Plateau

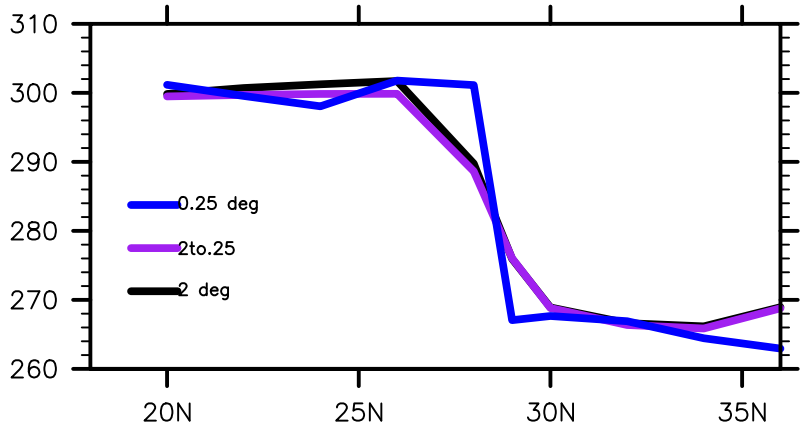

Fig. 5.2. Changes in h across transect a-b in figure 1a as a function of model resolution.

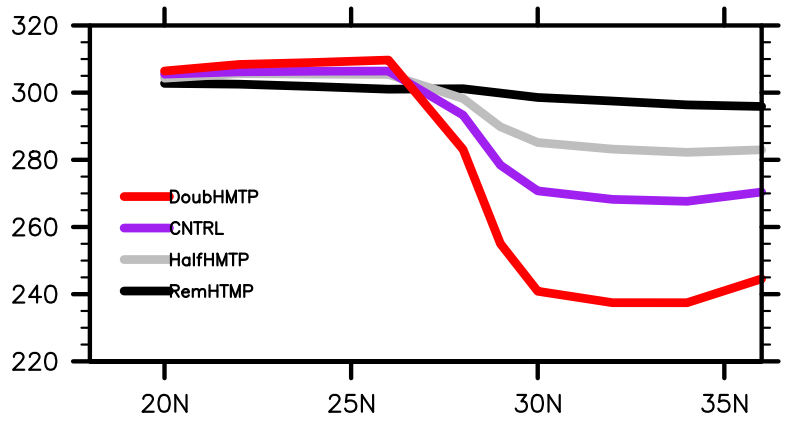

Fig. 5.3. Changes in h across transect in figure 1a as a function of changing Tibetan elevation.

h monotonically decreases the value of h (Fig. 5.3). Values found over India are relatively consistent but has the tendency to increase h as we increase the height of Tibet. However, a decrease in h at higher latitudes are more abrupt when we increase the height of Tibet. This is most likely due to non-linear qualities of moisture.

Qualitative comparison between actual elevation and calculated elevation when we alter the height of Tibet show major drawbacks in using the method. For instance, our result shows calculated heights from paleoenthalpy method overestimates the height of Tibet is lower, while substantially underestimates the elevation as when the Plateau is taller (5.4). The more quantitative comparison shows the residual error in meters (5.5). While the calculation of elevation when the height of Tibet is approximately half of the modern Tibet is accurate, at modern-day the residual error is 1000 (m). This 1000 m error has been noted by several studies [132,178]. However, We find that at the extreme heights the residual errors can be up to 3000 m and at lowest elevations, the estimated heights are negative heights. This demonstrates the paleoenthalpy method is unreliable in low and exceptionally high mountain ranges. This imply that paleoenthalpy values of an elevated terrain is either in the range of the actual elevation or severely underestimates the actual height of the topography.

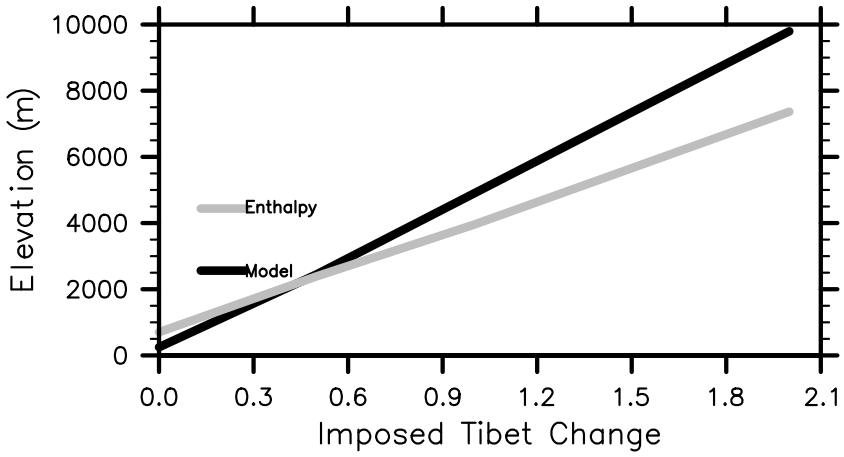

Fig. 5.4. Actual versus calculated elevations as a function of changes in Tibetan elevation.

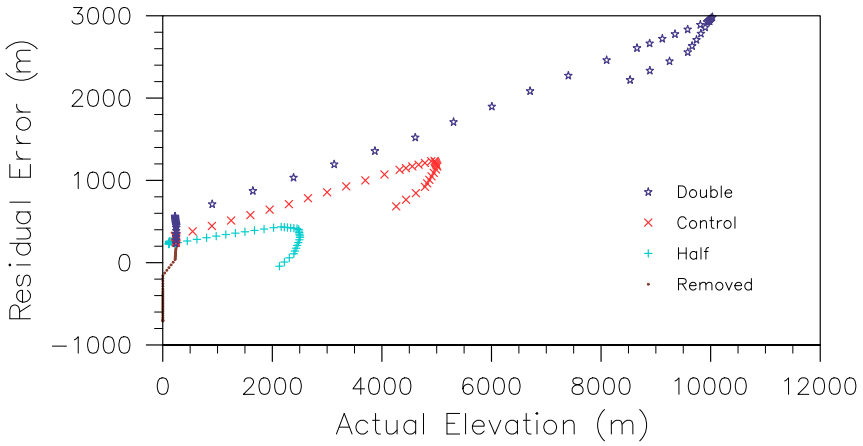

Fig. 5.5. Changes in h across transect in figure 1a as a function of increasing global temperature.

Since humidity is subject to changes as global surface temperature increases [Held and Soden, 2006], the vertical distribution of moist h is also altered. We test if h estimates of topography are consistent when global temperature is increased by varying degrees of CO_2 forcing similarly to Huber and Caballero [2011].

Qualitative analysis on surface h distributions shows an overall increase as global temperatures warm. Changes in h over lower elevation is 20 ($KJkg^{-}1$), while changes over higher elevation is 25 ($KJkg^{-}1$). The increase in global temperature results in a decrease in calculated maximum elevation (Table 2). The residual error is approximately 100 m decrease per degree of temperature change. This would suggest that the application of this method in the mid-latitude when we increase global temperature will result in much lower predicted topographic elevation. However, errors in h due to temperature changes are secondary in comparison to topographically driven errors.

5.3.1 Model diagnosis

Here we delve into understanding why we see such drastic bias in our topography test. Additionally, [177] suggested monsoon seasons have an impact in paleoenthalpy

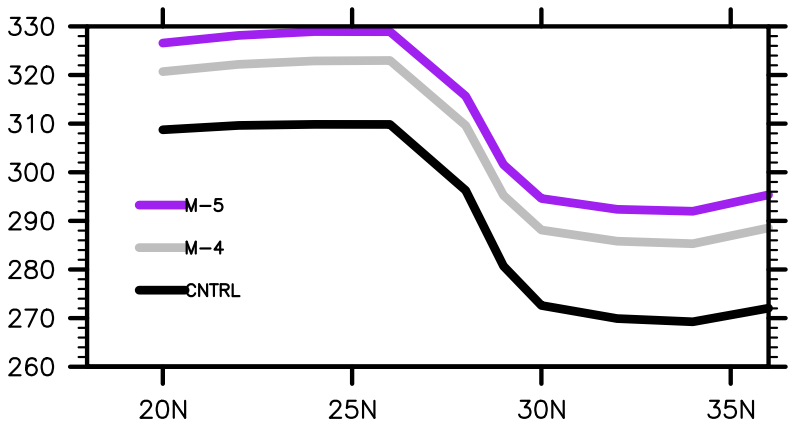

Fig. 5.6. Changes in h across transect in figure 1a as a function of increasing global temperature.

Table 5.2. Estimated elevations using paleoenthalpy method from warm climate simulations. Note: The maximum used height along the transect is 5001.3 (m)

Case	Sea level (h)	Topography (h)	Calculated maximum Z
CNTRL	309.857	269.214	4143.017
M-4	322.993	285.288	3843.527
M-5	328.97	291.993	3769.317
Mio	326.571	287.79	3953.24

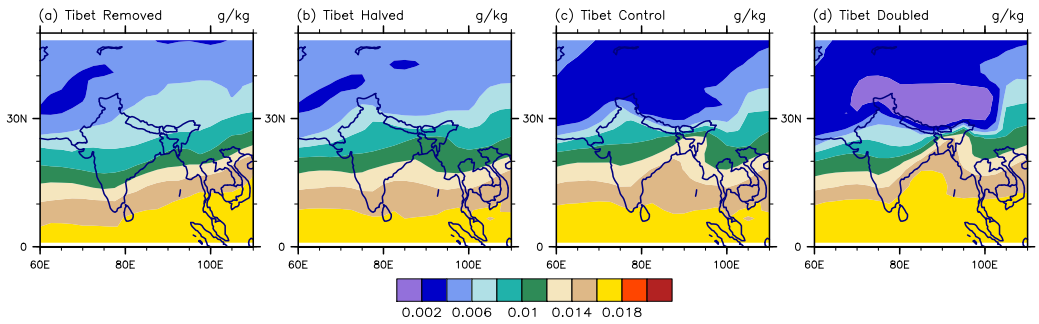

Fig. 5.7. Changes in humidity distribution as model height is varied.

calculations, thus we present seasonal changes in temperature and humidity and calculations height given a season. We extend this analysis in our CO_2 test.

Further diagnosis shows that difference in temperature and humidity between lower and higher elevated surface substantially widens as we increase the height of the Tibetan Plateau. This makes the top of topography increasingly drier and wetter, and in contrast, increasing temperature and moisture near the surface. Such contrast increases the back-calculated topographic height. However, the change in temperature and humidity is not enough to fully capture the actual height of the terrain. Thus either a much hotter or moister surface or a colder (dryer) elevated region or both would yield higher back-calculated terrain height.

Seasonal changes in regional circulation have a substantial impact on the calculated paleoaltimetry estimates. Northern Hemisphere warming generally increases both low and elevated surfaces. However, the Indo-Asian Monsoon brings an abundant onshore moisture that leads to increases in atmospheric humidity, thus increase in latent heating. Here we find increasing temperature and humidity over elevated regions lead to substantial underestimation of topographic height. Similar results are found in our CO_2 warming case, where increase temperature leads to increase humidity over elevated surface which then also leads to underestimation of topography height.

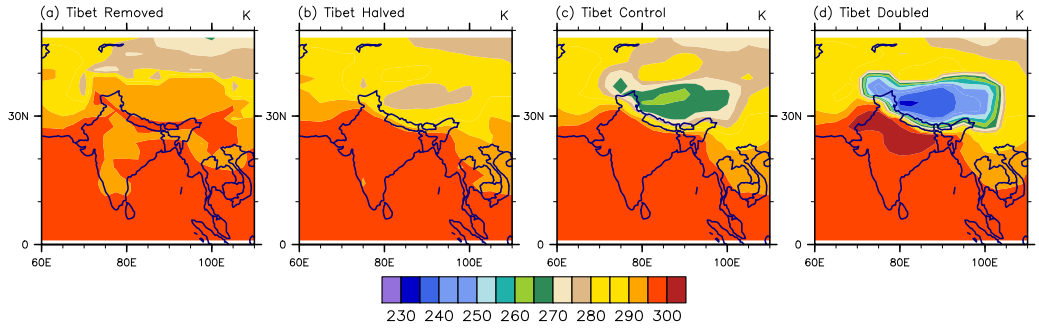

Fig. 5.8. Changes in temperature distribution as model height is varied.

Table 5.3. Estimated elevations using paleoenthalpy method from seasonal experiment. Note: The maximum used height along the transect is 5001.3 (m)

Case	Sea level (h)	Topography (h)	Max Z
Jan	295.4	253.6	4268.8
April	308	264.6	4423.8
July	306.6	281.1	2593.1
Oct	303.6	267.1	3720.7

5.4 Discussion

The paleoenthalpy method has been actively used to estimate the height of the Tibetan Plateau. Although, the field has highlighted GCMs as a tool that can minimize the uncertainties arising from local climate variability and discrepancies between modern and paleo analogs, a GCM based the paleoenthalpy study have not been presented. We test the limits of the paleoenthalpy method with the following hypotheses:

1. Are climate model estimates of h consistent as we increase model resolution?
2. Are h estimates of topography truly conserved as we modify topographic boundary conditions?
3. Are h estimates of topography consistent as we vary the modeled climate regime.

By utilizing a suite of model complexities we can elucidate the viability and setbacks of using such method.

Our analysis shows that changing model resolution does not substantially change the distribution of moist enthalpy between the sea-level and the chosen elevated region. This was clearly demonstrated by our Hybrid simulation. Although high resolution modeling have major impacts on the circulation, especially over Indo-Asia, such result highlights the robustness of physics of the climate model. Our result further encourages the field to use high-resolution models for general paleoclimate studies. Changing topographic boundary conditions presents complications in estimated moist enthalpy.

However, even with the simplest example, calculating a standard modern-day topographic elevation with the paleoenthalpy method results in a lower estimated height. Furthermore, such error increases as we continuously increase the height of the Tibetan Plateau. This result has major implication not only for Tibet Plateau and other high mountainous regions on Earth but also the expansion of this method to other terrestrial planets. Perhaps the largest complication using this method presents itself when we apply such method to different seasons and different climate regimes. In particular, during the monsoon season, moisture distribution over elevation begin to

match those found in lower elevation, resulting into a much lower estimated elevation. Additionally, at higher temperatures regimes, the predicted terrain height is also lowered. These results highlight the systematic bias of utilizing this method for predicting the height of the Tibetan Plateau throughout the Cenozoic.

Forest et al., [1999] argued that in the mid-latitudes upper-troposphere the zonal distribution of moist h follow that of a conserved trajectory. Such an assumption enabled this method to be applied to meridionally orientated mountain ranges found in the mid-latitudes, like the Sierras and various parts of the Andes. Since an adiabatic lapse-rate profile is a requirement for this method, such assumption is often not met in the mid-latitudes, where the lapse-rates vary drastically in a given season [Yang and Smith, 1985]. Additionally, the western coasts that are highly impacted by upwelling regions, and variation on sea surface temperature may implicate paleoenthalpy estimates [Meyer, 2007]. Moreover, moisture source over the region are not only generated west to east, for example, summertime rain can move up from the Gulf of California illustrating a south-to-north trajectory.

Under convective quasi-equilibrium, the surface (h) can be estimated as the subcloud θ_e Xu and Emanuel, [1989]. In these regions, the boundary layer equivalent potential temperature (θ_e) (or subcloud θ_e is approximately equal surface (h), which ultimately allows back calculation of paleoaltimetry. Today these regions extend mainly to the subtropics (30 N to 30 S) and potentially further depending on the time of the year. However, recent findings using theory on slantwise convection suggest that these regions are expected to expand into extratropics during in warmer climatic regimes [179]. As convectively neutral regions expand during a warmer climate regime, one could hope to use the paleoenthaly method at higher latitudes. However, results from this study should present caution.

Perhaps the combination of proxy data corrected with a modeling framework similar to seminal work by Fang and Poulsen [2016] can alleviate the biases we presented in this article. Under the assumption of slantwise convection and incorporation of a proxy-model framework, we can truly discern paleoaltimetry of various mountain

ranges. Our work corroborates with the findings of Fang and Poulsen [2016] and encourages the field to incorporate a model base correction factor to the paleoaltimetry study. Additionally, isotope modeling studies have been found useful, and could potentially increase the robustness of paleoaltimetry estimates.

Although our Hybrid model calculated similar results to our low-resolution model, it has been shown that moisture flux transport is highly impacted by model resolution. This is especially the case during the monsoon season where the Indo-Gangetic LLJ is active. We showed that seasonality of h varies quite dramatically. Thus, it is crucial to know the plant physiology and growing season to produce fruitful h calculations.

5.5 Conclusion

This study looked at the viability of using using the paleoaltimetry method, paleoenthalpy on the Tibetan Plateau complex. Results presented here were generated using the family of NCAR climate models that varied in complexities such as model resolutions and ocean model components. As a first order test we demonstrated that results from high-resolution models are consistent with its low-resolution counter part. However, we demonstrated that the paleoenthalpy method fail to reproduce the standard modern day height of Tibetan Plateau. Additionally, the calculation consistently underrepresented terrain height as we increase the height of the Tibetan Plateau, while overestimating simulations with substantially lower terrains. As we increase model temperature we find consistently lower predicted terrain height. Overall we find that sensitivity to changes in temperature and humidity over elevated surface lead to errors in topography estimations.

6. FUTURE DIRECTION

6.1 Unraveling the phenology of the Indo-Gangetic Low-Level Jet and its influence on the Himalayan water towers.

The nature of the Indo-Gangetic Low-Level Jet (IG LLJ) is not fully understood. While the work presented in Chapter two illustrates a modeling perspective, true observations have yet to be collected. Thus to prove its existence would require a vast network of in situ based observations along the Indo-Gangetic Plain (referred to as the Plain hereafter). Thus, as new products are generated, the discovery of how the LLJ impacts the IAM circulation and society represents a new frontier.

Nevertheless, its impacts are already being studied. A primary example of this is the persistence of aerosol mainly soot that lingers over Northern India. Satellite observations during the winter show an immense haze blanket that consists of dust, fog and industrial emissions, which lead to hazardous air quality. This is because the IG LLJ becomes dormant during this time and the lack of rainfall over the Plain, which normally scavenge particulates in the atmosphere, allows accumulation of Aerosols. Thus a modeling study of the IG LLJ with the proper aerosol physics should be completed.

Another impact the IG LLJ is its relation to the monsoon active phases which brings tropical disturbances that originate from the Bay of Bengal and moves along the Plain. We demonstrated in chapter two that the IG LLJ is active primarily during the peak summer season. Although modeling prediction of rainfall is difficult over the Plain is rather a difficult task, we speculate that the strength of the IG LLJ active phases can be correlated with the the monsoon low. Another avenue of this work is looking at a time-series analysis of the IG LLJ and precipitation patters over the Plain and the Himalayas.

Furthermore, there is an inherent link between the LLJ and orographic precipitation along the Himalayas. However, as we've shown before, climate models widely vary on how they simulate the types of orographic precipitation. This is primarily due to how each model treats the high entropy monsoon air within a cloud column. Since climate models lack the resolution to resolve convection, simplified parameterization schemes are used as solutions for overcoming their limitations. For instance, deep and shallow precipitation are often treated as separate schemes, which often leads to uncertainties when the model transition from convective storms to stratiform rain. Additionally, mechanically uplifting moisture can be readily converted to large-scale precipitation. Understanding how topography interacts with parameterization schemes can help shed some light orographic precipitation biases.

Perhaps the most compelling work yet to be done is understanding the fate of the Indo-Gangetic LLJ under a warmer climate. Despite the projected weakening of the monsoon circulationalso known as the Wind-Precipitation Paradox" modeling evidence derived from the Coupled Model Intercomparison Project Phase 5 (CMIP5) projects an increase in precipitation rates across monsoon regions during the end of the century. However, controversy exists whether the monsoon systems are subject to tipping elements. This is in part because tropical monsoonal regions are driven by the continuous flux of moisture into the region, and weakening of overturning circulation should intuitively weaken regional convergence of moisture. As previously shown, especially in the case of the Indo-Asian monsoon, many of the models found in CMIP5 have difficulty capturing topographically driven low-level jets, and as a result, many models overestimate regional and orographic precipitation rates. Thus, to accurately project the evolution of the monsoon precipitation regime with climate change we must understand the evolution of near-surface moisture converge in the context of global climate change.

Climate change simulations found in the CMIP5 archive suggest that the Somali Low-Level Jet (LLJ) is strengthening, bringing more moisture and rain on the western Indo-Asian monsoon region Sandeep and Ajayamohan, [2015]. As this transition

occurs, due to the expansion of the monsoon Hadley-Cell circulation, the Somali Jet is also expected to shift poleward. As a result, future climate change project using CCSM4 at high-resolution, demonstrate an overall increase in precipitation rates across the Indian Subcontinent. However, observational evidence recognizes that when the Somali Jet is extremely active, moisture flux from the Bay of Bengal weakens, limiting transport of high entropy air to the far eastern side of Indo-Asia. This inability to move moisture from the Bay of Bengal into the Indo-Gangetic region suffocates the formation of precipitation over the Ganges Basin and Central India.

Additionally, historical trends from both observations and simulations identify the excess anthropogenic aerosol over the Indo-Gangetic Plains as the cause of weakening rainfall rates. While, under extreme climate change projections, increase in greenhouse gasses eventually overcomes the negative feedback aerosols provide and suggest strengthening of precipitation over the region. Although radiative balance in the model is robust, increasing model resolution show large changes in regional monsoon circulation.

An alternate plausible outcome is presented, where the expansion of the Somali Jet limits the formation of the Indo-Gangetic Jet and augmented by aerosol direct and indirect forcing could ultimately switch the Ganges Basin and Central into a dry state. Since the Indo-Gangetic LLJ is only resolved in climate models at ultra-high resolution, the goal of this project is to run an atmospheric model capable of producing the aerosol effects at ultra-high resolution.

Previous work has shown through high-resolution regional climate modeling that the cyclonic circulation found in Ganges Basin may be shifting toward Bangladesh and ultimately suppressing the eastern branch of the IAM. This weakening of easterly flow decreases precipitation across the Ganges Basin and the IGP. This is supported by other high-resolution regional climate models that also project monsoon suppression for the end of the century. Further, historical rainfall trends analysis by Latif et al., [2016] showed an overall weakening of moisture flux over BOB into the IGP, this results in lower precipitation rates across the Himalayan Foothills and the Ganges

Basin. This weaker eastward flow was found anti-correlated with the strength of the westerly Somali Jet. It may be the case, that using climate models that can simulate the easterly flow across the IGP give us a different future projection than from those presented in the current CMIP5 archive.

6.2 The Iranian Plateau

Paleoclimate proxy records suggest that the IAM activity was further enhanced during the Miocene, and have been linked to the full development of the Tibetan orogeny. However, we demonstrated in chapter 4 that moisture flux and increase in precipitation rate across the Western Ghats is accounted for with Iranian Plateau present. Thus, further analysis ocean Sverdrup transport should reveal that the increase bioproductivity along the coast of Somalia during the Miocene is most likely due to the Iranian Plateau orogeny.

Interpretations of proxy records regarding the IAM is closely tied to the uplift or existence of the Tibetan Plateau. Often, interpretations from a paleorecord are extrapolated to try and explain the broader climatic regime or the elevation of Tibetan Plateau. Marine sedimentary records from the Indian Ocean, which primarily reflect shifts in the strength of the Southwesterly Somali Jet, have been used to interpret changes in the uplift rate of the Tibetan Plateau. However, results from the previous chapters show that the enhancement of moisture convergence flux over the coast of Somalia is primarily simulated with the Iranian Plateau is orogeny. Such results deemphasize the role of the Tibetan Plateau on initiating the strong upwelling system found over Somalia during the Miocene. Regional topography plays an immediate role on the regional circulation thus, interpretations of sediment records, especially those found in the Arabian Sea should be recognized as a regional signal.

The Iranian Plateau have been largely understudied, primarily due to the immense focus of the community on the Tibetan Plateau complex. The synergy between geologic and climatic studies of the area represents a new avenue of research. Determining

how the Iranian Plateau impacts the IAM environment, without the presence of the Tibetan Plateau or Himalayan Mountains is timely and is crucial to further developing our insight on the paleoclimate evolution of the Asian continent. This work is compelling because it links the climate modelling community to Asias geological history. Specifically, this study has implications for the interpretation of proxy data from current and future Asian monsoons IODP expeditions, and reinterpretation of IAM theory using high-resolution modeling.

7. SUMMARY

There are degrees of success elucidating the relationship between topography and climate systems. Most of which utilizes sophisticated tools like general circulation models and laid the ground work for the studies presented in this dissertation (Fig. 7.1). My work delved into theoretical mechanisms, thermal and mechanical, and builds upon seminal work on the interaction between the Tibetan Plateau and its influence on the surrounding hydrological system, the greater South Asian Monsoon system. The overall goal was to provide context for the competing monsoon theory and use such modeling tools to understand what are the roles of the surrounding topography on the general tropical monsoon system, if any. By applying such technique, we identified a secondary low-level jet that is crucial for the northern branch of the Indian monsoon. In addition, we demonstrated that model resolution has an immense impact on the low-level circulation, where crude model results led to false mechanism. Thus, my work also nullified previous theories that regarded the Himalayan-Tibetan Plateau as key features that control the South Asian Monsoon. From our analysis, we propose a new paradigm, where instead of the Tibetan Plateau, the Iranian Plateau acts as the gatekeeper to Indo-Asian Monsoon. To sum-up my dissertation, we utilize this framework to reevaluate the paleoenthalpy method and determined its strengths and weaknesses. Results from this study hope to clarify between competing monsoon theory, further our understanding about the role of topography on the general climate system, and better constraint paleoaltimetry records. This dissertation will be widely applicable to the modeling community, mountain-atmospheric dynamicist, and paleoclimatologists.

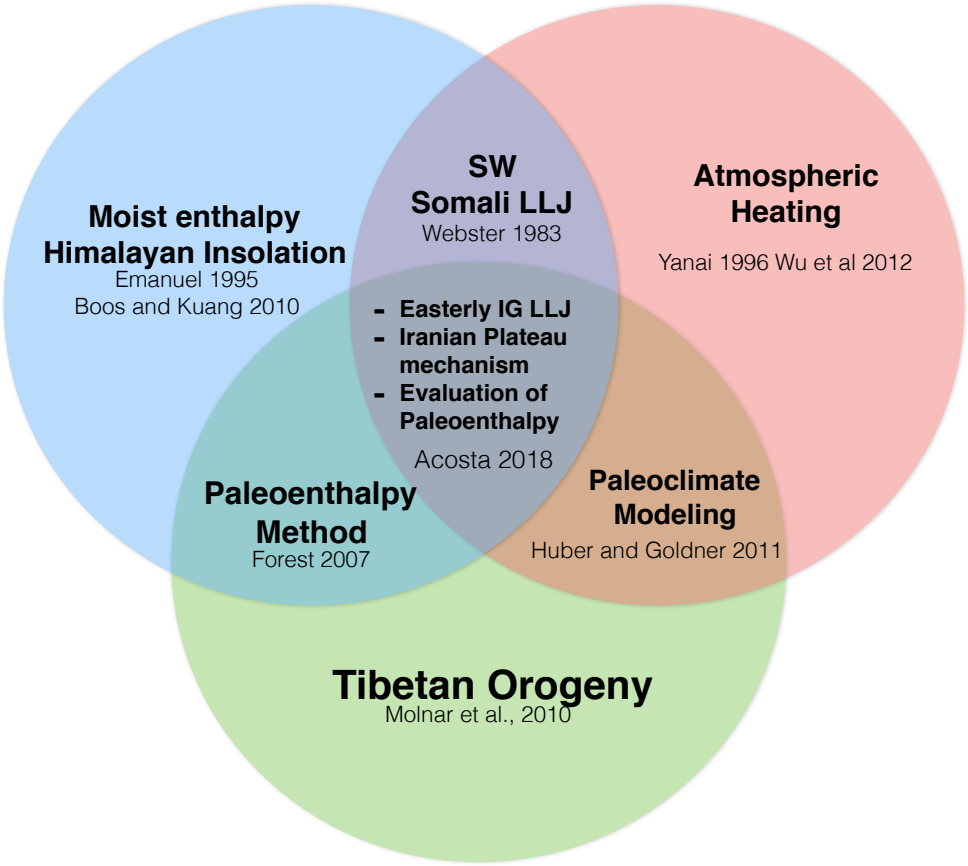

Fig. 7.1. Intersection of work presented in this dissertation.

REFERENCES

[1] M. E. Raymo and W. F. Ruddiman, "Tectonic forcing of late Cenozoic climate," *Nature*, vol. 359, no. 6391, pp. 117–122, 1992.

[2] J. E. Kutzbach, P. J. Guetter, W. F. Ruddiman, and W. L. Prell, "Sensitivity of climate to late Cenozoic uplift in southern Asia and the American west: Numerical experiments," *Journal of Geophysical Research*, vol. 94, no. D15, p. 18393, 1989.

[3] F. Ruddiman, J. E. Kutzbach, N. America, W. F. Ruddiman, and J. E. Kutzbach, "Forcing of Late Cenozoic Northern Hemisphere Climate by Plateau Uplift - I EO ," vol. 94, 1989.

[4] W. Prell and J. Kutzbach, "Sensitivity of the Indian monsoon to forcing parameters and implications for its evolution," *Nature*, vol. 360, pp. 647–652, 1992.

[5] A. Zhisheng, J. E. Kutzbach, W. L. Prell, S. C. Porter, Z. An, J. E. Kutzbach, W. L. Prell, S. C. Porter, A. Zhisheng, J. E. Kutzbach, W. L. Prell, and S. C. Porter, "Evolution of Asian monsoons and phased uplift of the Himalaya-Tibetan plateau since Late Miocene times." *Nature*, vol. 411, no. 6833, pp. 62–66, 5 2001.

[6] G. Zhuang, M. Pagani, and Y. G. Zhang, "Monsoonal upwelling in the western Arabian Sea since the middle Miocene," vol. 45, no. 7, pp. 655–658, 2017.

[7] P. Molnar, W. R. Boos, and D. S. Battisti, "Orographic Controls on Climate and Paleoclimate of Asia: Thermal and Mechanical Roles for the Tibetan Plateau," *Annual Review of Earth and Planetary Sciences*, vol. 38, no. 1, pp. 77–102, 4 2010.

[8] H. D. Reeves and Y.-L. Lin, "Effect of stable layer formation over the Po Valley on the development of convection during MAP IOP-8," *Journal of Atmospheric Sciences*, vol. 63, no. 2003, pp. 2567–2584, 2006.

[9] ——, "The Effects of a Mountain on the Propagation of a Preexisting Convective System for Blocked and Unblocked Flow Regimes," *American Meteorological Society*, vol. 64, pp. 2401–2421, 2007.

[10] R. H. White, D. S. Battisti, and G. H. Roe, "Mongolian mountains matter most: Impacts of the latitude and height of asian orography on pacific wintertime atmospheric circulation," *Journal of Climate*, vol. 30, no. 11, pp. 4065–4082, 2017.

[11] J. E. Martin, *Mid-latitude Atmospheric Dynamics A First Course*, 2nd ed. West Sussex, England: John Wiley & Sons, 2006.

[12] E. Halley, "An Historical Account of the Trade Winds, and Monsoons, Observable in the Seas between and Near the Tropicks, with an Attempt to Assign the Phisical Cause of the Said Winds, By E. Halley," *Philosophical Transactions of the Royal Society of London*, vol. 16, no. 179-191, pp. 153–168, 1686.

[13] M. Yanai and C. Li, "Mechanism of heating and the boundary layer over the Tibetan Plateau," *Monthly Weather Review*, vol. 122, pp. 305–323, 1994.

[14] M. Yanai and G.-x. Wu, "Effects of the Tibetan Plateau," in *The Asian Monsoon (ed. Wang, B.)*. Springer, 2006, no. 1950, pp. 514–539.

[15] W. R. W. R. Boos and Z. Kuang, "Dominant control of the South Asian monsoon by orographic insulation versus plateau heating," *Nature*, vol. 463, no. 7278, pp. 218–222, 2010.

[16] N. C. Privé and R. A. Plumb, "Monsoon Dynamics with Interactive Forcing. Part I: Axisymmetric Studies," *Journal of the Atmospheric Sciences*, vol. 64, no. 5, pp. 1417–1430, 5 2007.

[17] ——, "Monsoon Dynamics with Interactive Forcing. Part II: Impact of Eddies and Asymmetric Geometries," *Journal of the Atmospheric Sciences*, vol. 64, no. 5, pp. 1431–1442, 2007.

[18] S. Bordoni and T. Schneider, "Monsoons as eddy-mediated regime transitions of the tropical overturning circulation," *Nature Geoscience*, vol. 1, no. 8, pp. 515–519, 2008.

[19] T. A. Shaw, "On the Role of Planetary-Scale Waves in the Abrupt Seasonal Transition of the Northern Hemisphere General Circulation," *Journal of the Atmospheric Sciences*, vol. 71, pp. 1724–1746, 2014.

[20] W. C. Chao and B. Chen, "The Origin of Monsoons," *Journal of the Atmospheric Sciences*, vol. 58, no. 22, pp. 3497–3507, 2001.

[21] P. Webster and L. Chou, "Seasonal structure of a simple monsoon system," *Journal of the Atmospheric ...*, vol. 37, pp. 354–367, 1980.

[22] G.-S. S. Chen, Z. Liu, and J. E. Kutzbach, "Reexamining the barrier effect of the Tibetan Plateau on the South Asian summer monsoon," *Climate of the Past*, vol. 10, no. 1974, pp. 1269–1275, 2014.

[23] J. E. Kutzbach, W. L. Prell, and W. F. Ruddiman, "Sensitivity of Eurasian Climate to Surface Uplift of the Tibetan Plateau," *The Journal of Geology*, vol. 101, no. 2, pp. 177–190, 1993.

[24] H.-S. S. Park, J. C. H. Chiang, and S. Bordoni, "The Mechanical Impact of the Tibetan Plateau on the Seasonal Evolution of the South Asian Monsoon," *Journal of Climate*, vol. 25, no. 7, pp. 2394–2407, 4 2012.

[25] M. Rodwell and B. Hoskins, "Subtropical anticyclones and summer monsoons," *Journal of Climate*, vol. 14, pp. 3192–3211, 2001.

[26] K. A. Emanuel, "On thermally direct circulations in moist atmospheres," *Journal of the atmospheric sciences*, vol. 52, no. 9, pp. 1529–1534, 1995.

[27] P. Molnar and K. Emanuel, "Temperature profiles in radiative-convective equilibrium above surfaces at different heights," *Journal of Geophysical Research*, vol. 104, pp. 265–271, 1999.

[28] G. Wu, Y. Liu, Q. Zhang, A. Duan, T. Wang, R. Wan, X. Liu, W. Li, Z. Wang, and X. Liang, "The Influence of Mechanical and Thermal Forcing by the Tibetan Plateau on Asian Climate," *Journal of Hydrometeorology*, vol. 8, no. 4, pp. 770–789, 2007.

[29] J. Ling and C. Zhang, "Diabatic Heating Profiles in Recent Global Reanalyses," *Journal of Climate*, vol. 26, no. 10, pp. 3307–3325, 5 2013.

[30] J. S. Wright and S. Fueglistaler, "Large differences in reanalyses of diabatic heating in the tropical upper troposphere and lower stratosphere," *Atmospheric Chemistry and Physics*, vol. 13, pp. 9565–9576, 2013.

[31] M. Huber and A. Goldner, "Eocene monsoons," *Journal of Asian Earth Sciences*, vol. 44, pp. 3–23, 2012.

[32] M. J. Rodwell and B. J. Hoskins, "Monsoons and the dynamics of deserts," *Quarterly Journal of the Royal Meteorological Society*, vol. 122, no. 534, pp. 1385–1404, 1996.

[33] T. Tamura, K. Taniguchi, and T. Koike, "Mechanism of upper tropospheric warming around the Tibetan Plateau at the onset phase of the Asian summer monsoon," *Journal of Geophysical Research*, vol. 115, no. D2, p. D02106, 1 2010.

[34] A. E. Gill, "Some simple solutions for heat-induced tropical circulation," *Quarterly Journal of the Royal Meteorological Society*, vol. 106, no. 449, pp. 447–462, 1980.

[35] T. Schneider and S. Bordoni, "Eddy-Mediated Regime Transitions in the Seasonal Cycle of a Hadley Circulation and Implications for Monsoon Dynamics," *American Meteorological Society*, no. 1, pp. 915–934, 2008.

[36] P. J. Webster, V. O. Magafia, T. N. Palmer, J. Shukla, R. A. Tomas, M. Yanai, and T. Yasunari, "Monsoons : Processes , predictability , and the prospects for prediction," vol. 103, 1998.

[37] W. R. Boos and K. a. Emanuel, "Annual intensification of the Somali jet in a quasi-equilibrium framework: Observational composites," *Quarterly Journal of the Royal ...*, vol. 135, no. February, pp. 319–335, 2009.

[38] J. Zhai and W. Boos, "Regime Transitions of Cross-Equatorial Hadley Circulations with Zonally Asymmetric Thermal Forcings," *Journal of the Atmospheric Sciences*, p. 150904104933002, 2015.

[39] A. Arakawa and W. H. Schubert, "Interaction of a cumulus cloud ensemble with the large-scale environment, Part I," *Journal of the atmospheric sciences*, vol. 31, pp. 674–701, 1974.

[40] K. a. Emanuel, "Quasi-equilibrium dynamics of the tropical atmosphere," *The Global Circulation of the Atmosphere*, pp. 186–218, 2007.

[41] K.-M. Xu and K. a. Emanuel, "Is the Tropical Atmosphere Conditionally Unstable?" pp. 1471–1479, 1989.

[42] J. Fasullo and P. Webster, "A hydrological definition of Indian monsoon onset and withdrawal," *Journal of Climate*, vol. 16, pp. 3200–3211, 2003.

[43] V. S. Prasad and T. Hayashi, "Onset and withdrawal of Indian summer monsoon," *Geophysical Research Letters*, vol. 32, no. 20, p. L20715, 2005.

[44] K. a. Emanuel, J. David Neelin, and C. S. Bretherton, "On large-scale circulations in convecting atmospheres," *Quarterly Journal of the Royal Meteorological Society*, vol. 120, no. 519, pp. 1111–1143, 1994.

[45] J. Nie, W. R. Boos, and Z. Kuang, "Observational Evaluation of a Convective Quasi-Equilibrium View of Monsoons," *Journal of Climate*, vol. 23, pp. 4416–4428, 2010.

[46] G. Meehl, J. Arblaster, and J. Fasullo, "Model-based evidence of deep-ocean heat uptake during surface-temperature hiatus periods," *Nature Climate Change*, vol. 1, p. 360364, 2011.

[47] M. a. Bollasina and Y. Ming, "The general circulation model precipitation bias over the southwestern equatorial Indian Ocean and its implications for simulating the South Asian monsoon," *Climate Dynamics*, vol. 40, no. 3-4, pp. 823–838, 2013.

[48] J. L. Lin, "The double-ITCZ problem in IPCC AR4 coupled GCMs: Ocean-atmosphere feedback analysis," *Journal of Climate*, vol. 20, no. 18, pp. 4497–4525, 2007.

[49] a. Licht, M. van Cappelle, H. a. Abels, J.-B. Ladant, J. Trabucho-Alexandre, C. France-Lanord, Y. Donnadieu, J. Vandenberghe, T. Rigaudier, C. Lécuyer, D. Terry, R. Adriaens, A. Boura, Z. Guo, A. N. Soe, J. Quade, G. Dupont-Nivet, and J.-J. Jaeger, "Asian monsoons in a late Eocene greenhouse world." *Nature*, vol. 513, pp. 501–506, 2014.

[50] C. M. Bitz, K. M. Shell, P. R. Gent, D. a. Bailey, G. Danabasoglu, K. C. Armour, M. M. Holland, and J. T. Kiehl, "Climate Sensitivity of the Community Climate System Model, Version 4," *Journal of Climate*, vol. 25, no. 9, pp. 3053–3070, 5 2012.

[51] P. R. Gent, S. G. Yeager, R. B. Neale, S. Levis, and D. a. Bailey, "Improvements in a half degree atmosphere/land version of the CCSM," *Climate Dynamics*, vol. 34, no. 6, pp. 819–833, 2010.

[52] M. Ashfaq, Y. Shi, W.-w. Tung, R. J. Trapp, X. Gao, J. S. Pal, and N. S. Diffenbaugh, "Suppression of South Asian summer monsoon precipitation in the 21st century," *Geophysical Research Letters*, vol. 36, pp. 1–5, 2009.

[53] J. J. Hack, J. M. Caron, G. Danabasoglu, K. W. Oleson, C. Bitz, and J. E. Truesdale, "CCSMCAM3 Climate Simulation Sensitivity to Changes in Horizontal Resolution," *Journal of Climate*, vol. 19, no. 11, pp. 2267–2289, 2006.

[54] G. J. Zhang and N. a. McFarlane, "Sensitivity of Climate Simulations to the Parameterization of Cumulus Convection in the Canadian Climate Centre General Circulation Model," *Atmosphere-Ocean*, vol. 33, no. 3, pp. 407–446, 1995.

[55] S. J. Johnson, R. C. Levine, A. G. Turner, G. M. Martin, S. J. Woolnough, R. Schiemann, M. S. Mizielinski, M. J. Roberts, P. L. Vidale, M.-E. Demory, and J. Strachan, "The resolution sensitivity of the South Asian monsoon and Indo-Pacific in a global 0.35° AGCM," *Climate Dynamics*, 2015.

[56] S. Sandeep, R. S. Ajayamohan, W. R. Boos, T. P. Sabin, and V. Praveen, "Decline and poleward shift in Indian summer monsoon synoptic activity in a warming climate," 2018.

[57] J. Curio, F. Maussion, and D. Scherer, "A 12-year high-resolution climatology of atmospheric water transport over the Tibetan Plateau," *Earth System Dynamics*, vol. 6, no. 1, pp. 109–124, 2015.

[58] W. Dong, Y. Lin, J. S. Wright, Y. Ming, Y. Xie, B. Wang, Y. Luo, W. Huang, J. Huang, L. Wang, L. Tian, Y. Peng, and F. Xu, "Summer rainfall over the southwestern Tibetan Plateau controlled by deep convection over the Indian subcontinent," *Nature Communications*, vol. 7, p. 10925, 2016.

[59] a. F. Lutz, W. W. Immerzeel, a. B. Shrestha, and M. F. P. Bierkens, "Consistent increase in High Asia's runoff due to increasing glacier melt and precipitation," *Nature Climate Change*, vol. 4, no. 7, pp. 587–592, 2014.

[60] S. S. Amrith, "Risk and the South Asian monsoon," *Climatic Change*, no. February, pp. 1–12, 2016.

[61] V. Mishra, "Climatic uncertainty in Himalayan water towers," *Journal of Geophysical Research Atmospheres*, vol. 120, pp. 2689–2705, 2015.

[62] K. E. Trenberth, D. P. Stepaniak, and J. M. Caron, "The Global monsoon as Seen through the Divergent Atmospheric Circulation," *Journal of Climate*, vol. 13, pp. 3969–3993, 2000.

[63] K. L. Rasmussen and R. A. Houze, "A flash-flooding storm at the steep edge of high terrain," *Bulletin of the American Meteorological Society*, vol. 93, no. 11, pp. 1713–1724, 2012.

[64] V. Stolbova, E. Surovyatkina, B. Bookhagen, and J. Kurths, "Tipping elements of the Indian monsoon: Prediction of onset and withdrawal," *Geophysical Research Letters*, pp. 3982–3990, 2016.

[65] R. Knutti, J. Sedl, B. M. Sanderson, R. Lorenz, and E. Fischer, "A climate model projection weighting scheme accounting for performance and interdependence," pp. 1–10, 2017.

[66] T. L. Delworth, A. Rosati, W. Anderson, A. J. Adcroft, V. Balaji, R. Benson, K. Dixon, S. M. Griffies, H.-C. Lee, R. C. Pacanowski, G. A. Vecchi, A. T. Wittenberg, F. Zeng, and R. Zhang, "Simulated climate and climate change in the GFDL CM2.5 high-resolution coupled climate model," *Journal of Climate*, vol. 25, no. 8, pp. 2755–2781, 2012.

[67] D. Ma, W. Boos, and Z. Kuang, "Effects of orography and surface heat fluxes on the South Asian summer monsoon," *Journal of Climate*, vol. 27, no. 17, pp. 6647–6659, 2014.

[68] C. A. Shields, J. T. Kiehl, and G. A. Meehl, "Future changes in regional precipitation simulated by a half-degree coupled climate model: Sensitivity to horizontal resolution," *Journal of Advances in Modeling Earth Systems*, vol. 6, pp. 863–884, 2016.

[69] D. P. Dee, S. M. Uppala, A. J. Simmons, P. Berrisford, P. Poli, S. Kobayashi, U. Andrae, M. A. Balmaseda, G. Balsamo, P. Bauer, P. Bechtold, A. C. M. Beljaars, L. van de Berg, J. Bidlot, N. Bormann, C. Delsol, R. Dragani, M. Fuentes, A. J. Geer, L. Haimberger, S. B. Healy, H. Hersbach, E. V. Holm, L. Isaksen, P. Kallberg, M. Kohler, M. Matricardi, A. P. Mcnally, B. M. Monge-Sanz, J. J. Morcrette, B. K. Park, C. Peubey, P. de Rosnay, C. Tavolato, J. N. Thepaut, and F. Vitart, "The ERA-Interim reanalysis: Configuration and performance of the data assimilation system," *Quarterly Journal of the Royal Meteorological Society*, vol. 137, no. 656, pp. 553–597, 2011.

[70] S. Kobayashi, Y. Ota, Y. Harada, A. Ebita, M. Moriya, H. Onoda, K. Onogi, H. Kamahori, C. Kobayashi, H. Endo, K. Miyaoka, and K. Takahashi, "The JRA-55 Reanalysis: General Specifications and Basic Characteristics," *Journal of the Meteorological Society of Japan. Ser. II*, vol. 93, no. 1, pp. 5–48, 2015.

[71] F. Maussion, D. Scherer, T. Mölg, E. Collier, J. Curio, and R. Finkelnburg, "Precipitation seasonality and variability over the Tibetan Plateau as resolved by the high Asia reanalysis," *Journal of Climate*, vol. 27, no. 5, pp. 1910–1927, 2014.

[72] G. a. Meehl, W. M. Washington, J. M. Arblaster, A. Hu, H. Teng, J. E. Kay, A. Gettelman, D. M. Lawrence, B. M. Sanderson, and W. G. Strand, "Climate Change Projections in CESM1(CAM5) Compared to CCSM4," *Journal of Climate*, vol. 26, no. 17, pp. 6287–6308, 9 2013.

[73] R. B. Neale, J. Richter, S. Park, P. H. Lauritzen, S. J. Vavrus, P. J. Rasch, and M. Zhang, "The Mean Climate of the Community Atmosphere Model (CAM4) in Forced SST and Fully Coupled Experiments," *Journal of Climate*, vol. 26, no. 14, pp. 5150–5168, 2013.

[74] S. Sandeep and R. S. Ajayamohan, "Poleward shift in Indian summer monsoon low level jetstream under global warming," *Climate Dynamics*, pp. 337–351, 2015.

[75] W. R. Boos and T. Storelvmo, "Near-linear response of mean monsoon strength to a broad range of radiative forcings," *Proceedings of the National Academy of Sciences*, vol. 113, no. 6, pp. 1510–1515, 2016.

[76] J. Chen and S. Bordoni, "Orographic Effects of the Tibetan Plateau on the East Asian Summer Monsoon: An Energetic Perspective," *Journal of Climate*, vol. 27, no. Tao 1987, pp. 3052–3072, 4 2014.

[77] R. Zhang, D. Jiang, Z. Zhang, and E. Yu, "The impact of regional uplift of the Tibetan Plateau on the Asian monsoon climate," *Palaeogeography, Palaeoclimatology, Palaeoecology*, vol. 417, pp. 137–150, 2015.

[78] S. L. Thompson and D. Pollard, "A Global Climate Model (GENESIS) with a Land-Surface Transfer Scheme (LSX). Part I: Present Climate Simulation," *Journal of Climate*, vol. 8, pp. 732–761, 1994.

[79] R. Jacob, C. Schafer, I. Foster, M. Tobis, and J. Anderson, "Computational Design and Performance of the Fast Ocean Atmosphere Model , Version One," *International Journal of Computational Science*, pp. 175–184, 2001.

[80] G. J. Huffman, D. T. Bolvin, E. J. Nelkin, D. B. Wolff, R. F. Adler, G. Gu, Y. Hong, K. P. Bowman, and E. F. Stocker, "The TRMM Multisatellite Precipitation Analysis (TMPA): Quasi-Global, Multiyear, Combined-Sensor Precipitation Estimates at Fine Scales," *Journal of Hydrometeorology*, vol. 8, pp. 38–55, 2007.

[81] A. Yatagai, K. Kamiguchi, O. Arakawa, A. Hamada, N. Yasutomi, and A. Kitoh, "Aphrodite constructing a long-term daily gridded precipitation dataset for Asia based on a dense network of rain gauges," *Bulletin of the American Meteorological Society*, vol. 93, no. 9, pp. 1401–1415, 2012.

[82] G. Flato, J. Marotzke, B. Abiodun, P. Braconnot, S. C. Chou, W. Collins, P. Cox, F. Driouech, S. Emori, V. Eyring, C. Forest, P. Gleckler, E. Guilyardi, C. Jakob, V. Kattsov, C. Reason, and M. Rummukainen, "Evaluation of Climate Models," *Climate Change 2013: The Physical Science Basis. Contribution of Working Group I to the Fifth Assessment Report of the Intergovernmental Panel on Climate Change*, pp. 741–866, 2013.

[83] S. Patwardhan, A. Kulkarni, and S. Sabade, "Projected Changes in Semi Permanent Systems of Indian Summer Monsoon in CORDEX-SA Framework," no. June, pp. 133–146, 2016.

[84] D. J. Kirshbaum and D. R. Durran, "Factors governing cellular convection in orographic precipitation," *Journal of the Atmospheric Sciences*, vol. 61, no. 6, pp. 682–698, 2004.

[85] J. Galewsky and A. Sobel, "Moist Dynamics and Orographic Precipitation in Northern and Central California during the New Years Flood of 1997," *Monthly Weather Review*, vol. 133, pp. 1594–1612, 2005.

[86] J. Galewsky, "Orographic Clouds in Terrain-Blocked Flows : An Idealized Modeling Study," *Journal of Atmospheric Scienceso*, vol. 65, pp. 3460–3478, 2008.

[87] P. J. Neiman, F. M. Ralph, A. White, D. E. Kingsmill, and P. O. G. Persson, "The Statistical Relationship between Upslope Flow and Rainfall in California s Coastal Mountains : Observations during CALJET," *Monthly Weather Review*, vol. 130, pp. 1468–1492, 2002.

[88] A. P. Barros and T. J. Lang, "Monitoring the Monsoon in the Himalayas : Observations in Central Nepal , June 2001," *Monthly Weather Review*, vol. 131, pp. 1408–1427, 2003.

[89] B. N. Goswami, R. S. Ajayamohan, P. K. Xavier, and D. Sengupta, "Clustering of synoptic activity by Indian summer monsoon intraseasonal oscillations," *Geophysical Research Letters*, vol. 30, no. 8, p. 1431, 2003.

[90] V. Krishnamurthy and R. S. Ajayamohan, "Composite structure of monsoon low pressure systems and its relation to Indian rainfall," *Journal of Climate*, vol. 23, no. 16, pp. 4285–4305, 2010.

[91] M. Rajeevan, D. S. Pai, and R. Kumar, "New statistical models for long-range forecasting of southwest monsoon rainfall over India," *Climate Dynamics*, pp. 813–828, 2007.

[92] S. Y. Wang, B. M. Buckley, J. H. Yoon, and B. Fosu, "Intensification of pre-monsoon tropical cyclones in the Bay of Bengal and its impacts on Myanmar," *Journal of Geophysical Research Atmospheres*, vol. 118, no. 10, pp. 4373–4384, 2013.

[93] J. Karmacharya, M. New, R. Jones, and R. Levine, "Added value of a high-resolution regional climate model in simulation of intraseasonal variability of the South Asian summer monsoon," *International Journal of Climatology*, 2016.

[94] A. Levermann, J. Schewe, V. Petoukhov, and H. Held, "Basic mechanism for abrupt monsoon transitions," 2009.

[95] A. Levermann, V. Petoukhov, J. Schewe, and H. Joachim, "Abrupt monsoon transitions as seen in paleorecords can be explained by moisture-advection feedback," vol. 113, no. 17, pp. 2348–2349, 2016.

[96] P. R. Gent, G. Danabasoglu, L. J. Donner, M. M. Holland, E. C. Hunke, S. R. Jayne, D. M. Lawrence, R. B. Neale, P. J. Rasch, M. Vertenstein, P. H. Worley, Z.-L. Yang, and M. Zhang, "The Community Climate System Model Version 4," *Journal of Climate*, vol. 24, no. 19, pp. 4973–4991, 10 2011.

[97] T. A. O'Brien, F. Li, W. D. Collins, S. A. Rauscher, T. D. Ringler, M. Taylor, S. M. Hagos, and L. R. Leung, "Observed scaling in clouds and precipitation and scale incognizance in regional to global atmospheric models," *Journal of Climate*, vol. 26, no. 23, pp. 9313–9333, 2013.

[98] Y. Liu, G. Wu, J. Hong, B. Dong, A. Duan, Q. Bao, L. Zhou, Y. Liu, B. Dong, X. Liang, A. Duan, Q. Bao, and J. Yu, "Revisiting Asian monsoon formation and change associated with Tibetan Plateau forcing: II. Change," *Climate Dynamics*, vol. 39, no. 5, pp. 1183–1195, 3 2012.

[99] X. Xu, T. Zhao, C. Lu, and Y. Guo, "An important mechanism sustaining the atmospheric" water tower" over the Tibetan Plateau," *Atmospheric Chemistry and Physics*, pp. 11 287–11 295, 2014.

[100] G. H. Roe, Q. Ding, D. S. Battisti, P. Molnar, M. K. Clark, and C. N. Garzione, "A modeling study of the response of Asian summertime climate to the largest geologic forcings of the past 50 Ma," *Journal of Geophysical Research: Atmospheres*, vol. 121, no. 10, pp. 5453–5470, 2016.

[101] J. M. Walker, S. Bordoni, and T. Schneider, "Interannual variability in the large-scale dynamics of the South Asian summer monsoon," *Journal of Climate*, vol. 28, no. 9, pp. 3731–3750, 2015.

[102] A. Chakraborty, R. S. Nanjundiah, and J. Srinivansan, "Theoretical aspects of the onset of Indian summer monsoon from perturbed orography simulations in a GCM," *Annales Geophysicae*, no. 2003, pp. 2075–2089, 2006.

[103] A. Chakraborty, R. S. Nanjundiah, and J. Srinivasan, "Impact of African orography and the Indian summer monsoon on the low-level Somali jet," vol. 992, no. June 2008, pp. 983–992, 2009.

[104] G. Wu, Y. Liu, B. He, Q. Bao, A. Duan, and F.-F. Jin, "Thermal controls on the Asian summer monsoon." *Scientific reports*, vol. 2, p. 404, 1 2012.

[105] G. de Boer, W. Chapman, J. E. Kay, B. Medeiros, M. D. Shupe, S. Vavrus, and J. Walsh, "A Characterization of the Present-Day Arctic Atmosphere in CCSM4," *Journal of Climate*, vol. 25, no. 8, pp. 2676–2695, 4 2012.

[106] A. Zhisheng, W. Guoxiong, L. Jianping, S. Youbin, L. Yimin, Z. Weijian, C. Yanjun, D. Anmin, L. Li, M. Jiangyu, C. Hai, S. Zhengguo, T. Liangcheng, Y. Hong, A. Hong, C. Hong, and F. Juan, "Global Monsoon Dynamics and Climate Change," *Annual Review of Earth and Planetary Sciences*, vol. 43, no. 1, pp. 29–77, 2015.

[107] B. Rajagopalan and P. Molnar, "Signatures of Tibetan Plateau heating on Indian summer monsoon rainfall variability," *Journal of Geophysical Research: Atmospheres*, vol. 118, no. 3, pp. 1170–1178, 2013.

[108] L. Cheng, K. E. Trenberth, J. Fasullo, T. Boyer, J. Abraham, and J. Zhu, "Improved estimates of ocean heat content from 1960 to 2015," pp. 1–11, 2017.

[109] Z. Wang, A. Duan, G. Wu, and S. Yang, "Mechanism for occurrence of precipitation over the southern slope of the Tibetan Plateau without local surface heating," *International Journal of Climatology*, pp. n/a–n/a, 2015.

[110] C. Chou and J. Neelin, "Mechanisms Limiting the Northward Extent of the Northern Summer Monsoons over North America, Asia, and Africa*," *Journal of climate*, vol. 16, pp. 406–425, 2003.

[111] R. F. Adler, G. J. Huffman, A. Chang, R. Ferraro, P.-P. Xie, J. Janowiak, B. Rudolf, U. Schneider, S. Curtis, D. Bolvin, A. Gruber, J. Susskind, P. Arkin, and E. Nelkin, "The Version-2 Global Precipitation Climatology Project (GPCP) Monthly Precipitation Analysis (1979Present)," *Journal of Hydrometeorology*, vol. 4, no. January 1997, pp. 1147–1167, 2003.

[112] S. Prakash, C. Mahesh, and R. M. Gairola, "Comparison of TRMM Multisatellite Precipitation Analysis (TMPA)-3B43 version 6 and 7 products with rain gauge data from ocean buoys," *Remote Sensing Letters*, vol. 4, no. 7, pp. 677–685, 2013.

[113] M. M. Rienecker, M. J. Suarez, R. Gelaro, R. Todling, J. Bacmeister, E. Liu, M. G. Bosilovich, S. D. Schubert, L. Takacs, G. K. Kim, S. Bloom, J. Chen, D. Collins, A. Conaty, A. Da Silva, W. Gu, J. Joiner, R. D. Koster, R. Lucchesi, A. Molod, T. Owens, S. Pawson, P. Pegion, C. R. Redder, R. Reichle, F. R. Robertson, A. G. Ruddick, M. Sienkiewicz, and J. Woollen, "MERRA: NASA's modern-era retrospective analysis for research and applications," *Journal of Climate*, vol. 24, pp. 3624–3648, 2011.

[114] K. E. Trenberth and L. Smith, "Atmospheric Energy Budgets in the Japanese Reanalysis: Evaluation and Variability," *Journal of the Meteorological Society of Japan*, vol. 86, no. 5, pp. 579–592, 2008.

[115] S. Fueglistaler, B. Legras, A. Beljaars, J. Morcrette, A. Simmons, and A. M. Tompkins, "The diabatic heat budget of the upper troposphere and lower / mid stratosphere in ECMWF reanalyses," vol. 27, pp. 1–27, 2008.

[116] B. a. Cash, J. L. Kinter, J. Adams, E. Altshuler, B. Huang, E. K. Jin, J. Manganello, L. Marx, and T. Jung, "Regional structure of the Indian Summer Monsoon in observations, reanalysis, and simulation," *Journal of Climate*, vol. 28, no. 5, pp. 1824–1841, 2015.

[117] J.-L. Lin, W. Yuan, H. Chen, W. Sun, and Y. Zhang, "Precipitation over East Asia simulated by NCAR CAM5 at different horizontal resolutions," *Journal of Advances in Modeling Earth Systems*, vol. 7, pp. 774–790, 2015.

[118] S. P. Xie, H. Xu, N. H. Saji, Y. Wang, and W. T. Liu, "Role of narrow mountains in large-scale organization of Asian Monsoon convection," *Journal of Climate*, vol. 19, no. 14, pp. 3420–3429, 2006.

[119] A. Dai, H. Li, Y. Sun, L. C. Hong, L. Ho, C. Chou, and T. Zhou, "The relative roles of upper and lower tropospheric thermal contrasts and tropical influences in driving Asian summer monsoons," *Journal of Geophysical Research Atmospheres*, vol. 118, no. 13, pp. 7024–7045, 2013.

[120] B. He, G. Wu, Y. Liu, and Q. Bao, "Astronomical and Hydrological Perspective of Mountain Impacts on the Asian Summer Monsoon," *Scientific Reports*, vol. 5, p. 17586, 2015.

[121] R. B. Neale, J. H. Richter, and M. Jochum, "The Impact of Convection on ENSO: From a Delayed Oscillator to a Series of Events," *Journal of Climate*, vol. 21, no. 22, pp. 5904–5924, 2008.

[122] P. J. Rasch and J. E. Kristjánsson, "A Comparison of the CCM3 Model Climate Using Diagnosed and Predicted Condensate Parameterizations," *Journal of Climate*, vol. 11, no. 7, pp. 1587–1614, 1998.

[123] J. Boyle and S. a. Klein, "Impact of horizontal resolution on climate model forecasts of tropical precipitation and diabatic heating for the TWP-ICE period," *Journal of Geophysical Research: Atmospheres*, vol. 115, pp. 1–20, 2010.

[124] S. Sen Roy, S. B. Saha, S. K. Roy Bhowmik, and P. K. Kundu, "Analysis of monthly cloud climatology of the Indian subcontinent as observed by TRMM precipitation radar," *International Journal of Climatology*, vol. 2091, no. July 2014, pp. 2080–2091, 2014.

[125] W. I. Gustafson Jr., P.-L. Ma, and B. Singh, "Precipitation characteristics of CAM5 physics at mesoscale resolution during MC3E and the impact of convective timescale choice," *Journal of Advances in Modeling Earth Systems*, vol. 6, pp. 1271–1287, 2014.

[126] A. Cherchi, H. Annamalai, S. Masina, and A. Navarra, "South Asian summer monsoon and the eastern Mediterranean climate : the monsoon-desert mechanism in CMIP5 simulations," vol. 16, p. 13020, 2014.

[127] T. T. Manabe S., "The effects of mountains on the general circulation of the atmosphere as identified by numerical experiments," *Journal of the Atmospheric Sciences*, vol. 31, pp. 3–42, 1974.

[128] A. Kitoh, "Effects of Large-Scale Mountains on Surface Climate. A Coupled Ocean-Atmosphere General Circulation Model Study." *Journal of the Meteorological Society of Japan*, vol. 80, no. 5, pp. 1165–1181, 2002.

[129] P. C. Tada R., H. Zheng, "Evolution and variability of the Asian monsoon and its potential linkage with uplift of the Himalaya and Tibetan Plateau," *Progress in Earth and Planetary Science*, vol. 3, no. 1, pp. 1–26, 2016.

[130] H. Tang, A. Micheels, J. T. Eronen, B. Ahrens, and M. Fortelius, "Asynchronous responses of East Asian and Indian summer monsoons to mountain uplift shown by regional climate modelling experiments," *Climate Dynamics*, vol. 40, no. 5-6, pp. 1531–1549, 2013.

[131] W. R. Boos and Z. Kuang, "Sensitivity of the South Asian monsoon to elevated and non-elevated heating." *Scientific reports*, vol. 3, p. 1192, 1 2013.

[132] R. A. Spicer, J. Yang, A. B. Herman, T. Kodrul, N. Maslova, T. E. Spicer, G. Aleksandrova, and J. Jin, "Asian Eocene monsoons as revealed by leaf architectural signatures," *Earth and Planetary Science Letters*, vol. 449, pp. 61–68, 2016.

[133] A. K. Gupta, A. Yuvaraja, M. Prakasam, S. C. Clemens, and A. Velu, "Evolution of the South Asian monsoon wind system since the late Middle Miocene," *Palaeogeography, Palaeoclimatology, Palaeoecology*, vol. 438, pp. 160–167, 2015.

[134] P. Molnar, "Mio-Pliocene Growth of the Tibetan Plateau and Evolution of East Asian Climate," *Paleontologia Electronica*, vol. 8, no. 1, pp. 1–23, 2005.

[135] J. M. V. C. W. B. P. McQuarrie, N. Stock, "Cenozoic evolution of Neotethys and implications for the causes of plate motions," pp. 30–33, 2003.

[136] F. Mouthereau, "Timing of uplift in the Zagros belt/Iranian plateau and accommodation of late Cenozoic Arabia-Eurasia convergence," pp. 5–6, 2011.

[137] B. He, Y. Liu, G. Wu, Z. Wang, and Q. Bao, "The role of airsea interactions in regulating the thermal effect of the TibetanIranian Plateau on the Asian summer monsoon," *Climate Dynamics*, vol. 0, no. 0, pp. 1–19, 2018.

[138] A. Rohrmann, M. R. Strecker, B. Bookhagen, A. Mulch, D. Sachse, H. Pingel, R. N. Alonso, T. F. Schildgen, and C. Montero, "Can stable isotopes ride out the storms? The role of convection for water isotopes in models, records , and paleoaltimetry studies in the central Andes," *Earth and Planetary Science Letters*, vol. 407, pp. 187–195, 2014.

[139] R. P. Acosta and M. Huber, "The neglected Indo-Gangetic Plains low-level jet and its importance for moisture transport and precipitation during the peak summer monsoon," *Geophysical Research Letters*, 2017.

[140] K. E. Taylor, R. J. Stouffer, and G. A. Meehl, "An Overview of CMIP5 and the Experiment design," *American Meteorological Society*, vol. 3, no. april, pp. 485–498, 2012.

[141] J. J. Hack, "Parameterization of moist convection in the National Center for Atmospheric Research community climate model (CCM2)," *Journal of Geophysical Research*, vol. 99, no. 93, pp. 5551–5568, 1994.

[142] D. M. Lawrence, K. W. Oleson, M. G. Flanner, P. E. Thornton, S. C. Swenson, P. J. Lawrence, X. Zeng, Z.-L. Yang, S. Levis, K. Sakaguchi, G. B. Bonan, and A. G. Slater, "Parameterization improvements and functional and structural advances in Version 4 of the Community Land Model," *Journal of Advances in Modeling Earth Systems*, vol. 3, no. 3, pp. 1–27, 2011.

[143] S. Lindzen R., "On the Rold of Sea Surface Temperature Gradients in Forcing Low-Level Winds and Convergence in the Tropics," *Journal of Atmospheric Sciences*, vol. 44, pp. 2418–2436, 1987.

[144] W. R. Boos and J. V. Hurley, "Thermodynamic Bias in the Multimodel Mean Boreal Summer Monsoon*," *Journal of Climate*, vol. 26, no. 7, pp. 2279–2287, 2013.

[145] M. Huber and R. Caballero, "The early Eocene equable climate problem revisited," *Climate of the Past*, vol. 7, no. 2, pp. 603–633, 2011.

[146] a. Goldner, N. Herold, and M. Huber, "Antarctic glaciation caused ocean circulation changes at the EoceneOligocene transition," *Nature*, vol. 511, no. 7511, pp. 574–577, 7 2014.

[147] M. A. Bollasina, Y. Ming, and V. Ramaswamy, "Anthropogenic Aerosols and the Summer Monsoon," *Scientific reports*, vol. 334, pp. 502–505, 2011.

[148] G. Wu, Y. Guan, Y. Liu, J. Yan, and J. Mao, "Air-sea interaction and formation of the Asian summer monsoon onset vortex over the Bay of Bengal," *Climate Dynamics*, vol. 38, no. 1-2, pp. 261–279, 2012.

[149] T. Yao, F. Wu, L. Ding, J. Sun, L. Zhu, S. Piao, T. Deng, X. Ni, H. Zheng, and H. Ouyang, "Multispherical interactions and their effects on the Tibetan Plateau's earth system: A review of the recent researches," *National Science Review*, vol. 2, no. 4, pp. 468–488, 2015.

[150] S. R. A. S. T. E. B. S. Khan Mahasin Ali, Bera Meghma, "Palaeoclimatic estimates for a latest Miocene-Pliocene flora from the Siwalik Group of Bhutan: Evidence for the development of the South Asian Monsoon in the eastern Himalaya," *Palaeogeography, Palaeoclimatology, Palaeoecology*, vol. 31, pp. 3–42, 2019.

[151] M. B. Allen and H. A. Armstrong, "Reconciling the Intertropical Convergence Zone, Himalayan/Tibetan tectonics, and the onset of the Asian monsoon system," *Journal of Asian Earth Sciences*, vol. 44, pp. 36–47, 2012.

[152] C. S. C. K. K. G. J. J. L. J. A. N. Holbourn Ann E., Kuhnt Wolfgang, "Late Miocene climate cooling and intensification of southeast Asian winter monsoon," *Nature Communications*, pp. 1–13, 2018.

[153] H. Flohn, "Contributions to a Meteorology of the Tibetan Highlands," *Tech. Rep. 130, Colorado State University*, 1968.

[154] C. Li and M. Yanai, "The onset and interannual variability of the Asian summer monsoon in relation to land-sea thermal contrast," *Journal of Climate*, vol. 9, pp. 358–375, 1996.

[155] R. S. Lindzen and A. V. Hou, "Hadley circulations for zonally averaged heating centered off the equator," *Journal of the Atmospheric Sciences*, pp. 2416–2427, 1988.

[156] R. A. Plumb, "Dynamical constraints on monsoon circulations Sustained divergent ows : the circulation constraint in the upper troposphere," 2005.

[157] R. A. Plumb and A. Y. Hou, "The response of a zonally symmetric atmosphere to subtropical thermal forcing: Threshold behavior," *Journal of the atmospheric sciences*, vol. 49, no. 19, pp. 1790–1799, 1992.

[158] J. A. Day, I. Fung, and C. Risi, "Coupling of South and East Asian Monsoon Precipitation in July-August," *Journal of Climate*, p. 150227131327003, 2015.

[159] W. Dong, Y. Lin, J. Wright, Y. Xie, F. Xu, W. Xu, and Y. Wang, "Indian Monsoon Low-Pressure Systems Feed Up-and-Over Moisture Transport to the Southwestern Tibetan Plateau," *Journal of Geophysical Research: Atmospheres*, pp. 140–151, 2017.

[160] G. R. Goldsmith, N. J. Matzke, and T. E. Dawson, "The incidence and implications of clouds for cloud forest plant water relations," *Ecology Letters*, vol. 16, no. 3, pp. 307–314, 2013.

[161] T. Deng and L. Ding, "Paleoaltimetry reconstructions of the Tibetan Plateau: Progress and contradictions," *National Science Review*, vol. 2, no. 4, pp. 417–437, 2015.

[162] R. D. C. B. S. N. Zhu Bin, Kidd WSF, "Age of Initiation of the India Asia Collision in the East Central Himalaya," pp. 265–285, 2005.

[163] P. G. DeCelles, J. Quade, P. Kapp, M. Fan, D. L. Dettman, and L. Ding, "High and dry in central Tibet during the Late Oligocene," *Earth and Planetary Science Letters*, vol. 253, no. 3-4, pp. 389–401, 1 2007.

[164] J. E. Volkmer, P. Kapp, J. H. Guynn, and Q. Lai, "Cretaceous-Tertiary structural evolution of the north central Lhasa terrane, Tibet," *Tectonics*, vol. 26, no. 6, pp. n/a–n/a, 12 2007.

[165] S. R. A. B. S. G. R. Y. J. S. T. E. V. G. S.-x. S. T. J. F. G. P. J. Khan, Mahasin Ali, "Miocene to Pleistocene fl oras and climate of the Eastern Himalayan Siwaliks , and new palaeoelevation estimates for the NamlingOiyug Basin, Tibet," pp. 1–10, 2014.

[166] C. M. K. H. G. A. Dayem Katherine E, Molnar Peter, "Far-field lithospheric deformation in Tibet during continental collision," pp. 1–9, 2009.

[167] D. B. Rowley and C. N. Garzione, "Stable Isotope-Based Paleoaltimetry," *Annual Review of Earth and Planetary Sciences*, vol. 35, no. 1, pp. 463–508, 2007.

[168] R. A. Spicer, N. B. W. Harris, M. Widdowson, A. B. Herman, S. Guo, P. J. Valdes, J. A. Wolfe, and S. P. Kelley, "Constant elevation of southern Tibet over the past 15 million years," vol. 421, no. February, pp. 1–3, 2003.

[169] Q. J. D. D. L. D. P. G. K. P. A. D. L. Saylor, J. E., "The late Miocene through present paleoelevation history of southwestern Tibet," pp. 1–42, 2009.

[170] M. B. A. N. Tapponnier Paul, Zhiqin Xu, "Oblique Stepwise Rise and Growth of the Tibet Plateau," pp. 671–677, 2001.

[171] P. C. C. Mulch Andreas, "The rise and growth of Tibet," pp. 670–671, 2006.

[172] Q. J. D. C. P. G. B. R. F. Garzione C. N., Dettman D. L., "High times on the Tibetan Plateau: Paleoelevation of the Thakkhola graben, Nepal," pp. 339–342, 2000.

[173] E. J. Quade Jay, Garzione C., "Paleoelevation Reconstruction using Pedogenic Carbonates," pp. 53–87, 2000.

[174] H. W. Meyer, "A Review of Paleotemperature Lapse Rate Methods for Estimating Paleoelevation from Fossil Floras," *Reviews in Mineralogy & Geochemistry*, vol. 66, pp. 155–171, 2007.

[175] M. P. Wolfe Jack A, Forest Chris E, "Paleobotanical evidence of Eocene and Oligocene paleoaltitudes in midlatitude western North America," pp. 664–678, 1998.

[176] C. E. Forest, "Paleoaltimetry : A Review of Thermodynamic Methods," *Reviews in Mineralogy & Geochemistry*, vol. 66, pp. 173–193, 2007.

[177] R. Feng and C. J. Poulsen, "Refinement of Eocene lapse rates , fossil-leaf altimetry , and North American Cordilleran surface elevation estimates," *Earth and Planetary Science Letters*, vol. 436, pp. 130–141, 2016.

[178] C. J. Poulsen, T. A. Ehlers, and N. Insel, "Onset of Convective Rainfall During Gradual Late Miocene Rise of the Central Andes," vol. 328, no. April, pp. 490–494, 2010.

[179] R. Zamora, R. Korty, and M. Huber, "Thermal Stratification in Simulations of Warm Climates : A Climatology Using Saturation Potential Vorticity," *American Meteorological Society*, vol. 29, pp. 5083–5102, 2016.

VITA

Personal Background and Qualifications

During my dissertation, I investigated the linkages between major topographic features and atmospheric dynamics within an Earth System perspective. My work builds upon the foundations of theoretical atmospheric thermodynamics and dynamical principles and primarily addresses the interactions between the Tibetan Plateau and the Indo-Asian Monsoon.

For my first publication, I explored gaps in the current body of literature, mainly using observational datasets and reanalysis products. I added more sophisticated tools, such as general circulation models (GCMs) to investigate how topography influences climate with an emphasis on monsoonal features. To do so I explored drawbacks in using currently available GCMs found in the CMIP5 and demonstrated the necessity of model horizontal-grid resolution when studying atmosphere-terrain interactions. More specifically, my article shows two different topographic mechanisms between the low and high-resolution model, Community Earth System Model (CESM). We demonstrated that the degree of orographic diabatic heating impacts the static stability of the atmosphere, which determines if the onshore monsoon flow is channeled along or lifted above the mountains. This study bridges the gap between monsoon and topography by using the moist Froude number.

This work rose from analyzing the CMIP5 models and reanalysis products trying to understand how each product calculated diabatic heating across the tropics. The in-depth analysis led to running a suite of simulations that altered parameters in the deep and shallow convective schemes and with or without these elements. One key result of this study highlights how the persistent double Intertropical Convergence Zone (ITCZ) found in the Western Pacific changed as we alter the schemes. Additionally, testing how monsoon precipitation regimes change as the model resolution

was increased led to the conclusion that convective schemes parameterization scale incognizant problem.

After thoroughly testing the high-resolution version of CESM, I use this model to delve into the South Asian Monsoon theory. For this project, we demonstrate that counter to the classic notion where topography dictates the monsoon overturning circulation, its main purpose is to impose a regional influence on the monsoon thermal low found across northern India and Myanmar (in prep). For this study, we provide a complete surface energy budget and determined that cloud processes become fundamentally important for the monsoon circulation. For instance, the rise of Tibetan Plateau increased the production of latent heating, which then changed the regional cloud forcing. The key result from this study is that moist versus dry monsoon regimes is highly dependent on topography.

I applied these modeling tools to paleoclimate and more specifically reevaluation of the paleoaltimetry method. This method uses fossil assemblages to back-calculate moist static quantities such as temperature and moisture. From the paleoenthalpy quantities, we can use the hypsometric equation to then estimate the height of a mountain range when the fossil record existed. For my last project, I used paleoclimate simulations to create an extensive dataset that measures the paleoelevation of the Tibetan Plateau, the Andes, and the Sierra Nevada mountain range. This dataset will be used to provide a better topographic history of the mountain and plateaus around the world and has large implications in fields such as geophysics, and paleoclimatology.

The overarching goal of my dissertation is to constrain the evolution of the regional topography understand its importance to the regional climate and hydrological cycle. Additionally, prior to continuing my dissertation at Purdue, I spent several years at University of New Hampshire (UNH) where I worked on a project that looked at the impacts of climate change on New England, US (in review). There, I primarily used Weather Forecasting Model (WRF), regional climate model and was a part of a research team that dynamically downscaled GCM simulations into WRF. As the

primary data manager and analyst, I became familiar with the large-cluster systems such as Yellowstone. My time at UNH has allowed me to gain a greater understanding of convective resolving models and regional scale interactions, which better prepared me for my dissertation.

Research Interest, Scientific Agenda and Modeling Experiments

Research Interest

During the 2017 NCAR ASP summer colloquium, I had the privilege to see a talk on the fate of mountain ranges at the end of the 21st century. Amid the Professors presentation, I realized that his modified aqua planet results only focused on the mid-latitudes, and meridionally orientated mountains like the Sierras. As a graduate student that works on tropical, zonally orientated mountain range like the Himalayas, I felt compelled to ask what is the fate of such alternative types of mountains. The professors answer was simple We do not know. He further elaborated and said that our projection in the tropics is limited by our knowledge about the model parametrization schemes which are based on modern observations. As a Filipino-American that grew up in California and majored in Geology, I had the propensity to admire mountain ranges as well as Tropics. The uncertainty about the future of tropical montane regions and tropical dynamics compel me to continue my research and further broaden my knowledge of other tropical atmospheric phenomena.

My research interest broadly encompasses tropical dynamics and warm climate systems. I want to pursue research on monsoon systems, Walker Circulation, and Madden-Julian Oscillation dynamics. My true passion lies in understanding how such circulations impact mountainous regions found in the tropics. I gravitate toward this research because the nexus between mountain regions and tropical dynamics represents systems that are influenced by climate change. It has cumulative impacts on the hydrological cycle and inevitably overlaps with societal issues. To accomplish such goals, I plan to use data-model comparison methods that include modern and paleo records and state-of-the-art general circulation models.

Scientific Agenda

Despite the projected weakening of the tropical circulation, modeling evidence derived from the Coupled Model Intercomparison Project Phase 5 (CMIP5) projects an increase in rainfall rates across the tropics by the end of the century (4, 5). However, uncertainties persist in our current theories and the mechanisms that drive decadal and centennial changes. For these reasons both future and paleoclimate studies on the tropics remain an active area of research. The following are some of the issues I would like to investigate in my career: 1) Paleoenthalpy is used to estimate the uplift history of various topography around the world (6, 7). This method is predicated upon the annual mean atmospheric temperature profile close to a moist adiabat and is reliable in tropical environments. Additionally, the emergence of isotope-enabled models (8) allows accurate tracking of onshore moisture flow, which can also be used to estimate terrain elevation. Using a modeling framework, we can simulate both moist enthalphy and isotope-enabled models to validate the accuracy of such methods. 2) Tropical monsoonal regions are inland branch of the intertropical convergence zone. They are driven by a continuous influx of moisture, and weakening of the overturning circulation should intuitively weaken the regional convergence of moisture (9). Thus, monsoon systems are subject tipping elements (10, 11). 3) Observed modern ocean surface winds and Ocean-Atmosphere General Circulation models suggest that the Walker Circulation is weakening (12). Furthermore, various paleoclimate proxy from the Pliocene suggest a period with a perpetual state of El Nio (13). Transitioning to such a state provides a new area of research. 4) Tropical montane regions are impacted by the various tropical circulations and any changes in intensity and duration implicate the livelihood of such mountain ranges. One way to study the climate system of mountains is by understanding the fate of the moisture. Using climate models and isotopes we can derive the fate of the montane moist air.

For my post-doctoral appointment, I want to study the dynamics of tropical regions using high-resolution models from the Coupled Model Intercomparison Project as well as Convective resolving model such as the Weather Research Forecast model.

Lastly, I want to use isotope enable models to better understand the evolution of moisture driven regions.

Teaching Philosophy

The focal point of teaching in science is to distill complex ideas into a simple and readily usable information. To do so, we must enlighten our audience that physical sciences are tools for real-world problems, we must encourage critical problem-solving skills that will demand further self-induce exploration, as well as mastering oral and written communication skills. As a previous teaching assistant for Purdue EAPS, 191 Dynamic Earth and a Purdue Climate Change Research Center Undergrad mentor I found that students respond well and are more successful in learning the subject when they apply the material to topics they are interested in. I find starting with broad analogies then synthesizing them a more specific and favorable example allows students to connect to the subject. This is primarily way done through relating everyday life examples to the subject. During my time as a mentor, I encouraged students to take on task above their skill level, whether its a topic they struggle on or applying their knowledge beyond that of the classroom setting. I firmly believe that struggling and developing critical thinking skills are the stepping stones to success. Lastly, I believe that as teachers it is our task to develop the students communication skills either through in-class dialogue or written examples. However, I understand that this teaching method is only applicable in small classroom settings, and the dynamics of a large class will make personalized connections difficult. With an undergrad degree in geology and environmental sciences, masters in atmospheric science, and dissertation work in Earth system processes my work have always revolved around the nexus between Energy and Society. Given my previous teaching experiences and my expertise, I am equipped and accustomed to the many duties of teaching, running recitations and labs experiments, and prepared for any mentoring tasks.

Curriculum Vitae

Research Interest

Climate change variability, mountain dynamics, and tropical monsoons using high and low resolution numerical models.

Education Background

1. Current: Doctoral Candidate at EAPS Department, Purdue University
2. Previously a graduate student at University of New Hampshire (2014-2016)
3. Master of Science, Purdue University, Indiana (August 2012-December 2013) Academic Adviser: Matthew Huber, Ernie Agee, Alex Gluhovsky, Affiliation: Climate Dynamic Prediction Laboratory
4. Bachelor of Science in Earth Science with concentration in Environmental Science University of California Santa Cruz (September 2008-June 2012), Academic Adviser: Peter Weiss, Russel Flegal, Lisa Sloan

Awards

1. Purdue EAPS Outstanding Atmospheric Graduate Student (2018)
2. Purdue EAPS Outstanding Graduate Student Poster Presentation Award (2018)
3. Purdue Climate Change Research Center Conference Travel Grant (Nov 2016-17)
4. NCAR ASP Summer Program NSF funded (June 2017)
5. Purdue, EAPS Graduate Student Presentation Award (2017)
6. Univeristy of Chicago, Rossbypalooza NSF travel grant (July 2016)
7. University of New Hampshire NRESS Student Science Award (Feb 2016)
8. University of New Hampshire NRESS Department Travel Grant (Dec 2015)
9. EPSCoR NSF Student Grant (January 2014 August 2016)
10. Purdue Graduate Student Government Travel Grant (Dec 2013)
11. NCAR CESM summer tutorial travel scholarship (July 2013)
12. Purdue Doctoral Ross Fellowship (2012-2013)
13. Friends of Long Marine Lab Student Research and Education Award (2011-2012)

14. Senior Thesis: Total mercury concentration in sediment from continental shelf of central California

Peer Reviewed Publications

1. Acosta, R. P. and Huber, M. The neglected Indo-Gangetic Plains low-level jet and its importance for moisture transport and precipitation during the peak summer monsoon. Geophys. Res. Lett. (2017).
2. Acosta, R. P. (2013).The influence of the tibetan plateau elevation on the global and asian monsoons(Order No. 1553487). Available from Dissertations and Theses ; ProQuest Dissertations and Theses Global. (1518149402).
3. Weiss-Penzias, P. S., C. Ortiz Jr., R. P. Acosta, W. Heim, J. P. Ryan, D. Fernandez, J. L. Collett Jr., and A. R. Flegal (2012), Total and monomethyl mercury in fog water from the central California coast, Geophys. Res. Lett., 39, L03804.

Current Research Projects

1. (In review) Improved Regional Climate Projections Using Dynamical Downscaling
2. (In prep) Modifying the resilient South Asian monsoon-low through topographic forcings
3. (In review) Iranian Plateau Gatekeeper of the Indo-Asian Monsoon Environment
4. (In prep) Evaluating paleoenthalpy as a measure of paleotopography using climate models
5. (In prep) Analysis on Future Climate Change impacts using dynamically downscaled simulation from High Resolution WRF [Collaboration with University of New Hampshire]

Presentations

1. Acosta R. P. Rising to the Heavens, Purdue EAPS 591 graduate course Southeast Asia Tectonics: Puzzles, Monsoons and Oil (Spring 2018) (Guess lecture)

2. Acosta R. P. Huber M Regional Climate Influence of the Himalayan Tibetan Plateau on the Indo-Asian Monsoon, AGU Fall 2017 (Talk)
3. Acosta R. P. and Huber M. Topographic controls on the Indo-Asian monsoon, CBEP paleoclimate meeting Sep 2017 (Talk)
4. Acosta R. P. Huber M. The Southeast Moisture Transport Across the Indo-Gangetic Plain during Peak Monsoon Season Presented at American Geophysical Union fall science meeting (Dec 2016)
5. Acosta R. P., Huber M. An over estimation of topographic diabatic heating and precipitation in NCAR CAM simulations during the Indo-Asian monsoon season Presented at AGU fall science meeting (Dec 2015)
6. Acosta R P., Huber M. The Indo-Asian monsoon with high-resolution CAM model Presented at New England EPSCoR meeting (March 2015) and University of New Hampshire, graduate research conference (April 2015) (Talk)
7. Acosta R. P., Huber M. Are model-data differences in the Indo-Asian monsoon due to model or data biases? Presented at American Geophysical Union fall science meeting (December 2014)
8. Muge Komurcu, R. Paul Acosta, Jonathan Buzan, Matthew Huber Dynamically Downscaling and Model Calibration for Simulating Regional Climate Change in New Hampshire. Presented at American Geophysical Union fall science meeting (Dec 2014)
9. Acosta R.P., Goldner A., Herold, N., Huber M. Does the Tibetan Plateau influence the upwelling system of the Arabian Sea and Bay of Bengal? Presented at American Geophysical Union ocean sciences meeting (2014)
10. Acosta R.P., Goldner A., Herold, N., Huber M. Is the Tibetan Plateau important for the global monsoon? Presented at American Geophysical Union fall meeting (2013)
11. R. Paul Acosta, Peter Scott Weiss-Penzias, Victoria Bauer, John Phillip Ryan, Arthur Russell Flegal. Total mercury concentration in sediment from the con-

tinental shelf of central California Presented at American Geophysical Union 2012, and Purdue GIS day

Short Courses and Summer Schools

1. NCAR ASP summer colloquium (June 2017)
2. University of Chicago climate and statistics workshop, Rossbypalooza (July 2016)
3. NCAR Community Earth System Model winter modeling meeting (Feb 2016)
4. Yale, Synoptic-Scale and Intraseasonal Variability in Monsoons (Apr 2015)
5. Mountains and High Plateaus University of Michigan Summer school (Aug 2015)
6. USGS COAWST Modeling System Training (Augt 2014)
7. NCAR Weather Research Forecasting, Regional Climate summer tutorial (Jul 2014)
8. NCAR Weather Research Forecasting summer tutorial (Jul 2014)
9. NCAR Community Earth System Model summer tutorial (Jun 2013)
10. Urbino Paleoclimate school (Jul 2012)

Masters Research Projects

1. Climatic impact of Himalayan-Tibetan Mountains on the Asian Monsoons using NCAR CAM4 GCM

Undergraduate Research Projects (December 2010-June 2012)

1. Measurement of total, monomethyl mercury and ions in the fog and rain at Santa Cruz CA
2. Measurement of total mercury speciation in ocean sediment at Santa Cruz, CA

Teaching Experience

1. Teaching assistant, Purdue Climate and Statistics EAPS 509. Planetary Geology EAPS 556. (08/2018-12/2018)

2. Teaching assistant, Purdue University. Energy and Scociety (EAPS 375) (05/2018)
3. Teaching assistant, Purdue University. Dynamic Earth (EAS 191) (08/2012-12/2012)
4. Purdue Climate Change Research Center Undergrad Mentor (2013)
5. Teaching assistant, UCSC. TAs apprentice in an upper-division earth science coursework (Evolution of Earth 110A) (09/2011-12/2011)
6. Research Assistant and lab technician, UCSC. Dr. Peter Weiss in Russ Flegal Laboratory, (12/2010- 06/2012) http://news.ucsc.edu/2012/12/coastal-mercury.html
7. Research Assistant and lab technician, UCSC. Dr. Priya Ganguli in Russ Flegal Laboratory, (12/2010- 06/2012) -http://www.priyaganguli.com/teaching-philosophy/field-lab-mentees

Computational Skills

1. Operating systems: Windows, Mac, Linux
2. Programming Language: C, Unix, NCL, NCO, Python, Matlab and Rstudio
3. Community Earth System Model (CESM)
4. Weather Research Forecasting Model (WRF)

Extracurricular and Outreach Experience

1. Purdue University, EAPS-Imagination Center Passport Day (11-2017)
2. Purdue EAPS Solar Eclipse outreach event (08-2017)
3. Purdue University, EAPS-Imagination Center Passport Day (11-2016)
4. University of New Hampshire, NRESS department social and outreach committee member (Fall and Spring 2016)
5. University of New Hampshire - Climate, Coffee and Tea meetings (2014-15)
6. Student judge for Undergraduate Research Conference Interdisciplinary Science and Engineering Symposium (2014 and 2016)
7. Volunteer Annual University of New Hampshire Oyster River Duck Race (2014-15)

8. Event coordinator for Graduate Student Association at Purdue Earth, Planetary and Atmospheric Department (2012-13)
9. Cowell college orientation leader, UCSC. Assist freshmen move in and plan various events and projects throughout the year (2009-12)